ANALYSIS OF TRACER AND THERMAL TRANSIENTS DURING REINJECTION

A DISSERTATION
SUBMITTED TO THE DEPARTMENT OF PETROLEUM ENGINEERING
AND THE COMMITTEE ON GRADUATE STUDIES
OF STANFORD UNIVERSITY
IN PARTIAL FULFILLMENT OF THE REQUIREMENTS
FOR THE DEGREE OF
DOCTOR OF PHILOSOPHY

By
Ibrahim Kocabas
October, 1989

Abstract

This work studied tracer and thermal transients during reinjection in geothermal reservoirs and developed a new technique which combines the results from interwell tracer tests and thermal injection-backflow tests to estimate the thermal breakthrough times.

Tracer tests are essential to determine the degree of connectivity between the injection wells and the producing wells. To analyze the tracer return profiles quantitatively, we employed three mathematical models namely, the convection-dispersion(CD) model, matrix diffusion(MD) model, and the Avdonin(AD) model, which were developed to study tracer and heat transport in a single vertical fracture.

We considered three types of tracer tests namely, interwell tracer tests without recirculation, interwell tracer tests with recirculation, and injection-backflow tracer tests. To estimate the model parameters, we used a nonlinear regression program to match tracer return profiles to the solutions.

We matched the appropriate solutions to the three sets of data obtained from the interwell tracer tests without recirculation at Wairakei, New Zealand. All model matches had small residuals but differed considerably in capturing the distinctive features such as peak time and tailing of the profiles.

We developed new solutions to the mathematical models to interpret the return profiles from interwell tracer tests with recirculation. These solutions are more generally applicable than previously used methods, since they specifically include the recirculation effects and can account for any number of recirculations.

We also developed solutions to the CD and MD models to interpret the return profiles of injection-backflow tracer tests. A comparison of the solutions to the

CD model for different boundary conditions showed that some should not be used for short injection period tests and/or when the dispersive transport is dominant. To obtain the MD model solution, we used a double Laplace transformation with respect to the time variables of the injection and backflow periods.

Finally we suggested thermal injection-backflow tests as a means to estimate the thermal transport parameters. The solution to the MD model can be used for interpreting thermal injection-backflow tests. In fact, the MD model was first developed by Lauwerier to study the temperature distribution in an oil layer during hot fluid injection. The Lauwerier model has two parameters namely, t_w, the water transit time, and λ which accounts for the heat transfer from the fracture into the adjacent matrix. We obtain the value of t_w from the interwell tracer tests and the value of λ from the thermal injection-backflow tests. Substituting these parameters into the model, we can estimate the thermal breakthrough times during reinjection. This new technique avoids some of the disadvantages of previously suggested methods namely, the ambiguity of the estimates from the non-thermal methods and the inappropriateness of the interwell thermal interference tests.

TABLE OF CONTENTS

List of Tables

List of Figures

Chapter 1

INTRODUCTION

This work involves a study of tracer and thermal transients during reinjection in fractured geothermal reservoirs. We considered three types of tracer tests, namely interwell tracer tests both with and without recirculation, injection-backflow tracer tests, and thermal injection-backflow tests. To interpret tracer and temperature return profiles, we used three mathematical models which had been developed previously for studying tracer and heat transport through a single vertical fracture.

Reinjection of the waste water[17,41,74] is commonly practiced in many liquid-dominated geothermal fields worldwide. Most of the time the objective of the reinjection is to dispose of the waste water[40,41], since it usually contains silica and toxic minerals such as arsenic, boron and mercury[14]. Reinjection of the waste water is also used to maintain the reservoir pressure[40,41] and to enhance the energy recovery[66]. Regardless of the objective, however, the low temperature of the waste water is a serious constraint upon the reinjection. Many field experiences have shown that the reinjected water may move through the fractures to the production zones in a very short time. The rapid migration of the reinjected water is undesirable, because it can produce thermal drawdown at the production wells, This thermal drawdown has two detrimental effects. First, it reduces the discharge enthalpy causing the steam discharge rates to decline. Second, it decreases the total production because of the increasing hydrostatic pressure of the fluid in the well[41]. We can avoid a rapid propagation of the thermal front if we are able to identify the

fast flow channels prior to the start of reinjection.

Analysis of the return profiles of tracer tests is the tool most commonly used to identify these fast flow channels and to estimate the fracture aperture, which is the most important parameter controlling the propagation of the thermal front[66]. Some researchers[66] also suggested using thermal interference tests to determine thermal characteristics of the system directly. However, there is little thermal drawdown data reported on this kind of a long term injection test. **A** quantitative analysis of tracer return profiles can be accomplished by matching return profiles with solutions to mathematical models.

1.1 MATHEMATICAL MODELS

A heterogeneous system is characterized by preferential flow paths due to dead end pores[20,24], aggregates[63,68], fissures[4,90], fractures[40], layering[10], and so on. Tracer transport in a heterogeneous porous system may be modelled in four ways[8]:

1. the very near field: tracer transport in a single well defined preferential flow path, possibly with transport into the adjacent porous matrix is considered.
2. the near field: tracer transport in a set of well defined preferential flow paths is considered.
3. the far field: tracer transport is modelled by using two superposed continua, a mobile phase composed of a network of preferential flow paths and an immobile phase representing the rest of the system.
4. the very far field: entire medium is treated as a single continuum representing characteristics of both mobile and immobile phases.

Names of these various approaches are related to the scale of heterogeneities with respect to the scale of flow.

The far field and the very far field approaches are more widely used than the other two approaches. The far field approach has been commonly used to model laboratory experiments[10,35,68]. Mathematical models used for the far field approach assume that immobile phase acts as a uniformly distributed source in mobile phase. Transfer from mobile phase into immobile phase may be assumed proportional to the difference between average concentrations of two phases[20,24]. Alternatively, a diffusive transport may be assumed between the two phases[5,21,68]. In this case a definite geometry such as spherical, cylindrical, cubic, and so on, is assigned to the immobile phase. Despite different immobile phase geometries and transfer mechanisms assumed to take place between mobile and immobile phases, Barker[5] has obtained a standard mobile phase equation which is valid for all geometries. In his treatment, Barker used the block geometry functions(BGF).

Most of the time, groundwater field experiments have been modelled by using the very far field approach[67,77,90,93]. This is appropriate if the scale of heterogeneities is much smaller than the scale of flow.

In geothermal reservoirs, extremely fast fluid movements (up to 100 m/hr in some instances[40,41]) and asymmetric tracer return profiles indicate that flow takes place mainly in fractures between injection well and producing wells. Since the scale of fractures is in the order of the scale of flow, the very near field approach is appropriate to model the tracer transport.

There are three commonly used mathematical models to represent tracer transport through fractures. The first of these models, the convection-dispersion(CD) model, assumes a purely dispersive flow in the fracture. The form of the dispersion parameter depends on how the fracture is modelled.

Most of the time, we consider the fracture to be a plane between two parallel plates[31,39]. Since the flow is slow and laminar, we can assume a parabolic velocity profile across the fracture. This velocity profile gives rise to both a convective dispersion of the tracer along the transport path, and a large concentration gradient across the narrow width of the fracture. Molecular diffusion, on the other hand, rapidly equalizes the concentrations across the fracture and reduces the effect of the convective dispersion. The combination of transverse molecular diffusion

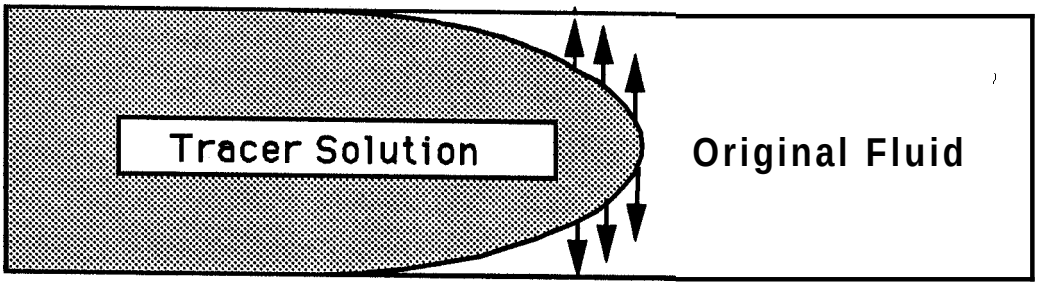

Figure 1.1: Taylor Dispersion

and convective dispersion along the flow direction is known as Taylor dispersion [Fig 1.11, which Taylor[84] described for flow in a capillary tube. Taylor also derived an expression for longitudinal dispersivity for capillary flow; and Horne and Rodriguez[39] derived an equivalent expression for fracture flow. The net result of Taylor dispersion is that the tracer front propagates with the mean speed of the flow, and the transition zone increases at a rate proportional to the square root of time.

Within the prescription of the convection-dispersion model, we could also consider the fracture as a porous stream tube[34]. In this case, we assume that the rough fracture walls and the bridging materials form a system of interconnected passages. There may be several local flow paths across the fracture which may also be significantly tortuous. There will be a velocity distribution within each path [Fig. 1.2a] and variations in the velocities of adjacent paths, in both magnitude [Fig. 1.2b] and direction [Fig. 1.2c]. This will cause spreading of the tracer with respect to mean flow, which is called mechanical dispersion. At the same time, in each of these local flow paths molecular diffusion causes an additional mixing [Fig. 1.31 of the tracer, which makes the dispersion irreversible. This combined effect of mechanical dispersion and molecular diffusion is called hydrodynamic dispersion[7]. The expression of the mechanical dispersion is given by the product of dispersivity,

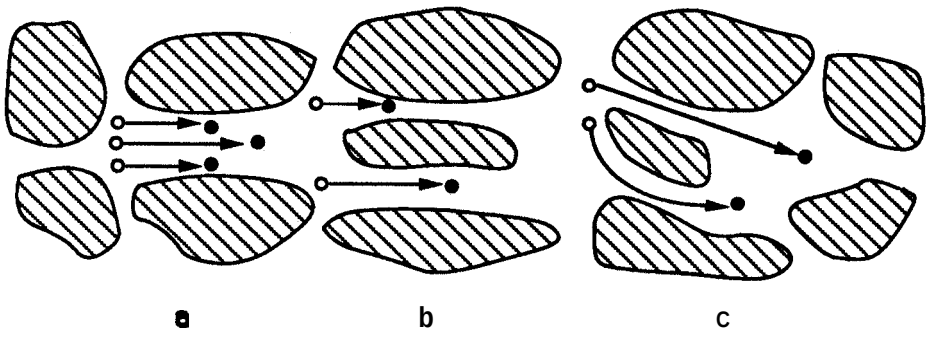

Figure 1.2: Mechanical Dispersion a) effect of pore walls b) effect of pore dimensions c) effect of tortuosity [After de Smedt *et. al.,* 1981]

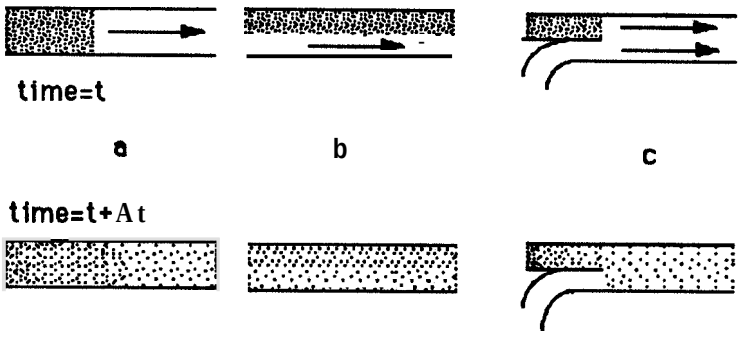

Figure **1.3:** Mixing in Local Flow Paths by Molecular Diffusion [After Fried, 1971]

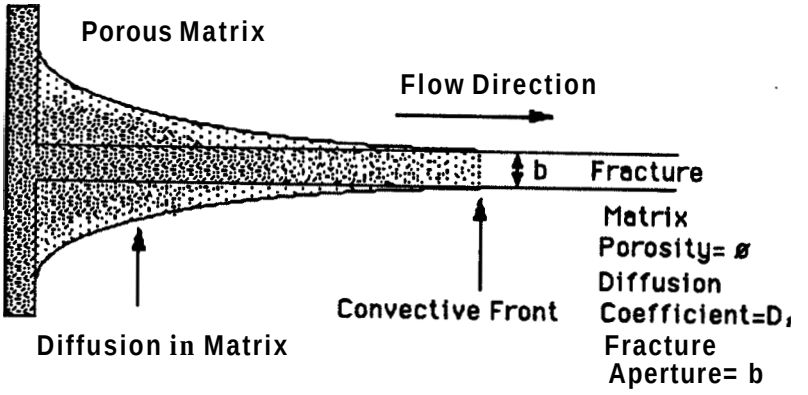

Figure 1.4: Matrix Diffusion Model [After Neretnieks, 19801

a characteristic mixing length[34], and the average **flow** speed.

The differential equation of the convection-dispersion model is given by

$$\frac{\partial C}{\partial t} + u\frac{\partial C}{\partial x} - D\frac{\partial^2 C}{\partial x^2} = 0 \qquad (1.1)$$

The variables used in Eq. 1.1 and in all other equations in this dissertation are defined in the nomenclature.

The second model is called the matrix diffusion(MD) model. It represents a system consisting of a fracture in which the tracer fluid is mobile located in a porous matrix in which the reservoir fluid is virtually immobile. The model considers the diffusion of the tracer from the fracture into the adjacent porous matrix as the main mechanism spreading the tracer along the transport region. It neglects longitudinal dispersion and assumes that tracer concentrations across the fracture are equalized before any significant effect of the convection appears [Fig. 1.41. Since the characteristic time for diffusion in the fracture is much less than that in the porous matrix[63], no concentration gradient across the fracture is likely. The matrix diffusion provides a time dependent storage, and the rate of change of storage

within the matrix is related to Fick's second law of diffusion. Within the matrix, diffusive transport is assumed to occur only perpendicular to the flow direction in the fracture.

Thus, two coupled one-dimensional equations are used to represent tracer transport. The equations are coupled by using the continuity of the flux and concentration across the fracture-matrix interface. The equation of tracer transport in the fracture[43,44,57,58,59] is:

$$\frac{\partial C}{\partial t} + u\frac{\partial C}{\partial x} + q = 0 \tag{1.2}$$

and the equation of transport in the matrix is:

$$D_a \frac{\partial^2 C_m}{\partial y^2} = \frac{\partial C_m}{\partial t} \tag{1.3}$$

The concentrations at the fracture-matrix interface are equated as:

$$C = C_m \quad at \quad y = o \tag{1.4}$$

and the continuity of the flux at the interface gives q in Eq. 1.2 as:

$$q = -\frac{2\phi D_a}{b} \left.\frac{\partial C_m}{\partial y}\right|_{y=0} \tag{1.5}$$

Matrix diffusion model is equivalent to the Lauwerier[50] model for heat transport.

The third model, called the Avdonin(AD) model, takes into account both longitudinal dispersion and diffusion into the matrix. It was developed by Avdonin[1] to study the temperature distribution in an oil layer during the injection of a hot incompressible fluid. Since then the model has been widely used to study the transport of tracers. Similar to the matrix diffusion model, tracer transport in the system is represented by two coupled one-dimensional equations. The fracture transport equation is given by:

$$\frac{\partial C}{\partial t} + u\frac{\partial C}{\partial x} - D\frac{\partial^2 C}{\partial x^2} + q = 0 \tag{1.6}$$

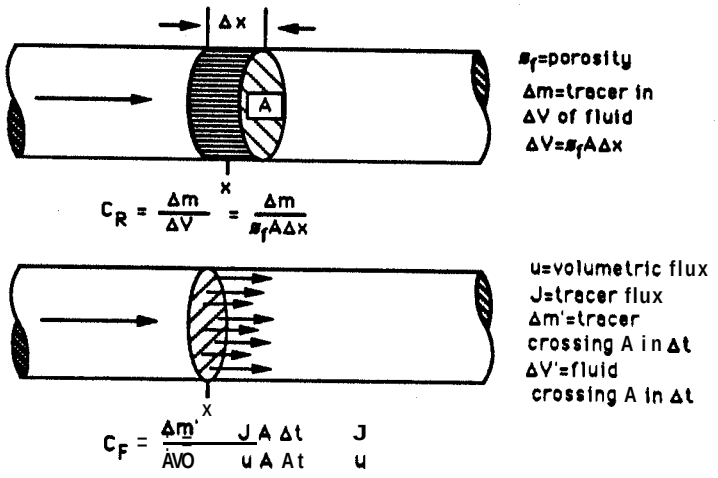

Figure **1.5:** Definitions of Resident and Flux Concentrations [After Kreft and Zuber, 1986]

Eq. **1.3,** Eq. **1.4** and Eq. **1.5** give the matrix transport equation and the equations describing the continuity of the concentration and the **flux** at the fracture-matrix interface.

1.2 FEATURES OF THE SOLUTIONS

A variable of a system is defined as a characteristic that may be measured and which assumes different numerical values when measured at different times[19], whereas a parameter is defined as a quantity characterizing the physical processes acting upon the variable, and remaining constant in time. In tracer studies, the use of two different concentration variables, namely resident and flux concentrations, has been equally common.

In development of the mathematical equations, the resident concentration C_R (the amount of the tracer per unit volume of the system at a given instant) [Fig. **1.51,** has always been taken as the variable of the system. In experiments, on the other hand, the flux concentration C_F (ratio of the tracer flux to the volumetric

flux) [Fig. 1.51, has been the most commonly measured quantity. As a result, tracer return profiles have been plotted mostly by using the flux concentration as the output variable. These two concentrations differ whenever the system is dispersive and there is a concentration gradient. Consequently, whenever a dispersive model is used for interpreting tracer return profiles, failure to distinguish between these two concentration variables leads to the use of solutions derived for initial and boundary conditions inconsistent with the actual conditions of the experiment(tracer test).

In solving the mathematical equations, Brigham[16] explained the proper specification of the initial and boundary conditions based on these two concentration variables. Later, Kreft and Zuber[47] provided a classification of the solutions to the convection-dispersion equation and the transformations linking the solutions. Parker and van Genuchten[60,87] also discussed the same concepts, and showed how the averaging techniques lead to different boundary conditions. This section summarizes the concepts discussed in these three articles, and the subsequent discussions on the subject by these authors.

The flux, C_F, and the resident, C_R, concentrations are related by:

$$Q \int_0^t C_F(x,t')dt' = \phi_f A \int_x^\infty C_R(x',t)dx' \tag{1.7}$$

where Q is the volumetric flow rate, A is the crossectional area, and ϕ_f is the porosity of flow path. Eq. 1.7 states that the material that passed the cross-section at **x** must be found between x and ∞.

If a dispersive model is used, the constitutive relation describing the flux is given by:

$$J = uC_R - D\frac{\partial C_R}{\partial x} \tag{1.8}$$

where J is the total flux, uC_R is the convective flux and $D\frac{\partial C_R}{\partial x}$ is the dispersive flux.

From the definition of the flux concentration, we can write:

$$J = uC_F \tag{1.9}$$

substituting Eq. 1.9 in Eq. 1.8 and rearranging yields:

$$C_F = C_R - \frac{D}{u}\frac{\partial C_R}{\partial x} \tag{1.10}$$

Eq. 1.7 and Eq. 1.10 serve for finding C_F whenever the theoretical form of C_R is known, or vice versa.

In an experiment, tracer is usually introduced into the system in either of two ways. In the first method, a slice of the system is uniformly filled with the traced fluid, which Kreft and Zuber[47] defined as injection in the resident concentration mode. In the second method, the tracer is uniformly distributed in the fluid stream entering the system, which Kreft and Zuber[47] defined as injection in the flux concentration mode. While the first method is formulated as an initial condition[27], the second method is formulated as a boundary condition[27].

As we have stated earlier, Eq. 1.1 has been formulated by using C_R as the variable of the system. However, one can show that the function C_F also satisfies Eq. 1.1(see Brigham[16] for details). Even though both functions C_R and C_F satisfy Eq. 1.1, we can obtain the solutions in terms of the function we want by properly specifying the initial and boundary conditions.

For an infinite system, if we assume that the part of the system from 0 to $-\infty$ is replaced with a traced fluid of constant concentration, then we have to formulate this assumption as an initial condition. If we want the solution in terms of the resident concentration, C_R, then the initial and boundary conditions are specified as follows:

$$C_R(x,0) = \begin{cases} 1 & x < 0 \\ 0 & x > 0 \end{cases} \tag{1.11}$$

$$\lim_{x\to\infty} C_R(x,t) = 0 \tag{1.12}$$

$$\lim_{x\to-\infty} C_R(x,t) = 1 \tag{1.13}$$

The solution to Eq. 1.1 subject to these initial and boundary conditions is called C_{CRR}, which corresponds to the infinitely extended injection in the resident fluid

and detection in the resident fluid.

If we want to obtain the solution in terms of the flux concentration variable, then we have to specify the initial and boundary conditions in terms of C_F. Substituting Eq. 1.11 through Eq. **1.13** into Eq. 1.10, we obtain:

$$C_F(x,0) = C_R(x,0)\left[1 + \frac{D}{u}\delta(x)\right] \tag{1.14}$$

$$\lim_{x\to\infty} C_F(x,t) = 0 \tag{1.15}$$

$$\lim_{x\to-\infty} C_F(x,t) = 1 \tag{1.16}$$

The solution to Eq. 1.1 subject to these initial conditions is called C_{CRF}, which corresponds to infinitely extended injection in the resident fluid and detection in the flux.

In a semi-infinite system, if we inject a traced fluid of constant concentration into the system at $x = 0$, we must formulate it as a boundary condition. If we want the solution in terms of C_R, then we can formulate the initial and boundary conditions as follows:

$$C_R(x,0) = 0 \tag{1.17}$$

Since injection of a fluid of constant concentration means keeping a constant flux at $x = 0$, we write the lower boundary condition(Danckwerts condition[22]) as:

$$\left[C_R(x,t) - \frac{D}{u}\frac{\partial C_R(x,t)}{\partial x}\right]_{x=0} = 1 \tag{1.18}$$

and finally the upper boundary condition is specified as:

$$\lim_{x\to\infty} C_R(x,t) = 0 \tag{1.19}$$

The solution to Eq. 1.1 subject to these conditions is called continuous injection in the flux and detection in the resident fluid, or C_{CFR}. To obtain the solution in the **flux** concentration variable, we specify:

$$C_F(x,0) = 0 \tag{1.20}$$

Since the tracer flux at the inlet is constant, we write:

$$C_F(0,t) = 1 \tag{1.21}$$

and substituting Eq. 1.12 into Eq. 1.10, we obtain the upper boundary condition.

$$\lim C_F(x,t) = 0 \tag{1.22}$$

In this case the solution to Eq. 1.1 is called C_{CFF}, continuous injection in the flux and detection in the flux.

Using the above technique Kreft and Zuber[47] classified the solutions to the CD model and showed how some of the solutions are related by different transformations. Here, the notation of Kreft and Zuber is used to represent solutions of governing differential equations. When the discussion is relevant to both instantaneous and continuous injection cases, the first letter of the subscript of C is omitted. For instance, C_{RR} refers to both the resident concentration solution for an infinitely extended injection C_{CRR} and the resident concentration solution for a planar injection C_{IRR}.

Tables 1.1 and 1.2 list the solutions in terms of C_R and C_F respectively, which are formed by rearranging the solutions in Tables 1 and 2 in the paper by Kreft and Zuber[47].

Table 1.3, which is also taken from the paper by Kreft and Zuber[47], shows how the solutions in Table 1.1 and Table 1.2 are linked by different transformations.

Many authors[10,16,60,94,95] have discussed the numerical differences between the solutions in terms of C_R and C_F. They stated that profiles of the concentration variables C_R and C_F become similar when the Peclet number P_e is high, which means that convective transport dominates dispersive transport. For $P_e \geq 30$ the differences are quite small, however, when the Peclet number is low, the difference between the profiles increases. Therefore, we have to use the solution closer to the physical situation, to interpret the return profiles of highly dispersive systems.

Inj.& Detec. Mode	IC & BC	Solution
infinitely extended injection and detection in resident fluid C_{CRR}	$C_R(x,0) = \begin{cases} 1 & for \quad x < 0 \\ 1/2 & for \quad x = 0 \\ 0 & for \quad x > 0 \end{cases}$ $\lim_{x\to-\infty} C_R(\cdot,t) = 1$ $\lim_{x\to\infty} C_R(x,t) = 0$	$C_{CRR} = \frac{1}{2} erfc\left(\frac{x-ut}{2\sqrt{Dt}}\right)$
planar injection in resident fluid and detection in resident fluid C_{IRR}	$C_R(x,0) = \frac{m}{\phi_f A}\delta(x)$ $\lim_{x\to-\infty} C_R(x,t) = 0$ $\lim_{x\to\infty} C_R(x,t) = 0$	$C_{IRR} = \frac{m}{\phi_f A}\frac{1}{\sqrt{4\pi Dt}} \exp\left(-(x-ut)^2/(4Dt)\right)$
continuous injection in flux concentration and detection in resident fluid C_{CFR}	$C_R(x,0) = 0$ $\left[C_R(x,t) - \frac{D}{u}\frac{\partial C_R(x,t)}{\partial x}\right]_{x=0} = 1$ $\lim_{x\to\infty} C_R(x,t) = 0$	$C_{CFR} = \frac{1}{2} erfc\left(\frac{x-ut}{2\sqrt{Dt}}\right) - \left[1 + \frac{u(x+ut)}{D}\right]$ $\frac{1}{2} \exp(ux/D)\ erfc\left(\frac{x+ut}{2\sqrt{Dt}}\right) +$ $\frac{ut}{\sqrt{\pi Dt}} \exp\left(-(x-ut)^2/(4Dt)\right)$
instantaneous injection in flux concentration and detection in resident fluid C_{IFR}	$C_R(x,0) = 0$ $\left[C_R(x,t) - \frac{D}{u}\frac{\partial C_R(x,t)}{\partial x}\right]_{x=0} = \frac{m}{\phi_f A}\delta(t)$ $\lim_{x\to\infty} C_R(x,t) = 0$	$C_{IFR} = \frac{m}{\phi_f A}\left[\frac{1}{\sqrt{\pi Dt}} \exp\left(-(x-ut)^2/(4Dt)\right) - \right.$ $\left.\frac{u}{2D} \exp(ux/D)\ erfc\left(\frac{x+ut}{2\sqrt{Dt}}\right)\right]$

Table 1.1: Resident Concentration Solutions

Ini.& D M	IC & BC	
infinitely extended injection and detection in flux concentration C_{CRF}	$C_F(x,0) = C_R(x,0)\left[1 + \frac{2D}{u}\delta(z)\right]$ *where* $C_R(x,0) = \begin{cases} 1 & for \quad x < 0 \\ 1/2 & for \quad x = 0 \\ 0 & for \quad x > 0 \end{cases}$ $\lim_{x\to-\infty} C_R(x,t) = 1$ $\lim_{x\to\infty} C_R(x,t) = 0$	$C_{CRF} = \frac{1}{2} erfc\left(\frac{x-ut}{2\sqrt{Dt}}\right) + \frac{D}{u}\frac{1}{\sqrt{4\pi Dt}} \exp\left(-(x-ut)^2/(4Dt)\right)$
planar injection in resident fluid and detection in flux concentration C_{IRF}	$C_F(x,0) = \frac{m}{\phi_f A}\left(1 + \frac{D}{ux}\right)\delta(x$ $\lim_{x\to-\infty} C_F(x,t) = 0$ $\lim_{x\to\infty} C_F(x,t) = 0$	$C_{IRF} = \frac{m}{Q}\frac{x+ut}{4\sqrt{\pi Dt^3}} \exp(-(x-u)^2/(4Dt)$
continuous injection in flux concentration and detection in flux concentration C_{CFF}	$C_F(x,0) = 0$ $C_F(0,t) = 1$ $\lim_{x\to\infty} C_F(x,t) = 0$	$C_{CFF} = \frac{1}{2}\left[erfc\left(\frac{x-ut}{2\sqrt{Dt}}\right) + \exp(ux/D)\, erfc\left(\frac{x+ut}{2\sqrt{Dt}}\right)\right]$
instantaneous injection in flux concentration and detection in flux concentration C_{IFF}	$C_F(x,0) = 0$ $C_F(0,t) = \frac{m}{Q}\delta(t)$ $\lim_{x\to\infty} C_R(x,t) = 0$	$C_{IFF} = \frac{m}{Q}\frac{x}{\sqrt{4\pi Dt^3}} \exp\left(-(x-ut)^2/(4Dt)\right)$

Table 1.2: Flux Concentration Solutions

Code	Transformation	Restriction
T_1	$C_F = C_R - \frac{D}{u}\frac{\partial C_R}{\partial x}$	$u \neq 0$
T_2	$C_F = \frac{1}{u}\int_x^\infty \frac{\partial C_R}{\partial t} dx'$	$u \neq 0$
T_3	$C_R = -u\int_0^t \frac{\partial C_F}{\partial x} dt'$	$u \neq 0$
T_4	$C_{CR} = \frac{\phi_f A}{m}\int_x^\infty C_{IR} dx'$	*none*
T_5	$C_{IR} = \frac{-m}{\phi_f A}\frac{\partial C_{CR}}{\partial x}$	*none*
T_6	$C_{CF} = \frac{Q}{m}\int_0^t C_{IF} dt'$	$u \neq 0$
T_7	$C_{IF} = \frac{m}{Q}\frac{\partial C_{CF}}{\partial t}$	$u \neq 0$

Table **1.3:** Transformations Linking The Solutions

Parker and van Genuchten[60] argue that the convection-dispersion model can effectively represent even media with large variations in pore velocities, and if we use the appropriate solution we should be able to match the return profiles of these systems.

A second issue discussed by researchers is choosing the appropriate boundary condition at the outlet of the system. When we use the infinite medium solutions for finite systems, we implicitly assume that a finite system acts like part of an infinite system. Parker and van Genuchten[60] say that this assumption imposes a mild restriction, since the outflow boundary should have no effect on the upstream velocity distribution inside the system. They also add that the only mechanism of backward transport is diffusion and when dispersion is dominant, the possible error is extremely small.

Brenner[9] has derived a finite system solution to Eq. 1.1 by imposing the following boundary conditions:

$$\left[C_R(x,t) - \frac{D}{u}\frac{\partial C_R(x,t)}{\partial x}\right]_{x=0} = 1.0 \qquad \textbf{(1.23)}$$

$$\left[\frac{\partial C_R(x,t)}{\partial x}\right]_{x=L} = 0 \qquad \textbf{(1.24)}$$

The finite system solution corresponds to a case of injection in the flux and detection in the resident fluid; therefore, its spatial concentration distribution matches with the semi-infinite medium solution, C_{CFR}, even for considerably small values($P_e \simeq 10$) of the Peclet number[10,26]. The finite system solution also produces the same numerical results as the semi-infinite medium C_{CFF} solution, at $x = L$ for the Peclet number as small as ten[10,26]. This is not surprising because upon substituting Eq. 1.24 into Eq. 1.10, we see that the zero gradient boundary condition practically transforms[94] the C_{FR} solution to C_{FF} at $x = L$.

Parker and van Genuchten[60] further claim that the semi-infinite medium C_{CFF} solution is more appropriate than Brenner's[9] solution to model finite systems. They say that a boundary layer interior to the outlet may arise as a result of treating the transition region, within which the transport parameters change from those of

the porous medium to those of bulk solution, as a boundary surface of infinitely small thickness. Therefore, a concentration discontinuity at the outlet boundary may exist. They support their argument by showing the inability of Brenner's solution to predict a short circuiting or zero impedance behavior. Zero impedance behavior is approached as $D/u \rightarrow \infty$ and the flux conditions imposed at $x = 0$ are instantaneously propagated through the medium. Therefore, C_{CFF} solution yields a flux concentration profile similar to the plug flow profile. They state that as $D/u \rightarrow \infty$ while Brenner's solution approaches the perfect mixing model, the semi-infinite medium C_{CFF} solution approximates the plug flow conditions which they claim that flow in fractured porous media is observed to approach. Therefore, they prefer C_{CFF} over Brenner's solution.

Kreft and Zuber[47] say that for a semi-infinite medium, the limiting case $D/u \rightarrow \infty$ has no physical meaning, but a high D/u may be understood as a result of a wide spectrum of microscopic velocities in the system. Even though he does not agree on the reasoning followed by Parker and van Genuchten[60], Zuber[95] also shares the opinion that C_{CFF} represents finite systems better than Brenner's[9] solution.

Finally, in the case of chemical reactions or adsorption a source/sink term appears in the mathematical equations. A material balance in terms of the resident concentration yields:

$$\frac{\partial C_R}{\partial t} + u\frac{\partial C_R}{\partial x} - D\frac{\partial^2 C_R}{\partial x^2} + q = 0 \tag{1.25}$$

where q is the reaction rate expressed in consistent units with C_R. If the reaction rate is of the first order, as follows;

$$q = kC_R \tag{1.26}$$

then C_F also satisfies[48] Eq. 1.25. If the reaction rate is of higher orders, then C_F does not satisfy Eq. 1.25. In such cases, C_F can be found through the application of transformation T_1 from Table **1.3,** whenever the theoretical form of C_R is known.

The discussion about the resident and flux concentrations also applies to dispersive models of the near field, the far field and the very far field approaches. In

fact, Baker[3] showed that both C_F and C_R satisfy the Coats-Smith model of the far field approach.

In summary, tracer tests are frequently used to identify the fast flow paths in geothermal reservoirs and to estimate some of the parameters controlling propagation of the thermal front. A quantitative interpretation of the return profiles requires matching the solutions of the mathematical models to field data. There are three commonly used mathematical models, namely the CD, MD and AD models, to study tracer and heat transport through fractures.

In tracer studies, use of the two concentration variables C_R and C_F has been equally common. Whenever a dispersive model is used, failure to distinguish between these two concentration variables leads to use of solutions which are inconsistent with actual conditions of the experiment. Differences between the two concentrations are significant at low Peclet numbers($P_e \leq 30$)[10]. For field experiments in fractured geothermal reservoirs the Peclet number can be as law as one[39,86]. Therefore, the distinction between resident and flux concentrations are necessary for analysis of tracer return profiles in geothermal reservoirs.

Several researchers have discussed the physical meaning of all the known solutions to the CD and AD models for unidirectional flow and presented the transformations linking them. These solutions have been used to interpret laboratory column experiments as well as tracer return profiles of interwell tracer tests without recirculation. There is, on the other hand, less work reported concerning either interwell tracer tests with recirculation or injection-backflow tracer tests.

Some researchers considered estimation of the thermal breakthrough time based on tracer tests as questionable. They suggested the use of thermal interference tests to determine thermal characteristics of the system. However, the extremely long injection period requirement makes thermal interference tests impractical most of the time. On the other hand, a thermal transient test in which fluid is first injected into a single well, and then produced from it (i.e. a thermal injection-backflow test), could be performed in a much shorter time.

The objectives of this study are two-fold: namely, a quantitative interpretation of the return profiles from tracer tests, and investigation of the applicability of

thermal injection-backflow tests. First, we present a unified approach to the classification of the solutions of dispersive mathematical models of the very near field, the near field, the far field and the very far field for unidirectional flow. Then we consider interpretation of tracer return profiles as an inverse problem. To study tracer return profiles of interwell tracer tests with recirculation and also injection-backflow tracer tests, we develop several new solutions by using single and double Laplace transformation methods. When the Laplace space functions were difficult to invert analytically, we use single **or** double numerical inversion methods. Finally, we investigate determining thermal characteristics of geothermal reservoirs from thermal injection-backflow tests. If we can identify fast flow paths and the mean speeds of flow in these paths by tracer tests and determine the heat transfer parameter between the flow path and the adjacent matrix, then we will be able to estimate the thermal breakthrough time.

Chapter 2

THEORY

This chapter will elaborate on three aspects of using the two concentration variables in dispersive systems. First, we will present a general treatment using different variables for all linear dispersive models. Second, we will clarify a solution to the convection-dispersion model, which Sauty[77] employed, but Kreft [47] and Zuber[94] criticized and rejected, apparently because of an ill-defined parameter, C_0. Using the concepts of resident and flux concentrations, we will also derive new solutions from this solution. Finally, we will present a new example of the differences between solutions in terms of the flux concentration variable and solutions derived by imposing zero gradient at the outlet boundary.

2.1 DEPENDENT VARIABLES OF DISPERSIVE SYSTEMS

In many cases, we represent the dispersive systems by:

$$\frac{\partial C}{\partial t} + u\frac{\partial C}{\partial x} - D\frac{\partial^2 C}{\partial x^2} + q = 0 \qquad (2.1)$$

Eq. 2.1 is derived by applying a material balance relation and C_R is used as the concentration variable of the system. We introduce the source term, q, to account for any of several phenomena such as chemical reaction, radioactive decay, adsorption,

and molecular diffusion into the adjacent porous matrix. If we use the constitutive relation given by Eq. 1.8, and if we transform the dependent variable C_R to J, we obtain:

$$\frac{\partial J}{at} + u\frac{\partial J}{\partial x} - D\frac{\partial^2 J}{\partial x^2} + uq - D\frac{\partial q}{\partial x} = 0 \tag{2.2}$$

We considered four specific forms of the source term, q. First, if the source term is equal to zero, then C_R and J both satisfy the convection-dispersion equation[16]. If there is no flow, then both variables satisfy the heat equation as pointed out by Carslaw and Jeager[18] for the diffusion equation.

Second, if the source term represents a linear type reaction such that:

$$q = kC_R \tag{2.3}$$

then both variables C_R and J again satisfy[47] the same equation.

Third, if the source term represents diffusion into the adjacent porous matrix, and the source term is given by Eq. 1.5, then we can show that the Laplace transform of Eq. *2.1* is given by:

$$D\frac{\partial^2 \overline{C}_R}{\partial x^2} - u\frac{\partial \overline{C}_R}{\partial x} - (s + 2\lambda\sqrt{s})\overline{C}_R = 0 \tag{2.4}$$

in which the Laplace transform of q, corresponds to:

$$\overline{q} = -2\lambda\sqrt{s}\ \overline{C_R} \tag{2.5}$$

where λ is:

$$\lambda = \frac{\phi\sqrt{D_a}}{b} \tag{2.6}$$

Then the Laplace transform of Eq. *2.2* can be obtained as:

$$D\frac{\partial^2 \overline{J}}{\partial x^2} - u\frac{\partial \overline{J}}{\partial x} - s\overline{J} - 2\lambda\sqrt{s}\,(u\overline{C}_R - D\frac{\partial \overline{C}_R}{\partial x}) = 0 \tag{2.7}$$

In Laplace space, since J and C_R are related by:

$$\overline{J} = u\overline{C}_R - D\frac{\partial \overline{C}_R}{\partial x} \tag{2.8}$$

Substituting Eq. 2.8 into Eq. 2.7:

$$D\frac{\partial^2 \overline{J}}{\partial x^2} - u\frac{\partial \overline{J}}{\partial x} - (s + 2\lambda\sqrt{s})\,\overline{J} = 0 \tag{2.9}$$

Comparing Eq. 2.4 and Eq. 2.9, we can see that both functions satisfy the same differential equation.

The corresponding dependent variable of the transport equation in the matrix J_m satisfies Eq. **1.3,** and the related boundary conditions are the same as those of C_m. The Laplace space solution for J_m is given by:

$$\overline{J}_m = \overline{J}\,\exp\left(-\frac{\sqrt{s}}{\sqrt{D_a}}\,y\right) \tag{2.10}$$

Substituting Eq . 2.8 into Eq. 2.10:

$$\overline{J}_m = \left(u\overline{C} - D\frac{\partial \overline{C}}{\partial x}\right)\,\exp\left(-\frac{\sqrt{s}}{\sqrt{D_a}}\,y\right) \tag{2.11}$$

Eq. 2.11 can be written as:

$$\overline{J}_m = u\overline{C}_m - D\frac{\partial \overline{C}_m}{\partial x} \tag{2.12}$$

Therefore, J and C, and J_m and C_m are correlated by the same relation. For all these cases, not only the variable J but also any other variable obtained by dividing J by a constant will satisfy Eq. 2.1. In fact, the variable C_F, one of the two concentration variables used in tracer studies, is obtained by dividing J by u.

The **AD** model corresponds to the third case, and its solutions can also be classified by using the methods discussed earlier. The solutions can be related to each other by using the transformations in Table **1.3,** except for the transformations T_2 and T_3 which will not work because of diffusion into the matrix. An infinitely extended injection is never realized in an actual experiment. For this mode there are two situations. First, initially the matrix is free of tracer over the whole domain, while the fracture is filled with the traced fluid from 0 to $-\infty$. Second, initially

both the matrix and fracture contain the traced fluid for $x \leq 0$. Both of these cases are unlikely to occur in an experiment.

Finally, if the source term represents a reaction of higher order, then Eq. 2.1 becomes nonlinear and neither of the functions J and C_F satisfies Eq. 2.1. In such a case, C_F does not loose its physical meaning and can be found from the theoretical expression for C_R by using the transformation T_1 in Table **1.3.**

So far all of the models discussed describe tracer transport in distinct fractures situated in matrix blocks(the very near field approach), and they suit well for studying tracer transport in geothermal reservoirs. However, the far field and the very far field approaches are widely used in other fields such as petroleum reservoir engineering, soil science, and hydrology. The very far field approach is modelled by the CD model which corresponds to the case $q = 0$. The far field approach models consist of the superposition of two continua in space, a mobile phase where convective transport occurs, and an immobile phase where only diffusive transport occurs. The models assume that immobile phase acts as a uniformly distributed source in the mobile phase. As a result, coefficients of accumulation and source terms are different from those of the corresponding terms of Eq. 2.1. The discussion on the resident and flux concentration also applies to these models.

Baker[3] showed that C_F and C_R both satisfy the Coats and Smith[20] model which is a special case of the far field approach models. The standard mobile phase equation which is valid for all immobile geometries is also satisfied by both concentration variables C_F and C_R as well as the flux variable J.

Several authors[2,11,13,21,69] used these models consistently with the two concentration variables to interpret laboratory experiments. Bretz and Orr[12] used the Coats-Smith and porous sphere model to investigate the effect of microscopic heterogeneities. Correa *et. al.*[21] used spherical and parallel plate geometries, and the Coats and Smith model to interpret miscible displacement experiments. They developed approximate solutions of the models for short and long times to estimate model parameters from displacement data.

2.2 NEW SOLUTIONS OF THE CD MODEL

The fundamental solution of a linear equation gives the response of a system to an instantaneous source acting at $x = 0$ and $t = 0$. The fundamental solution of the one-dimensional convection-dispersion equation is given by:

$$C = \frac{m}{\phi_f A} \frac{1}{\sqrt{4\pi D t}} \exp\left(-\frac{(x-ut)^2}{4Dt}\right) \tag{2.13}$$

If the strength of the source is time dependent in such a way that it will generate an amount of material equal to the total of the amount carried away in fluid flux and the amount dispersed, then it corresponds to the case of constant concentration at $x = 0$. This constant concentration at $x = 0$, however, is in terms of C_R and not C_F. If the source strength is constant in time, then the solution which will also be in terms of C_R can be obtained by either solving:

$$\frac{\partial C}{\partial t} + u\frac{\partial C}{\partial x} - D\frac{\partial^2 C}{\partial x^2} = \frac{m'}{\phi_f A}\delta(x) \tag{2.14}$$

subject to the following initial and boundary conditions:

$$C(x,0) = 0 \tag{2.15}$$

$$\lim_{x\to\infty} C(x,t) = 0 \tag{2.16}$$

$$\lim_{x\to-\infty} C(x,t) = 0 \tag{2.17}$$

or integrating Eq. **2.13** over time. By either of the methods we obtain:

$$C = \frac{m'}{u\phi_f A}\frac{1}{2}\left[erfc\left(\frac{x-ut}{2\sqrt{Dt}}\right) - \exp\left(\frac{ux}{D}\right) erfc\left(\frac{x+ut}{2\sqrt{Dt}}\right)\right] \tag{2.18}$$

for $x \geq 0$, and where m' is the amount of tracer released by the source per unit time. The integral does not result in a known function for $x \leq 0$.

These solutions were employed by Bear[7] and Sauty[77] in studying dispersion in aquifers. The solutions, however, were criticized and rejected by some

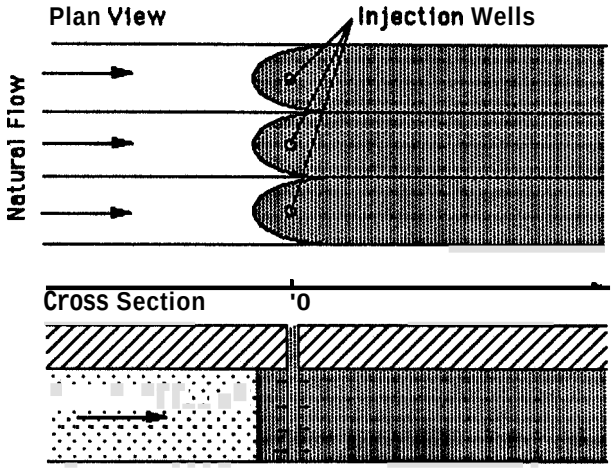

Figure 2.1: Tracer Sources in a Flow Field, [after Sauty, 1980]

authors[47,94], probably because of **an** ill-defined parameter, C_o. The parameter, C_o was defined by Sauty as the constant concentration of the injected fluid and substituted for $m'/\phi_f Au$ in **Eq. 2.18.** Considering this definition, we can see from **Eq.** 2.18 that C_o can be neither the flux concentration nor the resident concentration.

If we assume that the traced fluid injection rate is negligible compared to the volumetric flow rate in the system, then we can write:

$$\frac{m'}{\phi_f Au} = \frac{C_o Q_r}{\phi_f Au} = \frac{C_o Q_r}{Q} = C^* \qquad \textbf{(2.19)}$$

C^* is a reference concentration, which is similar to the flux concentration and expressed by the ratio of the amount of material generated in a unit time to the volumetric flow rate. In this system, the amount of material generated in **a** unit time is not equal **to** the tracer flux at the location of the source. Therefore, the solution is not in terms of C_F. In other words, since the source strength is expressed **as** the material generated per unit volume of the system per unit time, the solution is in terms of C_R.

Even though the solution is mathematically well formulated, we must investigate whether the initial and boundary conditions are consistent with the conditions of the experiment. Zuber[94] said that Figs. 2.a and 2.b in the paper by Sauty[77] correspond physically to the injection in flux concentration mode. Considering this argument, we conclude that the solutions are inappropriate for those cases studied by Sauty[77]. However, Fig. 2.a (see Fig. 2.1) in the paper by Sauty[77] indicates that there is a transport opposite to the direction of natural flow. If the injection is continuous, then the backward transport at the injection point may be significantly high. In such a case, using a solution for a continuous source at the origin may be more appropriate.

For detection in the flux concentration mode, the solution for an instantaneous source is obtained as:

$$C_{SIF} = \frac{m}{Q}\frac{x+ut}{2\sqrt{4\pi Dt^3}}\exp\left(-\frac{(x-ut)^2}{4Dt}\right) \qquad -\infty < x < \infty \tag{2.20}$$

and the solution for a continuous source is given by:

$$C_{SCF} = C^*\frac{1}{2}\left[erfc\left(\frac{x-ut}{2\sqrt{Dt}}\right)\right] \qquad for \quad x > 0 \tag{2.21}$$

For $x < 0$, the integration of Eq. **2.13** does not result in a known function. Therefore, Eq. **2.13** must be substituted into transformation T_1, and the resultant equation evaluated numerically.

2.3 THE OUTLET BOUNDARY CONDITION

All of the solutions discussed in the previous section are either infinite or semi-infinite medium solutions. In reality, however, all of the experiments must be carried out on finite systems, and choosing the appropriate boundary condition at the outlet of the system has lead to interesting discussions among researchers.

The general approach in specifying the boundary conditions in a finite system is to assume three units[91]: the first and the third being semi-infinite (see Fig. 2.2). The conservation of flux principle requires that the fluxes on both sides of the

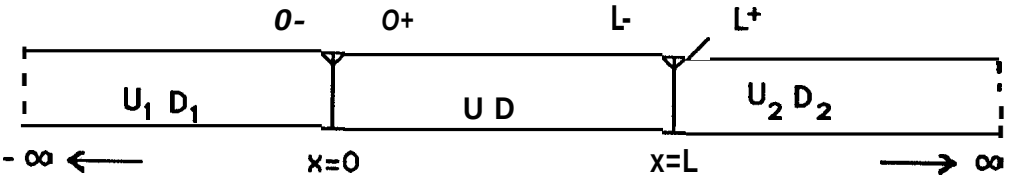

Figure **2.2:** Boundary Conditions of a Finite System

boundary (bounding surface) be equal. There can be no accumulation within the boundary surface because the surface has no volume.

$$\left[C_1 - \frac{D_1}{u_1}\frac{\partial C_1}{\partial x}\right]_{x=0^-} = \left[C - \frac{D}{u}\frac{\partial C}{\partial x}\right]_{x=0^+} \tag{2.22}$$

$$\left[C - \frac{D}{u}\frac{\partial C}{\partial x}\right]_{x=L^-} = \left[C_2 - \frac{D_2}{u_2}\frac{\partial C_2}{\partial x}\right]_{x=L^+} \tag{2.23}$$

The usual assumption that $D_1 = 0$ in the fore-section of the system reduces Eq. **2.22** to:

$$C_1 = C - \frac{D}{u}\frac{\partial C}{\partial x}\Big]_{x=0^+} \tag{2.24}$$

van Genuchten and Parker[62], in their response to Parlange *et.al.*[62], explain this result with the existence of a transition region within which the medium properties dispersivity and concentration vary continuously. Since the transition region is considered infinitely thin, apparent discontinuities result in both dispersivity and concentration.

However, there is no consensus over the treatment of the boundary condition at the outlet of the system. Brenner[9] derived a solution for the CD model by imposing **Eq. 2.24** and

$$\left[\frac{\partial C_R(x,t)}{\partial x}\right]_{x=L} = 0 \tag{2.25}$$

With the assumption that $D_2 = 0$ at the after-section of the system, Eq. 2.23 reduces to:

$$C - \frac{D}{u}\frac{\partial C}{\partial x}\Big]_{x=L-} = C_2 \tag{2.26}$$

Assuming that the macroscopic concentrations are continuous at the outlet boundary, then Eq. **2.26** is reduced to Eq. 2.25. Naumann and Buffham[56] explain this result by pointing out that when the flow is from a mixed region to a region where there is no mixing, there is no way in which the composition can change crossing the boundary.

van Genuchten and Parker[62] argue that even if a zero gradient exists at the after-section, it tells nothing about the mathematical boundary layer associated with the discontinuity in medium properties. They add that even though it is convenient to assume an infinitely thin boundary region within which the dispersion and porosity change from porous medium to bulk solution values, imposing discontinuities in these parameters must yield a discontinuity in macroscopic concentration.

Zuber[94] argues that Eq. 2.25 applies for the case of molecular diffusion, but in the case of hydrodynamic dispersion, its applicability becomes obscure. Eq. 2.25 means that there is no dispersive flux at the outlet boundary, which implies either all the flow lines have the same velocity, or the same concentration. Such a condition is highly unlikely to occur in natural systems.

A distinctive feature of Brenner's[9] solution is that both the time and space profiles conserve the material balance relation. Consequently, for large Peclet numbers, it generates identical profiles with C_{CFR} along the system, and with C_{CFF} in time at $x = L$. For small Peclet numbers, however, the results may differ considerably. Thus, the main difference between the semi-infinite and finite system solutions may be indicated in the differences between the resident and flux concentrations. In the semi-infinite medium approach, C_{FF} is always greater (smaller when convective

and dispersive fluxes are in opposite directions) than C_{FR}, and the difference between them is almost constant over the length of the system. In the finite system approach, however, the difference between C_{FF} and C_{FR} decreases as the distance from the inlet increases, and it becomes zero at the outlet boundary. The experimental results of Gaudet *et.al.* which are reported by de Smedt *et.al.*[26], and the results of the experiments presented by Parker[61], show that C_{FF} is greater than C_{FR}. Therefore, the known experimental results support the semi-infinite medium approach.

As there is no proof of the inappropriateness of either approach to model real systems, an intuitive decision is necessary on when to assume that the outlet boundary does not influence the system, or when to use an outlet boundary implying continuity of macroscopic concentrations. It is our purpose here to compare the two solutions: **one** assumes continuity of the macroscopic concentrations and the other does not. The example corresponds to the case where the flux concentration is smaller than the resident concentration.

Injection-backflow tracer tests have been performed in geothermal fields, and analysis of tracer return profiles is discussed in the next chapter. To obtain the solution for the backflow period, governing equations may be solved by using the injection period profile as the initial condition.

If a dispersive model is used, an appropriate outlet boundary condition is required at $x = 0$. The following initial and boundary conditions assume continuity of the macroscopic concentration at $x = 0$:

$$C(x,0) = f(x') \tag{2.27}$$

$$\lim_{x\to\infty} C(x,t) = 0 \tag{2.28}$$

$$\left.\frac{\partial C(x,t)}{\partial x}\right]_{x=0} = 0 \tag{2.29}$$

Using the Green's function method, Riley[72] gives a solution to the convection-dispersion model:

$$C(x,t) = \int_0^\infty f(x')\frac{1}{2}\left\{\frac{1}{\sqrt{\pi Dt}}\exp\left(-\frac{(x-x'+ut)^2}{4Dt}\right)\right.$$
$$+\frac{1}{\sqrt{\pi Dt}}\exp\left(-\frac{ux}{D}\right)\exp\left(-\frac{(x+x'-ut)^2}{4Dt}\right)$$
$$\left.-\frac{u}{D}\exp\left(\frac{ux'}{D}\right)erfc\left(\frac{x+x'+ut}{2\sqrt{Dt}}\right)\right\}dx' \qquad (2.30)$$

The function $f(x')$, which is the initial condition, is specified as C_{FR}, the resident fluid concentration at the end of the injection period:

$$f(x') = \frac{1}{2}erfc\left(\frac{x'-ut_j}{2\sqrt{Dt_j}}\right) - \frac{1}{2}\exp\left(\frac{ux'}{D}\right)erfc\left(\frac{x'+ut_j}{2\sqrt{Dt_j}}\right)$$
$$\left[1+\frac{u(x'+ut_j)}{D}\right] + \frac{u\sqrt{t_j}}{\sqrt{\pi D}}\exp\left(-\frac{(x'-ut_j)^2}{4Dt_j}\right) \qquad (2.31)$$

In an infinite medium, the solution to the convection dispersion model is:

$$C(x,t) = \int_{-\infty}^{\infty} f(x')\frac{1}{2\sqrt{\pi Dt}}\exp\left(-\frac{(x+ut-x')^2}{4Dt}\right)dx' \qquad (2.32)$$

where $f(x')$ is the initial condition. To obtain the flux concentration solution either of the two methods can be used. First, apply the transformation T_1 to Eq. 2.32. Alternatively, express the initial condition in terms of the flux concentration by applying the transformation T_1 to the initial resident concentration function.

Using the first method, the flux concentration solution is:

$$C(x,t) = \int_{-\infty}^{\infty} f(x')\frac{(x'+ut-x)}{4\sqrt{\pi Dt}}\left(-\frac{(x+ut-x')^2}{4Dt}\right)dx' \qquad (2.33)$$

Since the domain is infinite in both directions, the initial condition is:

$$f(x') = \frac{1}{2}erfc\left(\frac{|x'|-ut_j}{2\sqrt{Dt_j}}\right) - \frac{1}{2}\exp\left(\frac{u|x'|}{D}\right)erfc\left(\frac{|x'|+ut_j}{2\sqrt{Dt_j}}\right)$$
$$\left[1+\frac{u(|x'|+ut_j)}{D}\right] + \frac{u\sqrt{t_j}}{\sqrt{\pi D}}\exp\left(-\frac{(|x'|-ut_j)^2}{4Dt_j}\right) \qquad (2.34)$$

The three parameters affecting the return profiles are u, D and t_j. It is convenient to express the solutions in terms of dimensionless variables. The Green's function solution in dimensionless variables is:

$$\begin{aligned} C(x_D, t_{Dp}) &= \int_0^\infty f(x'_D)\frac{1}{2}\left\{\frac{1}{\sqrt{\pi t_D t_{Dp}}}\exp\left(-\frac{(x_D - x'_D + t_{Dp})^2}{4t_D t_{Dp}}\right)\right. \\ &\quad + \frac{1}{\sqrt{\pi t_D t_{Dp}}}\exp\left(-\frac{x_D}{t_D}\right)\exp\left(-\frac{(x_D + x'_D - t_{Dp})^2}{4t_D t_{Dp}}\right) \\ &\quad \left. - \frac{1}{t_D}\exp\left(\frac{x'_D}{t_D}\right) erfc\left(\frac{x_D + x'_D + t_{Dp}}{2\sqrt{t_D t_{Dp}}}\right)\right\} dx'_D \end{aligned} \tag{2.35}$$

$$\begin{aligned} f(x'_D) &= \frac{1}{2}erfc\left(\frac{x'_D - 1}{2\sqrt{t_D}}\right) - \frac{1}{2}\exp\left(\frac{x'_D}{t_D}\right) erfc\left(\frac{x'_D + 1}{2\sqrt{t_D}}\right) \\ &\quad \left[1 + \frac{(x'_D + 1)}{t_D}\right] + \frac{1}{\sqrt{\pi t_D}}\exp\left(-\frac{(x'_D - 1)^2}{4t_D}\right) \end{aligned} \tag{2.36}$$

where:

$$t_D = \frac{D}{u^2 t_j} \tag{2.37}$$

$$x_D = \frac{x}{u t_j} \tag{2.38}$$

$$x'_D = \frac{x'}{u t_j} \tag{2.39}$$

$$t_{Dp} = \frac{t}{t_j} \tag{2.40}$$

In a unidirectional flow, the parameter of the system is usually chosen to be the Peclet number, P_e, which is the ratio of the characteristic time for dispersion, $\frac{L^2}{D}$, to that of convection, L/u. For the injection-backflow, the parameter t_D is the ratio of the characteristic length (dispersivity) $\frac{D}{u}$, to the convective transport length ut_j, during the injection period. The parameter t_D is an inverse Peclet number in which

the distance travelled by the convective front during the injection period is used to set the length scale in the Peclet number.

Similarly the flux concentration solution in dimensionless variables is:

$$C(x_D, t_{Dp}) = \int_{-\infty}^{\infty} f(x'_D) \frac{x'_D + t_{Dp} - x_D}{4\sqrt{\pi t_D t_{Dp}^3}} \exp\left(-\frac{(x_D + t_{Dp} - x'_D)^2}{4 t_D t_{Dp}}\right) dx'_D \quad (2.41)$$

$$f(x'_D) = \frac{1}{2} erfc\left(\frac{|x'_D| - 1}{2\sqrt{t_D}}\right) - \frac{1}{2} \exp\left(\frac{|x'_D|}{t_D}\right) erfc\left(\frac{|x'_D| + 1}{2\sqrt{t_D}}\right) \left[1 + \frac{(|x'_D| + 1)}{t_D}\right] + \frac{1}{\sqrt{\pi t_D}} \exp\left(-\frac{(|x'_D| - 1)^2}{4 t_D}\right) \quad (2.42)$$

Tracer return profiles may be studied by varying the value of the only parameter, t_D.

Fig. **2.3** shows that for small values of t_D, which is equivalent to high P_e in solutions for unidirectional flow, zero gradient and infinite medium flux solutions yield identical results. This is due to the small value of the dispersion coefficient which makes the flow approach pure convective flow. Tracer return profile of pure convective flow is distinguished by a sudden drop to zero in the concentration value when $t_{Dp} = 1$.

As for the intermediate values of t_D, both methods produce almost identical numerical results despite the fact that tracer return profiles indicate a transition region. As the value of t_D becomes larger, (see Fig. *2.4* and 2.5), the two tracer return profiles separate. Experimental values of t_D are usually much less than *0.4.*

For large values of P_e (for small values of t_D for injection-backflow tracer tests), the solutions for different injection and detection methods yield similar tracer return profiles. These two solutions, however, produce similar profiles for a larger range of t_D, since imposing a zero gradient at the outlet virtually converts the resident concentration to the flux concentration.

The backflow period solutions in terms of C_R and C_F are tabulated later in Section *3.3.* Fig. *2.6* shows that among the solutions corresponding to different

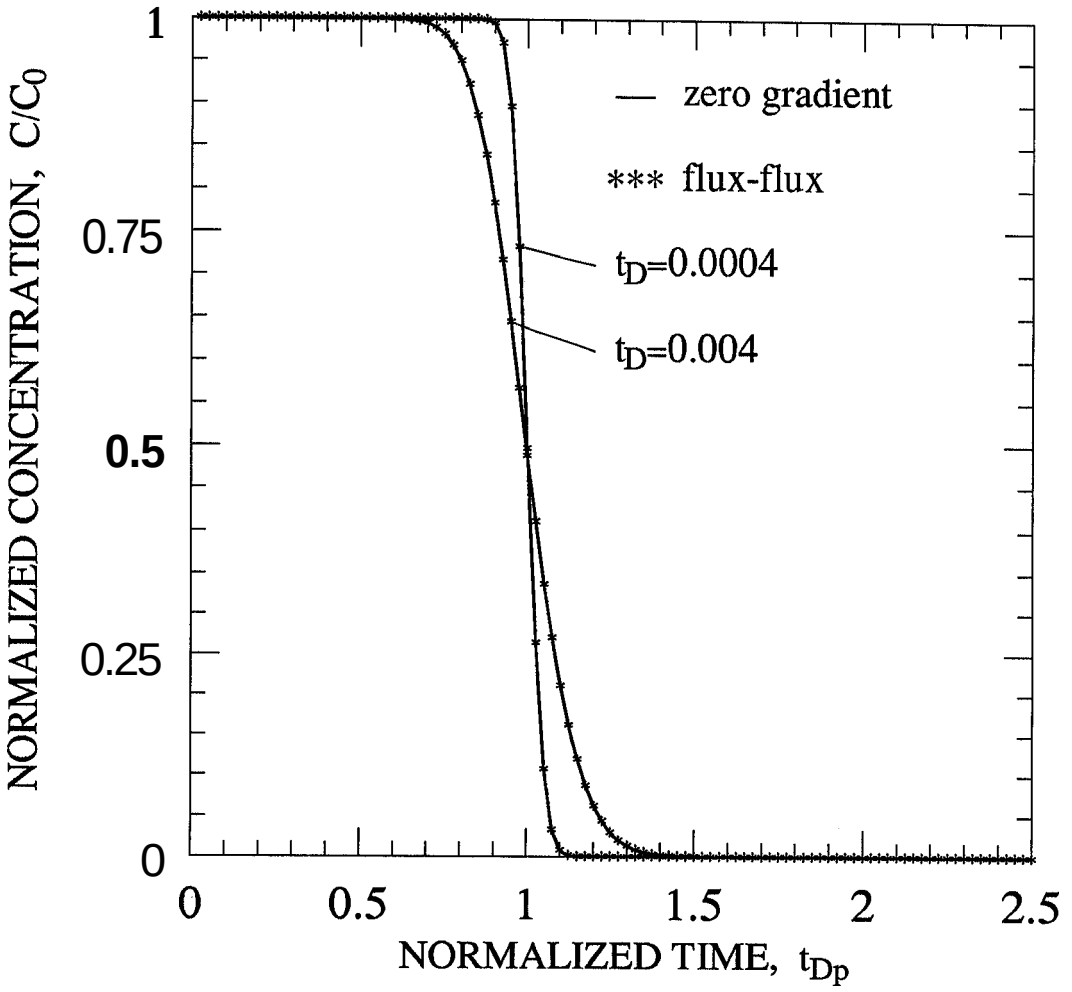

Figure **2.3:** Zero Gradient Solution and Flux-Flux Solution for Small t_Ds

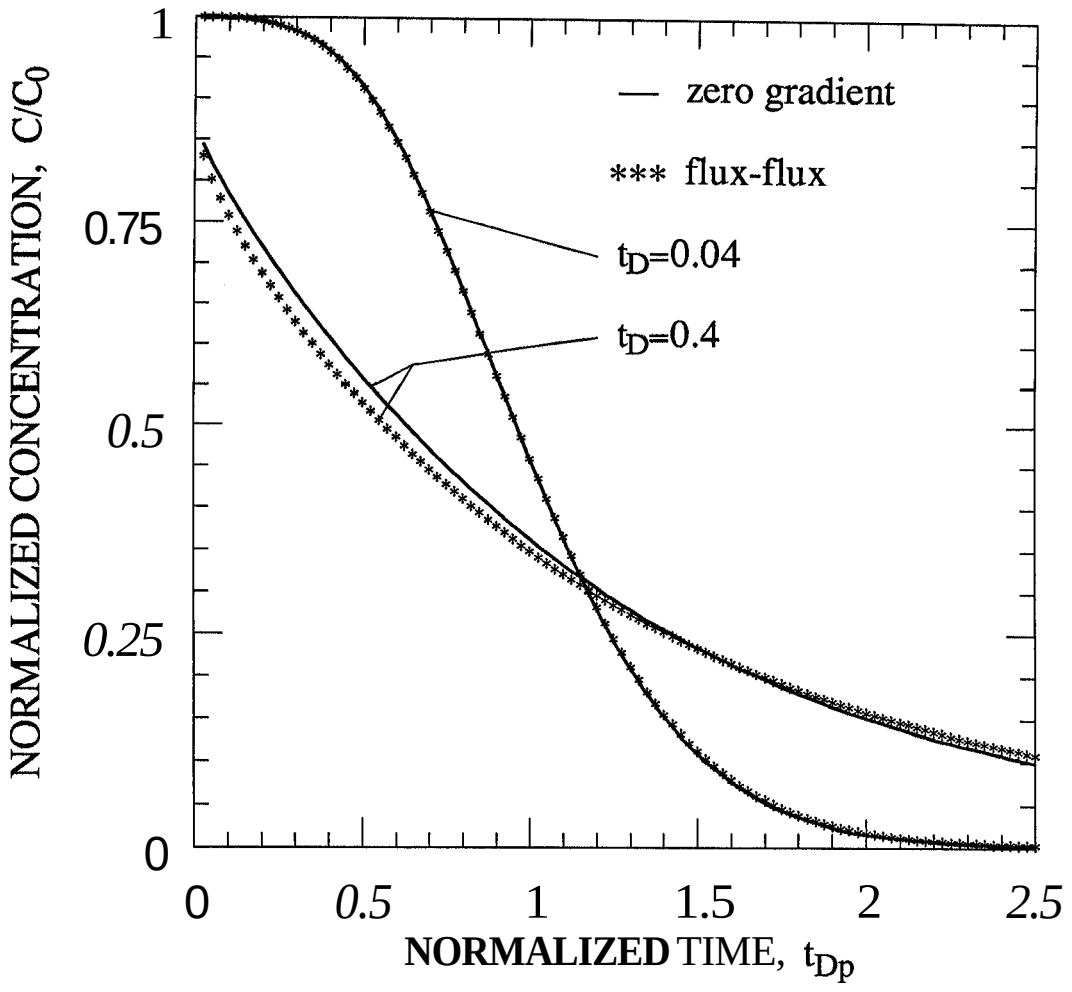

Figure 2.4: Zero Gradient Solution and Flux-Flux Solution for Intermediate t_Ds

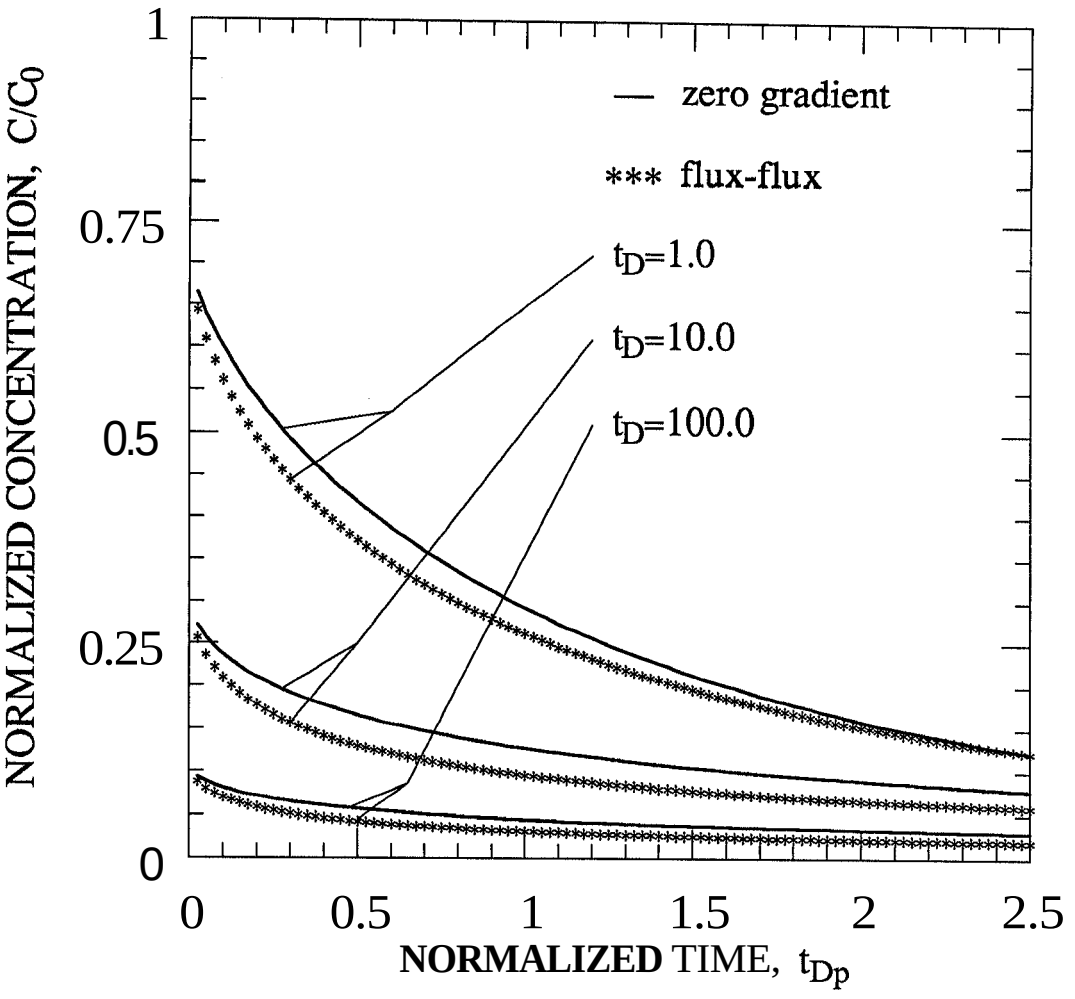

Figure **2.5:** Zero Gradient Solution and Flux-Flux Solution for Large t_Ds

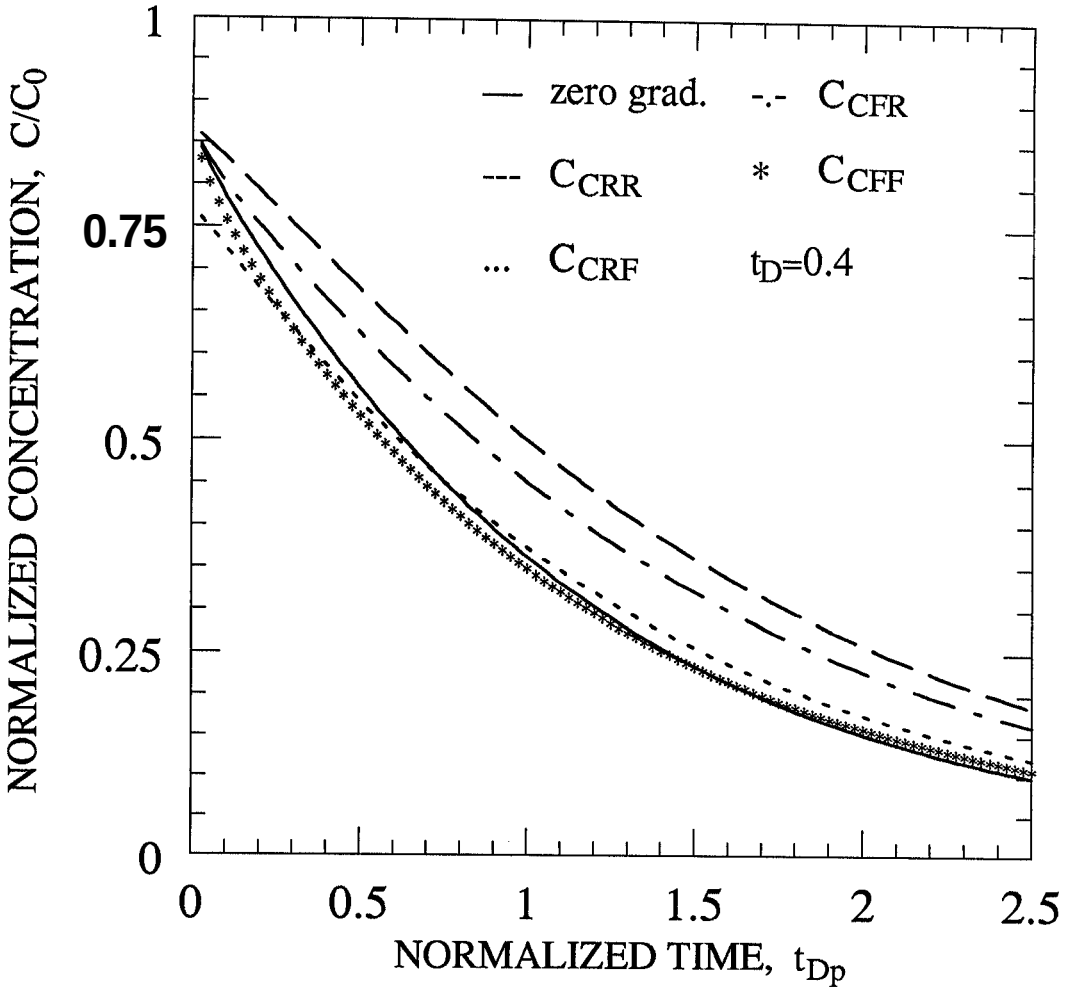

Figure 2.6: Zero Gradient Solution and Infinite Medium Solutions for an intermediate t_D

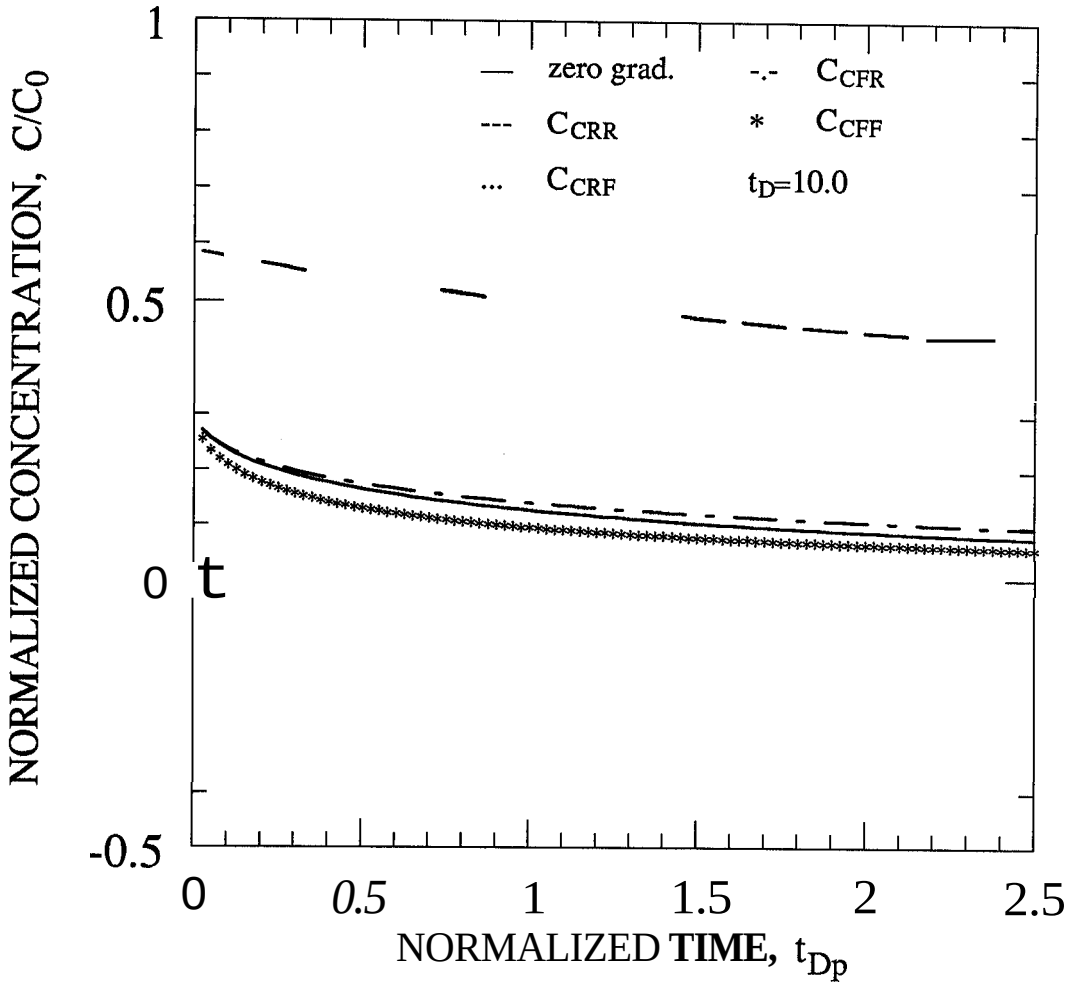

Figure 2.7: Zero Gradient Solution and Infinite Medium Solutions for a Large t_D

injection and detection modes, the zero gradient solution is the closest to the C_{CFF} solution. Since the parameter t_D is high differences between solutions are significant.

Fig. 2.7 shows that the difference between C_{CRR} and C_{CRF} solutions is large compared to the difference between C_{CFR} and C_{CFF} solutions. Also, C_{CRF} yields negative concentration values because it predicts that the total tracer flux is in the direction opposite to the flow. This is a result of the imposed initial condition which provides an infinite amount of tracer supply in the region $x \leq 0$. Thus a large negative gradient is generated in the system, which causes the dispersive flux to dominate the convective flux.

The difference between C_{CFR} and C_{CFF} profiles is small because the initial condition imposed during the backflow period does not allow material to be introduced into or removed from the system. Therefore, initial concentration gradients are quickly smoothed, and this decreases the dispersive flux. As a result, difference between C_{CFR} and C_{CFF} becomes smaller. The initially finite amount of the tracer which is symmetrically distributed about the origin seems to prevent the negative flux. This may be concluded from the fact that while C_{CRF} yields negative values, C_{IRF} given by:

$$\frac{V}{m}C_{IRF} = \frac{3 + t_{Dp} - x_D}{4\sqrt{\pi t_D (1 + t_{Dp})^3}} \exp\left(-\frac{(x_D - 1 + t_{Dp})^2}{4t_D(1 + t_{Dp})}\right) \tag{2.43}$$

does not yield negative values at $x_D = 0$. Eq. *2.43* gives the C_{IRF} solution normalized by the concentration that results if all the injected fluid were to be found only in the total volume of injected fluid.

In experiments, the flux concentration solution given by Eq. *2.41* is preferred on physical grounds and because of its simple form. A partial differential equation(PDE) is always formulated on an open, connected set called a domain Ω. An open set is chosen to avoid discussing the PDE on boundaries. Therefore, the general solution of PDE does not include boundary values. Boundary values are specified and related to interior values requiring the solution be continuous in the closed region composed of the domain and its boundary $\overline{\Omega} = \Omega + \partial\Omega$. Requring continuity of the solution on $\overline{\Omega}$ eliminates supurious solutions[81]. Therefore, the

outlet boundary condition must be known and specified in the case of finite system approach. For any system, if the solution is desired in terms of C_R, any of the following quantities must be specified on each boundary:

$$C_R, \quad \frac{\partial C_R}{\partial x}, \quad C_R - D\frac{\partial C_R}{\partial x}$$

Alternatively, if the solution is desired in terms of C_F, any of the following quantities must be specified on each boundary:

$$C_F, \quad \frac{\partial C_F}{\partial x}, \quad C_F - D\frac{\partial C_F}{\partial x}$$

A zero gradient in the resident concentration implies $C_F = C_R$, but a zero gradient in flux concentration does not[6]. Also, both resident and flux concentration gradients become zero only in the case of D = 0.

For a composite system, the flux must be continuous at the interface. The continuity of the dependent variable(concentration) at the interface, on the other hand, has been proven only for the case of continuous properties across the interface. It has been assumed that properties change rapidly but continuously across the interface[81]. For discontinuous properties there is no proof of neither continuity nor discontinuity of the dependent variable. However, Parker and van Genuchten[62] reasoned that discontinuous properties must yield a discontinuity in the dependent variable.

Eq. 2.22 states the continuity of fluxes at outlet boundary(interface). Assume the CD model is an exact formulation of reality and properties are continuous across boundaries. Then,

$$C_R]_{x=L^-} = C_R]_{x=L^+} \tag{2.44}$$

must hold at the interface because of the continuity of properties. If the resident concentration gradient is zero in the outer section:

$$\left.\frac{\partial C_R}{\partial x}\right]_{L^+} = 0 \tag{2.45}$$

Substituting Eq. 2.44 and Eq. 2.45 into Eq. 2.22 results in:

$$\frac{\partial C_R}{\partial x}\Big]_{L^-} = 0 \tag{2.46}$$

However, the CD model is a macroscopic scale approximation of reality. Reducing the boundary region within which properties change from those of porous medium to bulk solution to a surface yields discontinuities in properties. Imposing discontinuities in properties is likely to cause a discontinuity in the dependent variable of the system. Therefore, a zero gradient boundary condition is questionable.

Dispersive flux is an approximation of the transport due to variations of microscopic velocities with respect to the average macroscopic velocity. These variations in microscopic velocities still exist at the outlet, therefore, dispersive flux must not disappear. The infinite medium flux-flux solution C_{FF} includes dispersive flux at the outlet.

In the infinite medium approach, however, concentrations in the extended region beyond the outlet affect concentrations inside the system. This effect, is part of a fundamental problem in the formulation of tracer dispersion with the CD model[25]. In tracer experiments, since no backward mixing occur due to the velocity variations, mixing is only in the direction of convection[25]. Yet, this forward mixing is represented by the CD model which includes both forward and backward mixing. Therefore, if the CD model is satisfactory within the system, the infinite medium approach at the outlet is consistent with the assumptions of modelling. This reasoning, nevertheless, is not a proof of the appropriateness of infinite medium approach.

In conclusion, there is no proof supporting any of the two approaches for real systems. However, infinite medium approach makes the most sense on physical grounds, since there are some experimental data supporting it[10,26,61]. Furthermore, the infinite medium flux-flux solution C_{FF} is simpler than the zero gradient solution. Therefore, we prefer C_{FF} over the zero gradient solution. We turn now to interpretation of experimental results.

Chapter 3

INTERPRETATION OF TRACER RETURN PROFILES

Development of a method for forecasting the thermal breakthrough time during reinjection must be based on both tracer and thermal data. In this chapter, interpretation of interwell tracer tests with and without recirculation, injection-backflow tracer tests and thermal injection-backflow tests is considered. A new method of estimating the thermal breakthrough time is presented.

3.1 INTERWELL TRACER TESTS-NO RECIRCULATION

In an interwell tracer test without recirculation, the tracer is introduced into the system at the injection well and observed at the production well(s). The tracer can be transported either by a natural gradient of the flow system, or by a gradient caused by injection and production. The main purpose of interwell tracer tests in geothermal reservoirs is to determine the degree of connectivity between the injection well and the producers. A connectivity map of the reservoir permits selection of the appropriate locations for reinjection wells. Even though a qualitative analysis of tracer return profiles may be used to compare the flow paths leading to different

producers, to design a reinjection scheme, values of system's parameters must be estimated or measured.

3.1.1 The Analysis Technique

From a quantitative analysis of tracer return profiles, parameters of the system influencing both tracer and thermal transients can be estimated. An important parameter of flow is the mean arrival time (transit time) of the water:

$$t_w = \frac{L}{v} \tag{3.1}$$

If the system has a constant volume accessible to the tracer, such as within parallel fractures, then a mean transit time of the tracer can be defined as[53]:

$$t_{tr} = \frac{\int_0^\infty tC(x,t)dt}{\int_0^\infty C(x,t)dt} \tag{3.2}$$

If there is a porous matrix adjacent to the fracture, then the degree of fracture-matrix interaction is characterized by the parameter, λ, defined by Eq. **2.6.** Finally the dispersion coefficient, D, is the measure of the spreading of the tracer beyond the region of convective transport. The model response to both parameters λ and D is dependent on the fracture aperture, b, which is the most important parameter controlling propagation of the thermal front during reinjection.

The parameters of the system are estimated by a non-linear regression method. We have used a multiple parameter nonlinear regression program, VARPRO, developed by Stanford's Computer Science Department to match tracer return profiles to analytical solutions. To select the best of the three models representing the system, we applied three criteria which are often used in model evaluations[78]. First, the model-data match should have a small residual of sum of squares. Second, the model should capture distinctive features of data profiles, such as breakthrough time, peak arrival time and total tracer recovery. Finally, values of the field parameters recovered through curve fitting must be physically possible, and consistent with the basic assumptions of the model.

One of the most sought parameters is the fracture aperture, and it can be estimated by two methods. If the condition of the Taylor dispersion theory[85], namely:

$$\frac{L}{u} > \frac{L_t}{u} \gg \frac{0.5\,b^2}{D_m} \tag{3.3}$$

is satisfied, then an expression for the dispersion coefficient is given by [39]:

$$D = \frac{2}{105}\frac{b^2u^2}{D_m} \tag{3.4}$$

Rearranging Eq. 3.3:

$$1 > \frac{L_t}{L} \gg \frac{0.5\,b^2u}{D_mL} \equiv \frac{0.5\,b^2u^2}{D_m}\frac{1}{uL} \tag{3.5}$$

Substituting Eq. 3.4 into Eq. 3.5 results in:

$$\frac{4}{105}\frac{L_t}{L} \gg \frac{1}{P_e} \tag{3.6}$$

If L is twice the length of L_t, and a ten to one ratio is good for assuming a quantity is much greater than another, then the Peclet number is at least:

$$P_e \simeq 500 \tag{3.7}$$

In such a case, the fracture aperture may be estimated as:

$$b = 0.067345\sqrt{\frac{t_w}{P_e}}\ m \tag{3.8}$$

Using Eq. 2.6, the fracture aperture may also be estimated as:

$$b = \frac{2.934\,10^{-3}\,\phi}{\lambda}\ m \tag{3.9}$$

for the MD and AD models.

Since close initial estimates of parameters speeds convergence, some characteristics of the tracer return profiles may be used to provide good initial estimates. In fact, Bullivant[14] showed that the parameters of the solutions to the CD model can be expressed by water transit time t_w and peak arrival time t_p and to the MD

model by peak arrival time t_p and tracer breakthrough time t_b. The two parameters t_p and t_b can easily be determined from tracer return profiles.

In both laboratory experiments and field tests, both the injection and detection in the flux concentration is the most commonly employed mode. The C_{IFF} solutions may be used to illustrate the method of determining first estimates of regression parameters.

For an instantaneous injection in flux and detection in the flux concentration, the solutions of the three models with pertinent boundary conditions are given in Table 3.1. For the **AD** model a solution in the integral form is available[53,83], but we preferred to use a numerical Laplace inversion technique to evaluate the solution, because we had a computer program[92] based on an **accurate** inversion algorithm[23,29]. The theoretical peak arrival time can be determined from:

$$\left[\frac{\partial C(x,t)}{\partial t}\right]_{t=t_p} = 0 \tag{3.10}$$

Substituting the solution to the CD model into Eq. 3.10 and solving for t_p:

$$t_p = \sqrt{\frac{1}{\alpha_2^2} + 9\frac{\alpha_1^2}{\alpha_2^2}} - \frac{3\alpha_1}{\alpha_2} \tag{3.11}$$

The parameters α_1 and α_2 are defined in Table *3.1.* From Eq. **3.11,** t_w is always greater than t_p. This is because, due to the dispersion, the tracer moves faster than the fluid. Therefore, following Bullivant's[14] suggestion, we may assign an initial estimate value to t_w as:

$$t_w = 2t_p - t_b \tag{3.12}$$

Then the initial estimate of the Peclet number can be found from Eq. *3.11.* Zuber[94] pointed out that the transit time of the tracer for the CD model is the same as t_w only for the C_{FF} solution.

Similarly, an expression for t_p of the MD model is [14]:

$$t_p = \frac{2}{3}\alpha_1^2\alpha_2^2 + \alpha_2 \tag{3.13}$$

M	IC & BC	Parameters	
⊲D	$C(x,0)=0$ $C(0,t)=\frac{m}{Q}\delta(t)$ $\lim_{x\to\infty} C(x,t)=0$	$\beta=\frac{m}{Q}$ $\alpha_1=\frac{1}{P_e}=\frac{D}{uL}$ $\alpha_2=\frac{1}{t_w}=\frac{u}{L}$	$C=\frac{\beta}{\sqrt{4\pi\alpha_1\alpha_2 t^3}}\exp\left(-(1-\alpha_2 t)^2/(4\alpha_1\alpha_2 t)\right)$
MD	$C(x,o)=C_m(x,y,o)=0$ $C(0,t)=\frac{m}{Q}\delta(t)$ $C(x,t)=C_m(x,o,t)$ $\lim_{y\to\infty} C_m(x,y,t)=0$	$\beta=\frac{m}{Q}$ $\alpha_1=\lambda=\frac{\phi\sqrt{D_a}}{b}$ $\alpha_2=t_w=\frac{L}{u}$	$C=\frac{\beta H(t-\alpha_2)\alpha_1\alpha_2}{\sqrt{\pi(t-\alpha_2)^3}}\exp\left(-(\alpha_1\alpha_2)^2/(t-\alpha_2)\right)$
AD	$C(x,o)=C_m(x,y,o)=0$ $C(0,t)=\frac{m}{Q}\delta(t)$ $\lim_{x\to\infty} C(x,t)=0$ $C(x,t)=C_m(x,o,t)$ $\lim_{y\to\infty} C_m(x,y,t)=0$	$\beta=\frac{m}{Q}$ $\alpha_1=\frac{1}{P_e}=\frac{D}{uL}$ $\alpha_2=\frac{1}{t_w}=\frac{u}{L}$ $\alpha_3=\lambda=\frac{\phi\sqrt{D_a}}{b}$	$\overline{C}=\beta\exp(1/(2\alpha_1))\exp\left(-\sqrt{1/(4\alpha_1^2)+(s+2\alpha_3\sqrt{s})/(\alpha_1\alpha_2)}\right)$

Table 3.1: Solutions to Models of Non-recirculating Flow

In this case, since there is no dispersion, spreading of the tracer occurs only behind the pure convection region. Therefore, tracer breakthrough time is virtually equal to t_c, and t_p is greater than t_c. Choosing the time of the first detection as the initial estimate of t_c, the initial estimate of the parameter, λ can be calculated.

As for the AD model, initial estimates of the parameters should be based on the shape of the tracer return profile. For instance, a steep slope in the profile after breakthrough and long tailing after the peak is an indication of a dominant matrix diffusion effect. Therefore, t_p should be between t_b and t_p and an initial estimate of λ may be made from Eq. **3.13.** To estimate the Peclet number, a significantly smaller value is selected than the initial estimate of the CD model.

If the return profile varies smoothly between t_b and t_p and does not exhibit a long tail, then we should enter a value close to $2t_p - t_b$ as an initial estimate for t_c. Peclet number may be estimated from Eq **3.11.** The parameter λ is assigned an initial estimate value significantly smaller than the initial estimate for the MD model's same parameter.

3.1.2 Field Examples

We have obtained three data sets from tracer tests conducted in the Wairakei geothermal field[54]. In order to use the appropriate theoretical solution to interpret tracer return profiles, it is necessary to determine which of the two concentration variables correspond with the injection and detection modes. The tracer was introduced into the system at the wellhead of the injection well and allowed to be transported by the gradient created by the production wells [14]. The concentrations in samples taken from the outflowing fluid were measured to determine tracer return profiles. In this type of tracer test, the injection and the detection modes are both in the flux concentration variable. Therefore, the solutions in Table **3.1** can be used to interpret tracer return profiles.

The ability of each of the model solutions to match the field data is shown in Figs. **3.1** through **3.5.** For all the profiles analyzed, the residual error after fitting is of the same order for all three models. However, the models differed in matching the

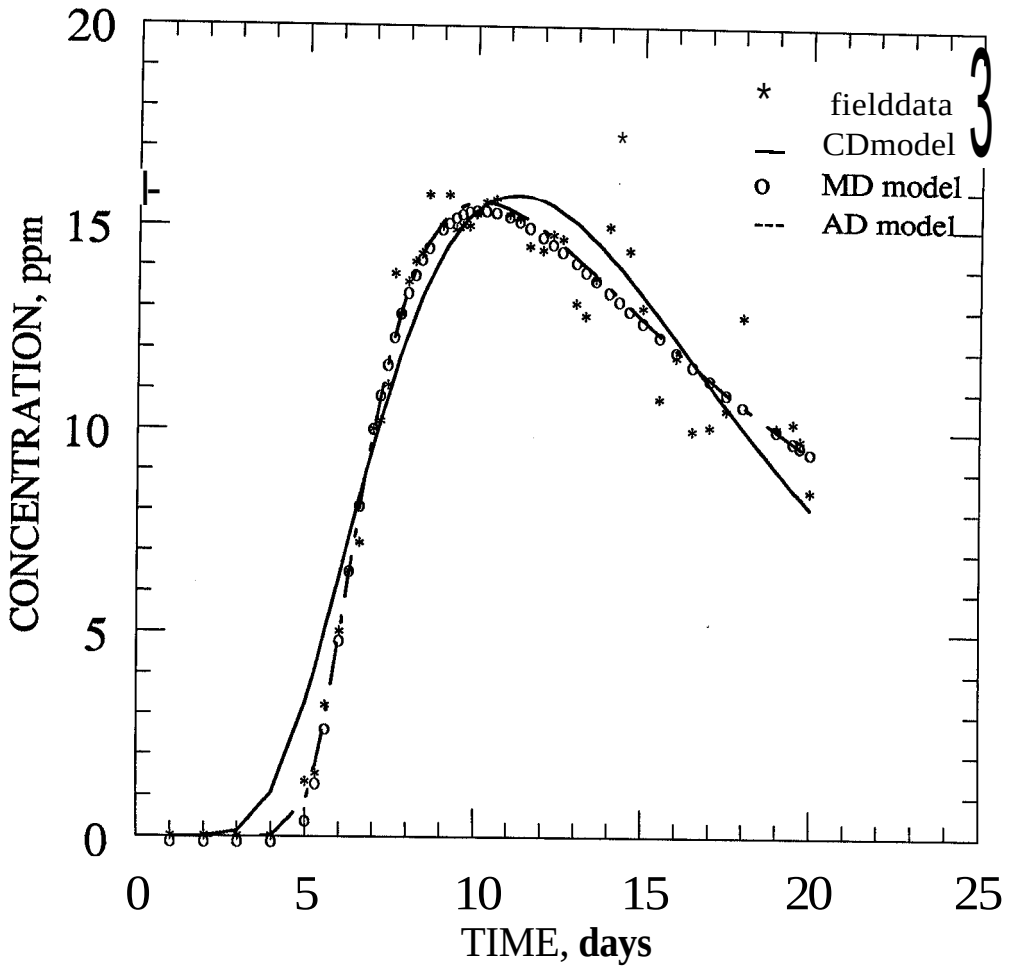

Figure 3.1: Model Fits to the Profile at WK108

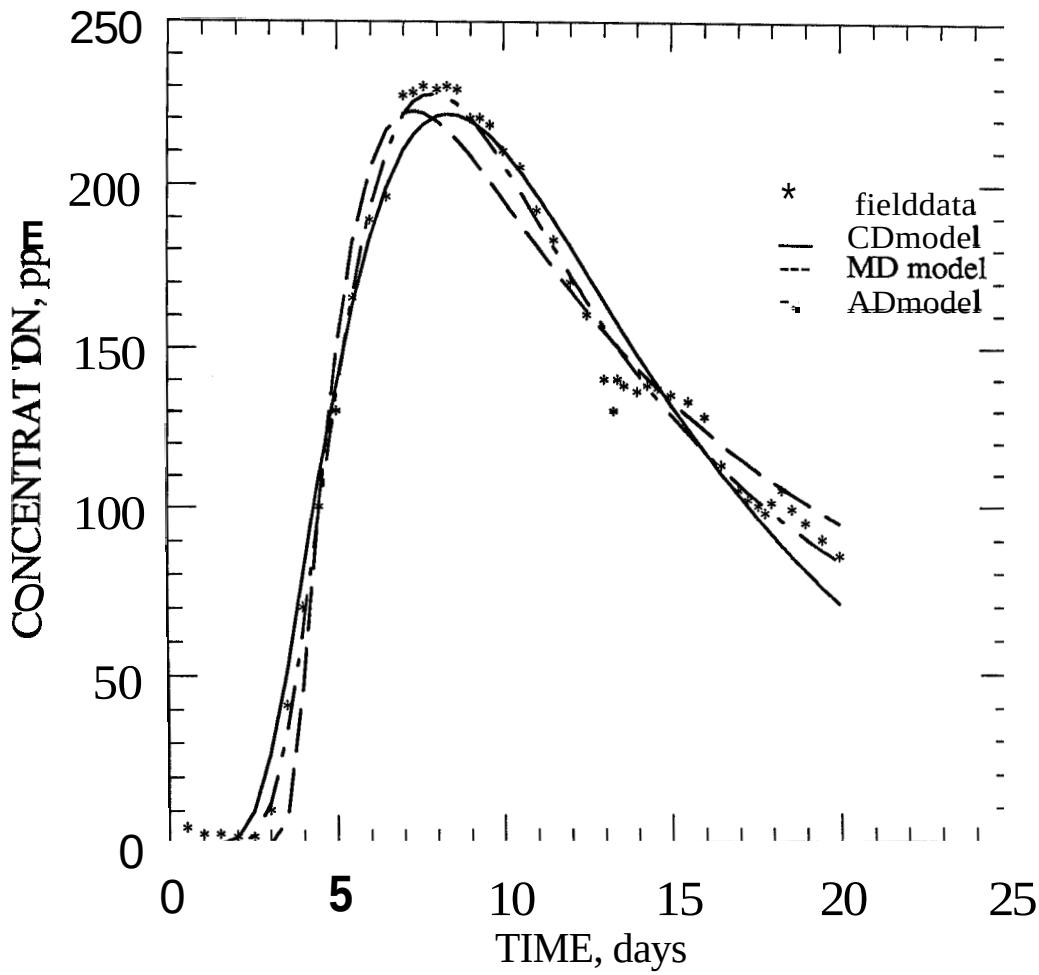

Figure 3.2: Model Fits to the Profile at WK116

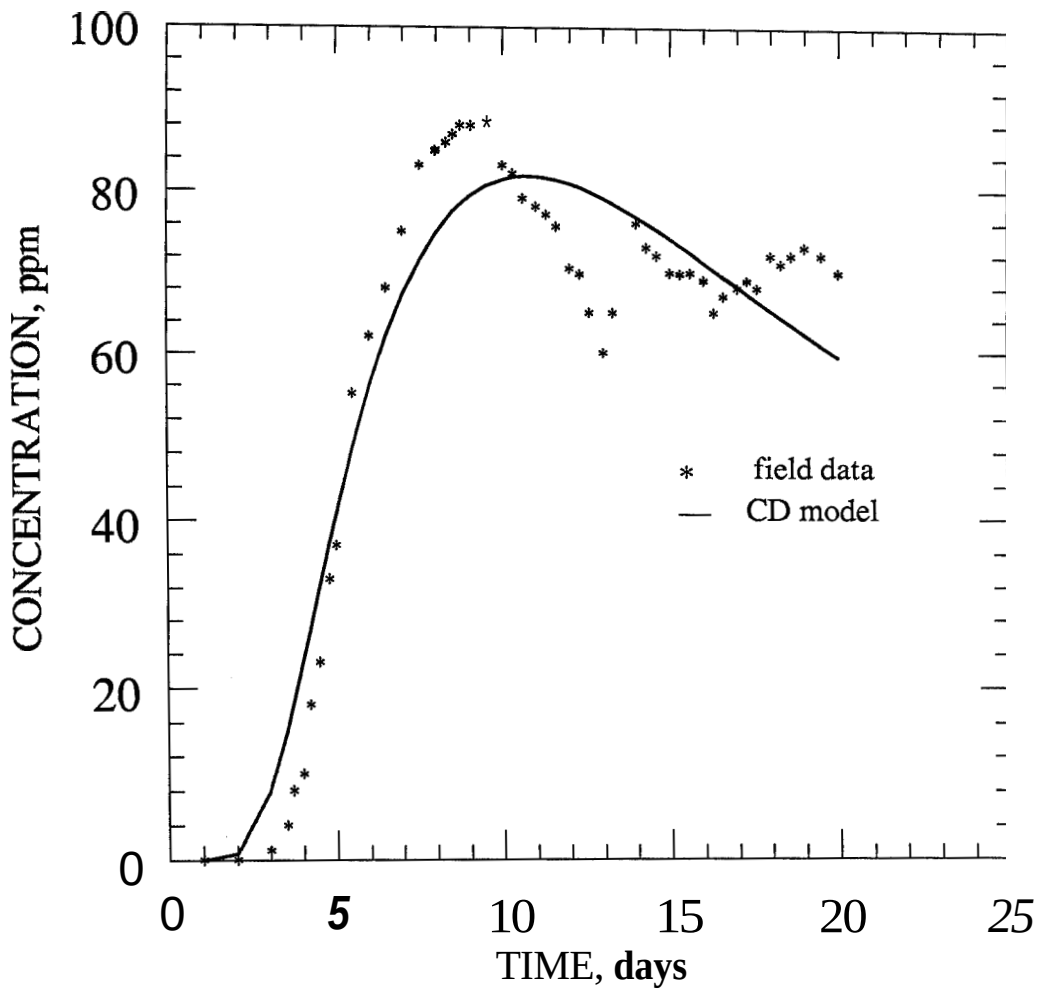

Figure 3.3: 1-Path CD Model's Fit to the Profile at WK76

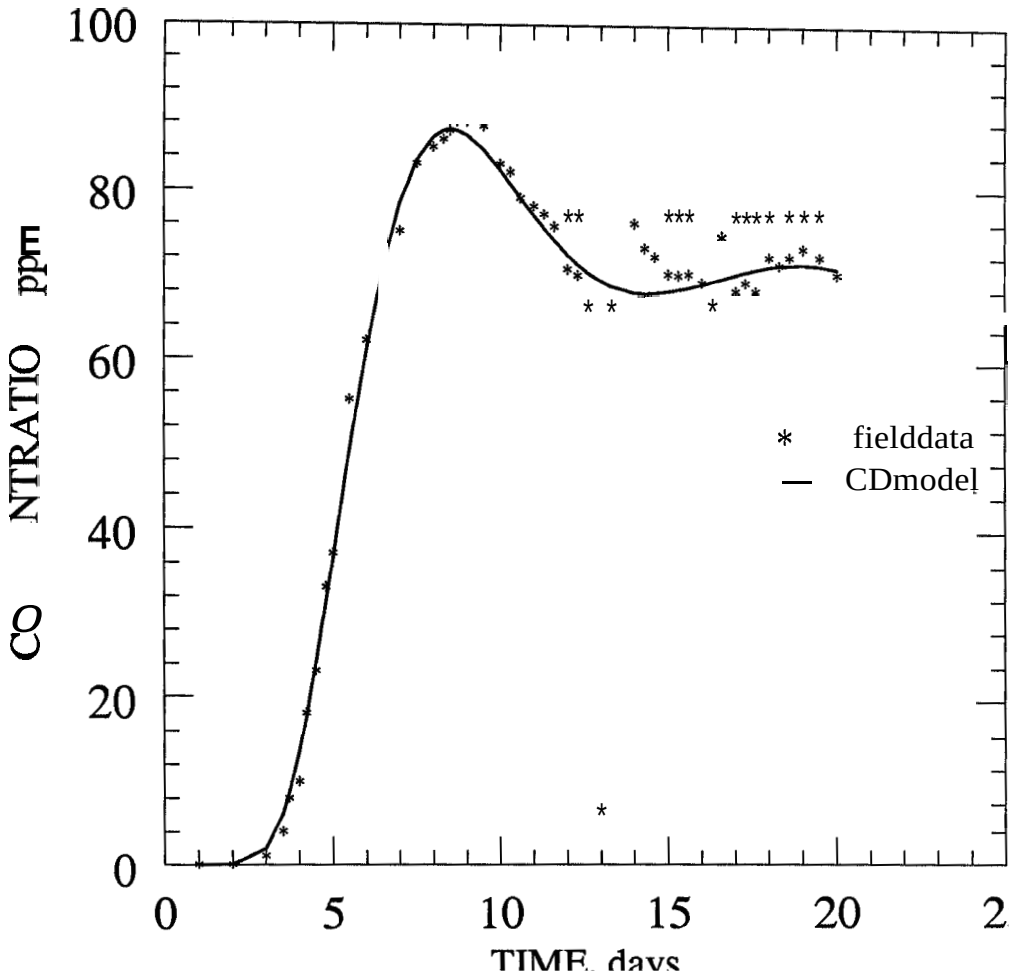

Figure **3.4:** 2-Path CD Model's Fit to the Profile at WK76

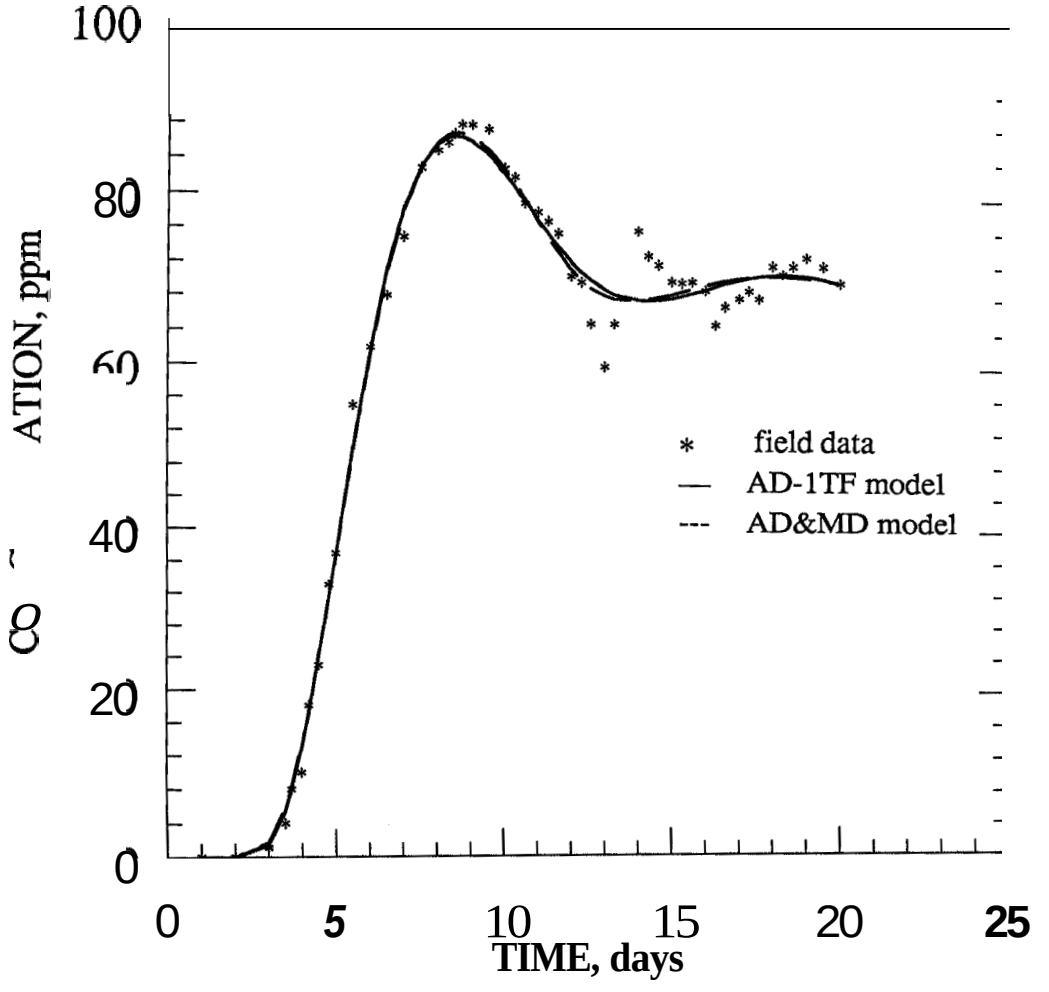

Figure 3.5: 2-Path AD and AD-MD Model's Fits to the Profile at WK76

Well WK108			
	CD	AD	MD
m/Q	0.2465 103	0.6327 103	0.6525 103
$1/P_e$	0.12832	0.00349	-
$1/t_w$	0.06123	0.2454	0.2716
λ	-	0.7457	0.8471

Well Wk116			
	CD	AD	MD
m/Q	$0.3089\ 10^4$	$0.5564\ 10^4$	$0.6929\ 10^4$
$1/P_e$	0.1749	0.0468	-
$1/t_w$	0.0723	0.1719	0.4005
λ	-	0.3495	1.0754

Well WK76			
	CD	MD	AD
m/Q	$0.2474\ 10^4$	no match	no match
$1/P_e$	0.4245	-	-
$1/t_w$	0.0322	-	-
λ	-	-	-

Table **3.2:** Regression Parameters

breakthrough and peak arrival times. Also, the values of the parameters determined differed greatly. Table **3.2** shows the estimated regression parameters for all three models.

Assuming the fracture length is equal to the distance between the injector and the producer, we obtained the flow speeds and the related dispersion coefficients, and estimated the corresponding fracture apertures (see Table **3.3).** For CD and AD models, the estimated fracture apertures based on the Taylor dispersion theory are quite large and do not satisfy **Eq. 3.3.** However, for MD and AD, the apertures estimated by using **Eq. 3.9** are consistent with the observations since a fast flow and a strong matrix diffusion are likely to occur in a narrow fracture.

Fig. 3.1 shows the return profile at well WK108 and the optimum fits of the models. In the return profile, considering the distance, **230** m, between the injection well and well WK108, we see that the breakthrough and peak arrival times are very small, indicating a fast **flow** path. The concentrations of the tail section are very

Well	injector to producer distance m	MODEL								
		CD			AD				MD	
		u m/day	D m^2/day	$b_{Eq.3.8}$ mm	u m/day	D m^2/day	$b_{Eq.3.8}$ mm	$b_{Eq.3.9}$ mm	u m/day	$b_{Eq.3.9}$ mm
WK108	230	14.1	414.5	98	45.5	0.8	8	0.19	62.5	0.17
WK76	145	4.7	287.0	105	–	–	–	–	–	–
WK116	500	36.2	3161.0	245	85.9	1991	34	0.42	58.2	0.14

Table **3.3:** Estimates of the Flow Parameters From Regression Results

close to the peak concentration which indicates a strong matrix diffusion effect. The dominant matrix diffusion effect becomes obvious, since the matrix diffusion model captures the breakthrough and the peak arrival times as accurately as does the Avdonin model.

Fig. **3.2** shows the return profile at the well WK116 and the effectiveness of the models in matching the observed data. The profile has the characteristics of a fast **flow and** strong matrix diffusion, however, in this case they are less pronounced compared to the characteristics of WK108. While CD and MD models have slight differences with the observed values, the AD model shows an excellent agreement with the data. The values of the parameter estimates from the regression, however, differed significantly. For example, Table **3.2** shows the values of t_w, a common parameter to all of the three models, is only 2.5 days for the MD model, **5.8** days for the AD model and **13.8** days for the CD model. The fracture apertures cannot be estimated by using Eq. **3.8** because Eq. **3.3** is not satisfied. The MD model yields a smaller fracture aperture and a higher flow speed than the AD model.

Fig, **3.3** shows the return profile at the well WK76 matched by the CD model. The error of residual to fit was similar in order to the residuals of the earlier matches. The model yielded a relatively small flow velocity and a high dispersion, but the fracture aperture cannot be estimated from Eq. **3.8,** because Eq. **3.3** is not satisfied. We could not match MD and AD models to this set of data. During the regression, sometimes illconditioning occurred which may be caused by either an unfortunate initial guess or a poor choice of the model. In other cases, the absolute and relative tolerance for the norm of the projection of the residual onto the range of the jacobian

of the variable projection functional is not satisfied.

The existence of the double peak suggests that the injection and the observation wells may be connected by at least two paths. The two path solution to the CD model gave a much better match, Fig. **3.4,** but neither of the two path solutions to MD and AD models matched the profile.

During the regression for a single path solution to the AD model, the Peclet number consistently diverged towards infinity. A two path solution was also unsuccessful, but this time either the Peclet number for the second path diverged to infinity or ill-conditioning occurred. We concluded that the ill-conditioning occurred because the flow rates of the two paths were almost the same. In this case, in the regression procedure, we need to use one transfer function(1TF) with six variables, three for each path.

As for the divergence of the Peclet number towards infinity for the second path, it could be because dispersion in the second path is negligible. Therefore, we matched the first peak by the AD model. Then the profile for this first path was subtracted from the observed profile and the resultant profile was matched by the MD model. The performances of the one transfer function for the AD model(1TF-AD) and for this combined AD&MD model are shown in Fig. **3.5.**

We also considered the possibility of three paths connecting the injection well and the producing well, since there is a small peak between the two main peaks. However, the data did not match any of the three-path solutions of the models, because error tolerance was not satisfied. Fig. 3.6 shows matching of the first peak with the AD model and the profile resulted from subtracting profile of the first path from the observed profile. The difference profile has the characteristics of a single flow path, an evidence of the failure in matching data with a three-path solution.

In summary, all three models had small residuals satisfying the first criteria of model evaluations. The AD model captured the characteristic features of the return profiles accurately whenever a match was possible, and the MD model was more successful than the CD model in this respect. As for the values of the parameter estimates, Table **3.3** shows that the flow speeds are extremely high compared to those normally reported in the groundwater literature. The estimates of P_e or the

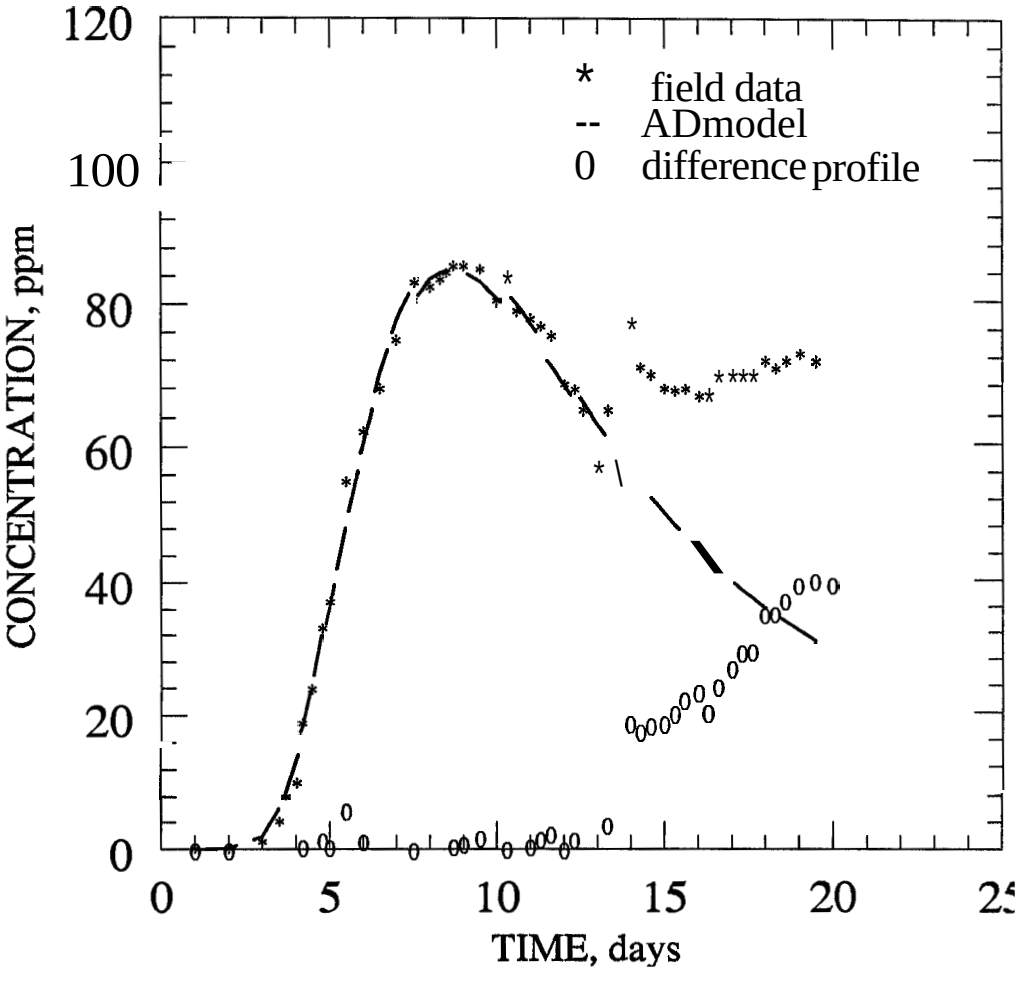

Figure **3.6:** Matching the first peak of WK76 data with the AD model

related estimates of the fracture aperture, b, did not satisfy the Taylor dispersion condition for any of the return profiles. The values of dispersion coefficients are difficult to accept as realistic for the **CD** model. For the **AD** model, the dispersion coefficient estimated for WK116 is similar to the one obtained by the **CD** model. The estimated D value for WK108 is, although less than the estimated **D** value for WK116, still 10 times higher than the largest value reported[69] in the groundwater literature, Even if the fracture is modelled as a porous stream tube so that hydrodynamic dispersion expression[7,15,65] can be used, we obtain dispersivity, D/u, values which are still extremely large compared to the values reported in the review paper by Pickens and Grisak[67].

Therefore, first, the fracture aperture estimations must not be based on Taylor dispersion theory, and second, considering the extremely high dispersion coefficient estimates, caution must be exercised in using the parameter estimates for forecasting the effect of future operations.

3.2 INTERWELL TRACER TESTS WITH RECIRCULATION

In an interwell tracer test with recirculation, the reservoir fluid is withdrawn from a production well and reinjected at an equal rate into the reservoir at the injection well. The procedure continues until the system reaches steady state. Then the tracer is introduced into the flowing stream at the injection well. While the recirculation continues, the concentration history of the fluid samples taken at the production well is analyzed to determine the system's parameters. These techniques of injecting and detecting the tracer correspond to injection and detection in flux concentration modes.

3.2.1 The Analysis Technique

Interwell tracer tests with recirculation are useful to estimate the volume of the fluid recirculating in the system[39]. Another advantage of this type of test is

that it enables larger distances and areas to be investigated[93].

Most of the researchers[36,67,90,94] who studied tracer tests with recirculation assumed an infinite homogeneous isotropic porous medium confined between two parallel horizontal planes. Thus, they were able to treat the flow field generated by an injection-production well pair as the superposition of the flow fields of a line source and a line sink. They divided the flow field between the injector and the producer into crescents and approximated the crescents by columns of finite length. A one-dimensional solution to the CD model was used to calculate the tracer return profile of each crescent. Then the individual return profiles were summed to obtain the composite return profile. The recirculation effect was considered by adding continuous injection solutions to the spike injection solution. The concentrations of the continuously injected fluid were equated to the average concentrations of different segments of the return profile. Only one recirculation was considered. While most of the researchers[36,67,90] used the finite system solution derived by Brenner[9] to model the tracer transport, Zuber[94] reported a work where he and his co-worker used C_{IFF} solution as the theoretical model.

Since a linear geometry is employed, we can use the approach of the previous studies to model the tracer transport in vertical fractures. However, the previously developed methods of analysis for this type test considered only one recirculation and were not able to account for the strong recirculation effects. Therefore the previous methods were applicable only in homogeneous layers with low dispersivity and wells situated at sufficient distances to minimize the recirculation effects. The solutions we have developed, on the other hand, not only specifically include recirculation, but also use the effects of the recirculation to determine the dominant mechanism of tracer spreading along the flow path. Assuming a semi-infinite domain, we developed solutions for the case of an instantaneous injection and detection in flux concentration mode. We preferred the semi-infinite medium flux-flux solution over the finite medium solution because the flux-flux solution represents real systems better than the finite medium solution. Furthermore, the semi-infinite flux-flux and finite medium solutions give numerically identical results over a large range of the values of the parameters, but the latter are more complicated. Table 3.4 shows the

solutions to the three models with the pertinent initial and boundary conditions. We can match these solutions to the field data to estimate the parameters.

3.2.2 Theoretical Return Profiles

The purpose of interwell tests with recirculation is to estimate the total reservoir volume accessible to the tracer as well as the parameters affecting the tracer transport. The total reservoir volume accessible to the tracer consists of the recirculating fluid volume, which corresponds to the fracture volume, and the stationary fluid volume, which corresponds to the matrix pore volume. In general, while the recirculating fluid volume affects the breakthrough time, the stationary fluid volume determines the final level of concentration reached after adequate recirculations.

In the study of tracer return profiles, it is convenient to normalize the concentration by a reference concentration, C_r, the final concentration that would be reached if all the tracer were to mixed only in the recirculating volume. Since the reference concentration C_r is:

$$C_r = \frac{m}{V_r} \tag{3.14}$$

the source strength in the equations of Table **3.4** can be expressed as:

$$\frac{m}{Q} = \frac{m}{V_r}\frac{L}{u} - C_r\frac{L}{u} \tag{3.15}$$

The normalized concentration functions are given in Table **3.5.** In Table **3.5** the CD model is scaled also to the pore volume injection, however, the MD and AD models cannot be scaled to the pore volume injection since the matrix diffusion is time dependent[52]. Therefore, in MD and AD models the influence of time does not disappear upon normalization of time by the mean arrival time of the water, t_w.

In the literature, the reported values for fracture apertures in groundwater aquifers are usually smaller than 0.2 mm. Considering the unusually high flow speeds in some geothermal reservoirs, we can expect fracture sizes to be greater than

Model	IC & BC	Parameters	Solution
CD	$C(x,0) = 0$ $\lim_{x\to\infty} C(x,t) = 0$ $C(0,t) = \frac{m}{Q}\delta(t) + C(L,T)$	$\beta = \frac{m}{Q}$ $\alpha_1 = \frac{1}{P_e} = \frac{D}{uL}$ $\alpha_2 = \frac{1}{t_w} = \frac{u}{L}$	$C = \beta \sum_{n=0}^{\infty} \frac{(n+1)}{2\sqrt{\pi\alpha_1\alpha_2 t^3}} \exp\left(-((n+1)-\alpha_2 t)^2/(4\alpha_1\alpha_2 t)\right)$
MD	$C(x,o) = C_m(x,y,o) = 0$ $C(0,t) = \frac{m}{Q}\delta(t) + C(L,t)$ $C(x,t) = C_m(x,o,t)$ $\lim_{y\to\infty} C_m(x,y,t) \doteq 0$	$\beta = \frac{m}{Q}$ $\alpha_1 = \lambda = \frac{\phi\sqrt{D_a}}{b}$ $\alpha_2 = t_w = \frac{L}{u}$	$C = \beta \sum_{n=0}^{\infty} H(t-(n+1)\alpha_2) \frac{(n+1)\alpha_1\alpha_2}{\sqrt{\pi(t-(n+1)\alpha_2)^3}}$ $\exp\left(-((\neg+1)\alpha_1\alpha_2)^2/(t-(n+1)\alpha_2)\right)$
AD	$C(x,o) = C_m(x,y,o) = 0$ $\lim_{x\to\infty} C(x,t) = 0$ $C(0,t) = \frac{m}{Q}\delta(t) + C(L,t)$ $C(x,t) = C_m(x,o,t)$ $\lim_{y\to\infty} C_m(x,y,t) = 0$	$\beta = \frac{m}{Q}$ $\alpha_1 = \frac{1}{P_e} = \frac{D}{uL}$ $\alpha_2 = \frac{1}{t_w} = \frac{u}{L}$ $\alpha_3 = \lambda = \frac{\phi\sqrt{D_a}}{b}$	$\overline{C} = \beta\left(\exp(-1/(2\alpha_1))\exp\left(\sqrt{1/(4\alpha_1^2) + (s+2\alpha_3\sqrt{s})/(\alpha_1\alpha_2)}\right) - 1\right)^{-1}$

Table 3.4: Solutions to Models of Recirculating Flow

Model	IC & BC	Parameters	Solution
CD	$C(x,0) = 0$ $\lim_{x\to\infty} C(x,t) = 0$ $C(0,t) = \frac{m}{Q}\delta(t) + C(L,T)$	$\alpha_1 = \frac{1}{P_e} = \frac{D}{uL}$ $\alpha_2 = \frac{t}{t_w} = \frac{ut}{L}$	$\frac{C}{C_r} = \sum_{n=0}^{\infty} \frac{(n+1)}{2\sqrt{\pi\alpha_1\alpha_2^3}} \exp\left(-((n+1)-\alpha_2)^2/(4\alpha_1\alpha_2)\right)$
MD	$C(x,o) = C_m(x,y,o) = 0$ $C(0,t) = \frac{m}{Q}\delta(t) + C(L,t)$ $C(x,t) = C_m(x,o,t)$ $\lim_{y\to\infty} C_m(x,y,t) = 0$	$\alpha_1 = \lambda = \frac{\phi\sqrt{D_d}}{b}$ $\alpha_2 = t_w = \frac{L}{u}$	$\frac{C}{C_r} = \alpha_2 \sum_{n=0}^{\infty} H(t-(n+1)\alpha_2) \frac{(n+1)\alpha_1\alpha_2}{\sqrt{\pi(t-(n+1)\alpha_2)^3}}$ $\exp\left(-((n+1)\alpha_1\alpha_2)^2/(t-(n+1)\alpha_2)\right)$
AD	$C(x,o) = C_m(x,y,o) = 0$ $\lim_{x\to\infty} C(x,t) = 0$ $C(0,t) = \frac{m}{Q}\delta(t) + C(L,t)$ $C(x,t) = C_m(x,o,t)$ $\lim_{y\to\infty} C_m(x,y,t) = 0$	$\alpha_1 = \frac{1}{P_e} = \frac{D}{uL}$ $\alpha_2 = \frac{t}{t_w} = \frac{ut}{L}$ $\alpha_3 = \lambda = \frac{\phi\sqrt{D_d}}{b}$	$\frac{C}{C_r} = \frac{1}{\alpha_2}\left(\exp(-1/(2\alpha_1))\exp\left(\sqrt{1/(4\alpha_1^2)+(s+2\alpha_3\sqrt{s})/(\alpha_1\alpha_2)}\right)-1\right)^{-1}$

Table 3.5: Normalized Solutions to Models of Recirculating Flow

0.2 mm. To generate the theoretical return profiles we used λ values corresponding to a range of fracture apertures from 0.14 *mm* ($\lambda = 1$) to 0.23 *mm* ($\lambda = 0.064$). We have assumed an apparent diffusion coefficient of $8.6410^{-6} m^2/day$ ($1.10^{-6} cm^2/sec$) and a porosity of 0.05.

The generated return profiles indicate (see Figs. **3.7** to **3.12)** as many local minima and maxima as the number of recirculations. If we try to determine the times of the local minima and maxima by equating the time derivative to zero, only the first peak time occurs in a linear equation. However, the equation of the time of the first peak allows us to make close initial estimates of the parameters.

Even though it is difficult to solve the theoretical equations for the times of the local minima and maxima, the generated profiles display several distinctive features, which are useful in analyzing field profiles.

The return profiles generated by the CD model in Fig. 3.7 display almost periodic patterns, and the amplitude of the peaks decreases with increasing time. The second peak occurs almost exactly at a time equal to twice the time of the first peak. Also the first local minimum occurs virtually at the midpoint of the first and second peaks. These features can be used to identify the number of recirculations in an experiment and to determine if a recirculation is completed or not. Therefore, in cases where there is not enough data, we can **look** for distinguishing features such as the slope after the first peak. It should be negative until the time is close to $1.5t_p$, and then positive until the time is close to $2t_p$.

Also, in the CD model profiles, the final level concentration should stay constant. Finally in cases of high dispersion, the profiles will reach a plateau earlier than t_c. It is desirable to continue measurements until twice the time of the maximum observed concentration, since it will help determine whether the plateau has been reached or not.

The MD model return profiles shown in Figs. **3.8** and 3.9 also have almost periodic patterns. On the other hand, their features are different from the features of the CD model profiles. First the peaks occurs immediately after t_w, and the section between t_w and t_p are characterized by a steep slope. Second the final level concentration is not constant but decreases with time. This results because

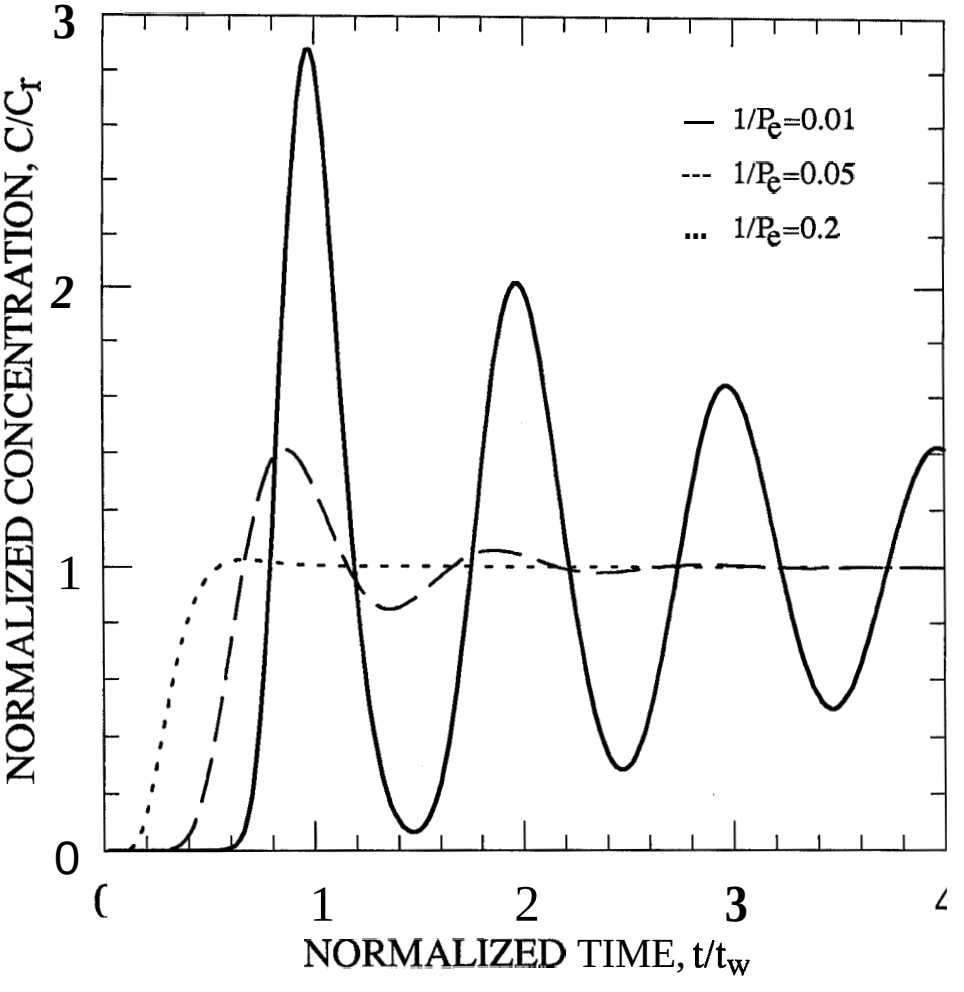

Figure 3.7: Normalized Solutions to CD Model For Recirculating Flow

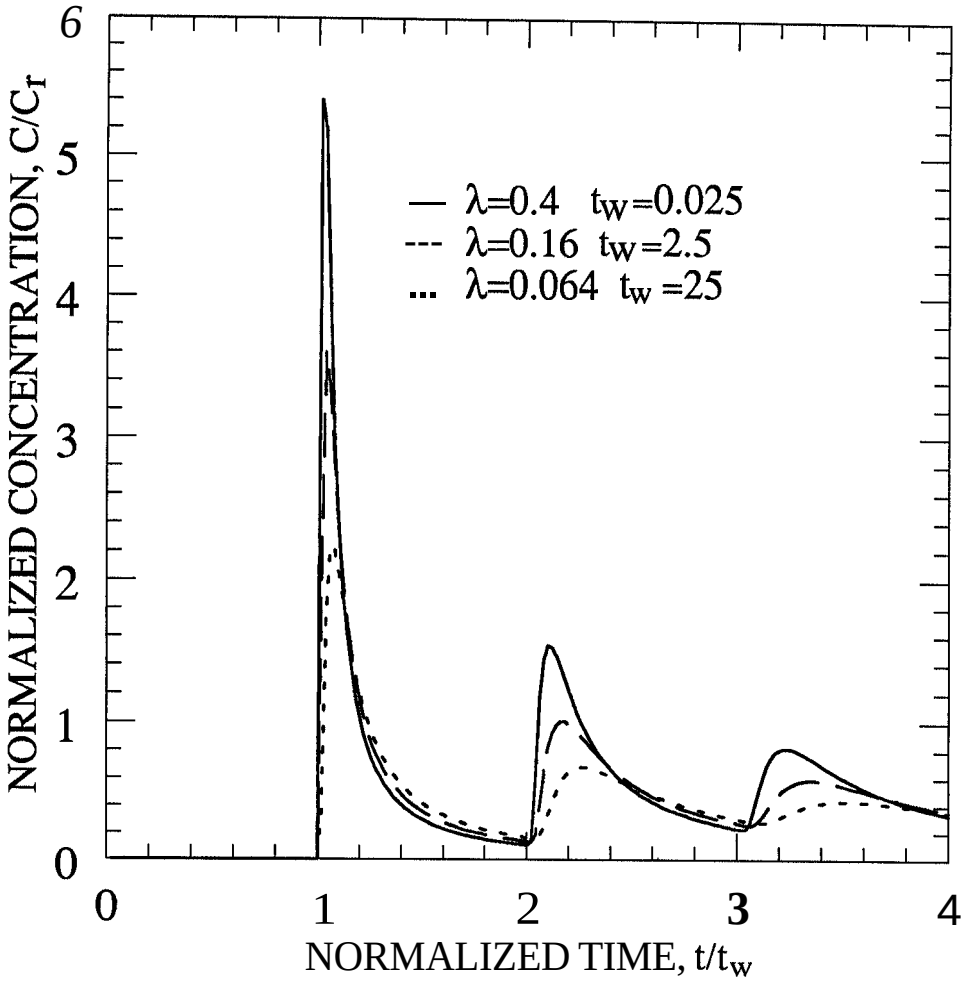

Figure **3.8:** Normalized Solutions to the MD Model for Small Amount of Diffusion

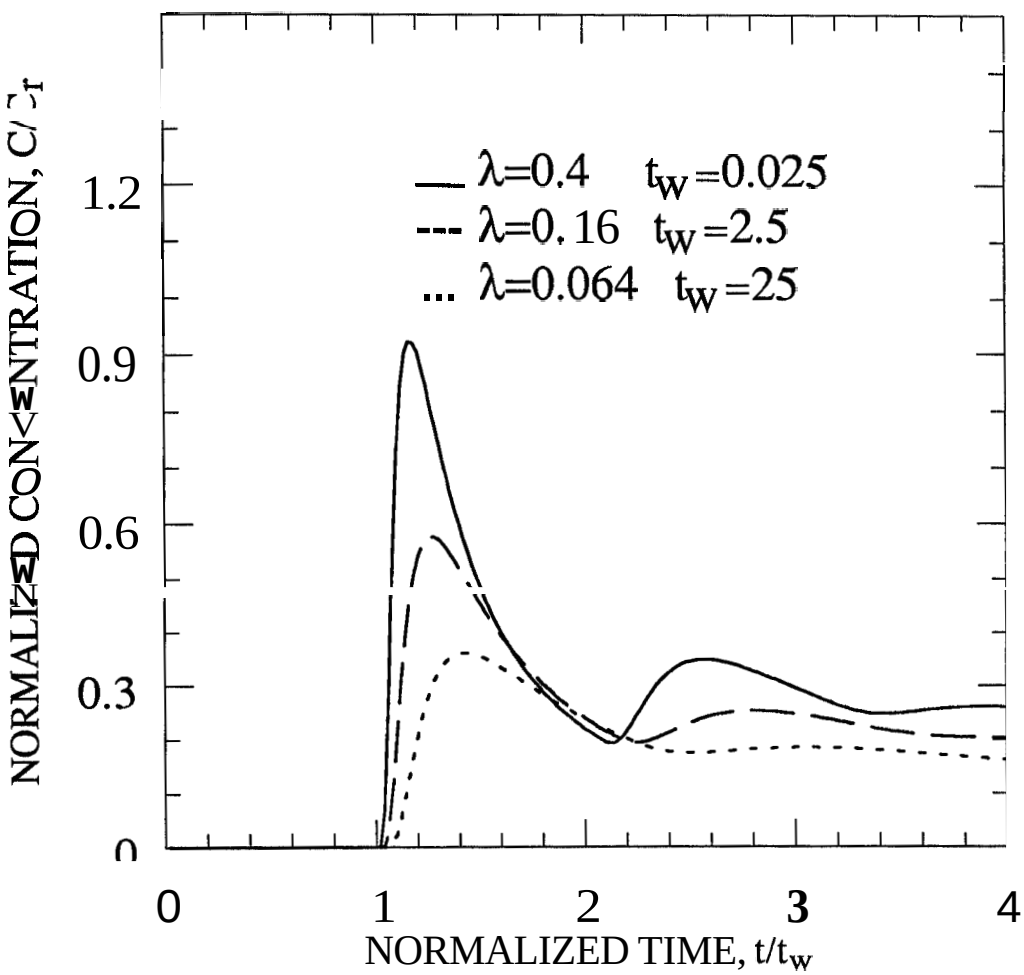

Figure 3.9: Normalized Solutions to the MD Model for Large Amount of Diffusion

of the assumption of flow in a single fracture. For the parallel fractures model, the final level concentration would have been constant. Finally, the influence of time is significant in determining the shape of the return profile. For example, both a system with a small λ and large t, and a system with a large λ and a small t, yield similar tracer return profiles. The parameter t, affects the injection period because the tracer reaches the observation point when $t > t_s$.

The generated return profiles of the **AD** model are shown in Figs. 3.10, 3.11 and **3.12.** The return profiles are characterized by the dominant mechanism mixing the tracer with the reservoir fluid. If dispersion is the dominant mechanism, appearance of the peaks may have the features of the peaks of the CD model profiles. On the other hand, if matrix diffusion is dominant, then profiles will be similar to those of the MD model. In both cases, however, for a single fracture model, there will not be a final concentration level, since the matrix pore volume is theoretically infinite. Because of matrix diffusion, the influence of time cannot be eliminated. As a result, it is possible to obtain similar profiles corresponding to short, intermediate and long t_s, by utilizing different combinations of P_e, λ and t_s. This is indicated by the similarities between the profiles for t, values of **0.25, 2.5** and **25.** However, the absolute amplitude of the peaks differ considerably, being high for a small t, and low for a large t_s.

De Smedt *et.al*[26] pointed out that for a test without recirculation the three parameters, t_s, P_e and λ are not likely to be correlated, since they affect different segments of the profiles. While t_w affects the breakthrough time, P_e affects the slope of the section between t_b and t_p, and λ affects the slope of the tail section. It is also possible to observe these distinct effects of the parameters on the return profiles of tracer tests with recirculation. In addition to the previously mentioned effects, several other features related to the parameters can be observed. First, as the Peclet number increases, t_b becomes smaller. Second, the parameter λ has significant effects on the magnitudes and the number of the peaks that can be distinguished by eye in the profiles. Finally the slopes at the limit are almost independent of the parameters, which can be observed in all the figures for the AD model. Again if the parallel fractures model were used, the final level concentration

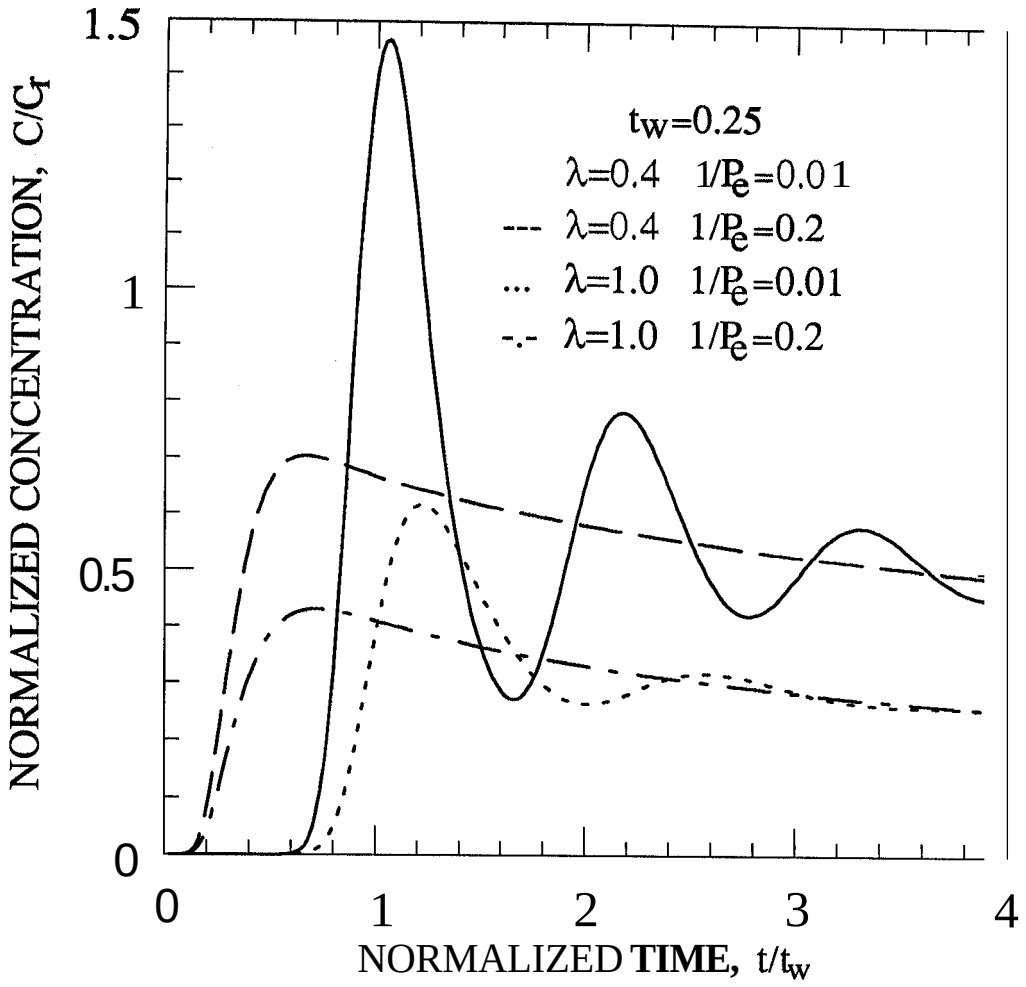

Figure 3.10: Normalized Solutions to the AD Model for Short Period Tests

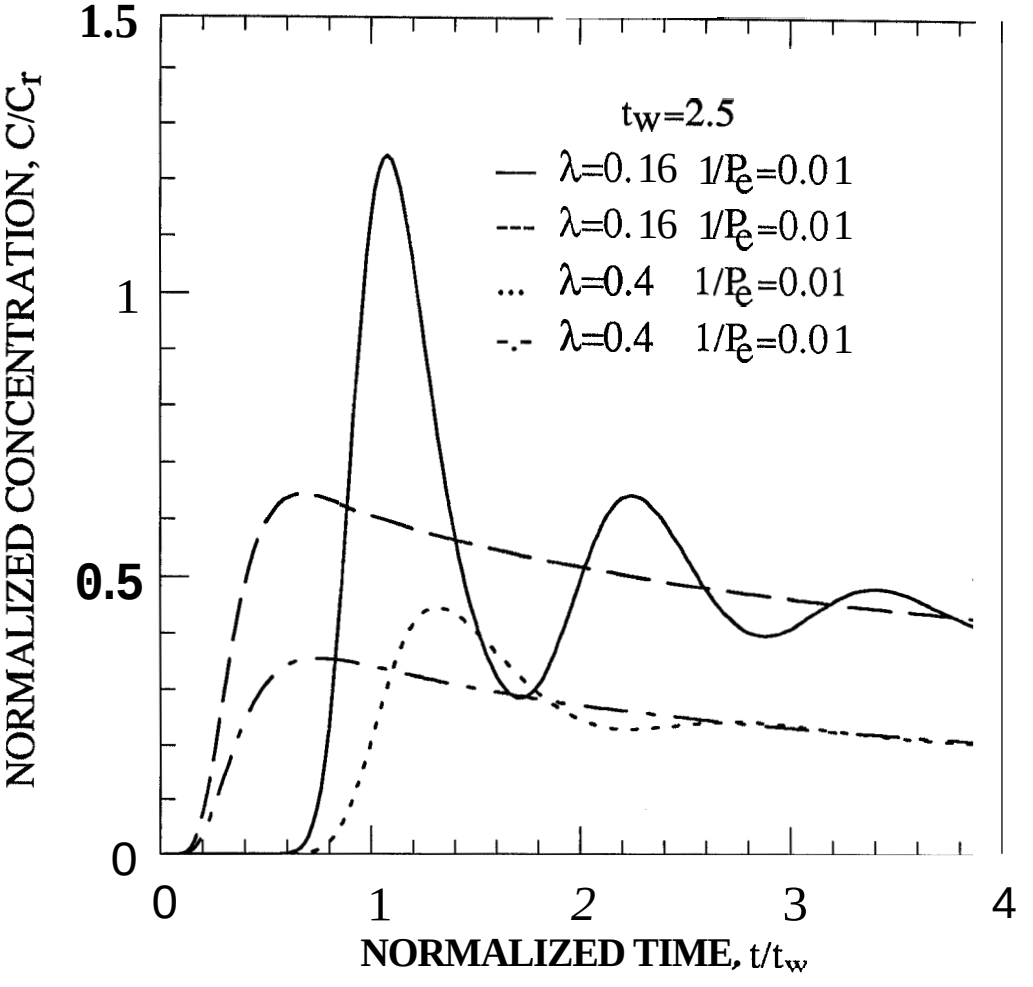

Figure 3.11: Normalized Solutions to the **AD** Model for Medium Period Tests

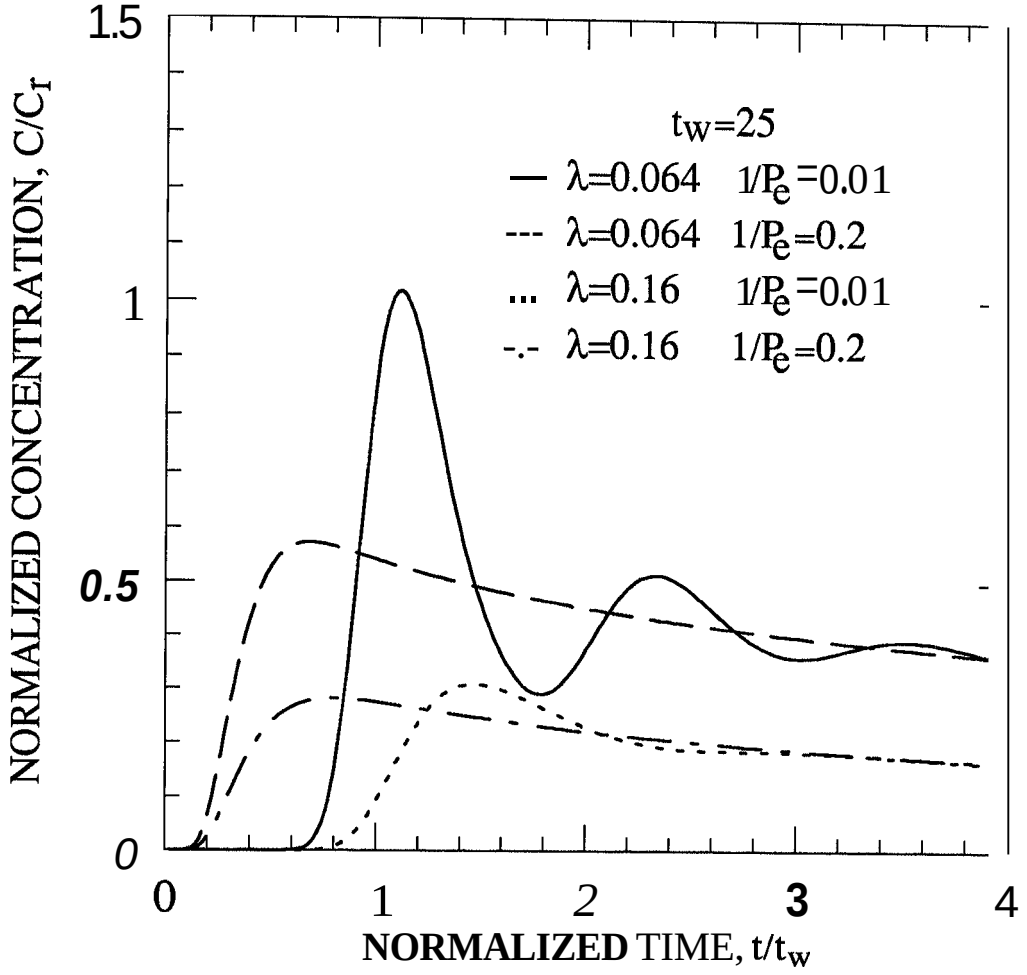

Figure 3.12: Normalized Solutions to the AD Model for Long Period Tests

would have been constant.

3.2.3 A Field Example

We matched the tracer return profile of a test conducted in Broadland, New Zealand with solutions to the models. Fig. **3.13** shows the tracer return profile matched by the CD model. The other two models did not match the data. For the MD model the error tolerance was not satisfied. For the AD model, when parameter estimates of the CD model and a small value for λ were entered as initial estimates, the regression value of λ became negative, and moreover, the error tolerance was not satisfied. When initial estimates are determined from correlations related to t,, t_w and t_b the error tolerance was not satisfied.

The tracer return profile does not show a fast flow path characteristic, namely, a steep slope between t_b and t,. Furthermore, since the tailing section was not measured, it was difficult to determine whether the matrix diffusion effects, which influence the tailing of the tracer return profile appeared or not. The early part of the tracer return profile could be matched by the CD model of the tracer transport without recirculation.

Since the shape of the tracer return profile is similar to those obtained in uniform formations[36,67,90] it seems reasonable to use the uniform porous medium approach. In all those profiles, t_p values were **3** to **13** times greater than t_b, and in the Broadland profile t_p was approximately equal to $7t_b$. If we divide the flow field into crescents such that the flow rates are equal, we can use one transfer function for multiple paths in the regression procedure. If the flow rates were unequal, we would have to use as many transfer functions as the number of paths. This is not feasible for more than few paths. If the flow velocities of the individual paths are specified explicitly, then the number of nonlinear parameters can be reduced significantly. Further assumptions on the form of the dispersion coefficient, for instance it can be taken as proportional to the velocity or to the square of the velocity, would greatly simplify the problem. Especially, assuming that the dispersion coefficient is proportional to the velocity square, the Taylor dispersion relation, the solution becomes a function of a single nonlinear parameter, dispersivity. The best approach

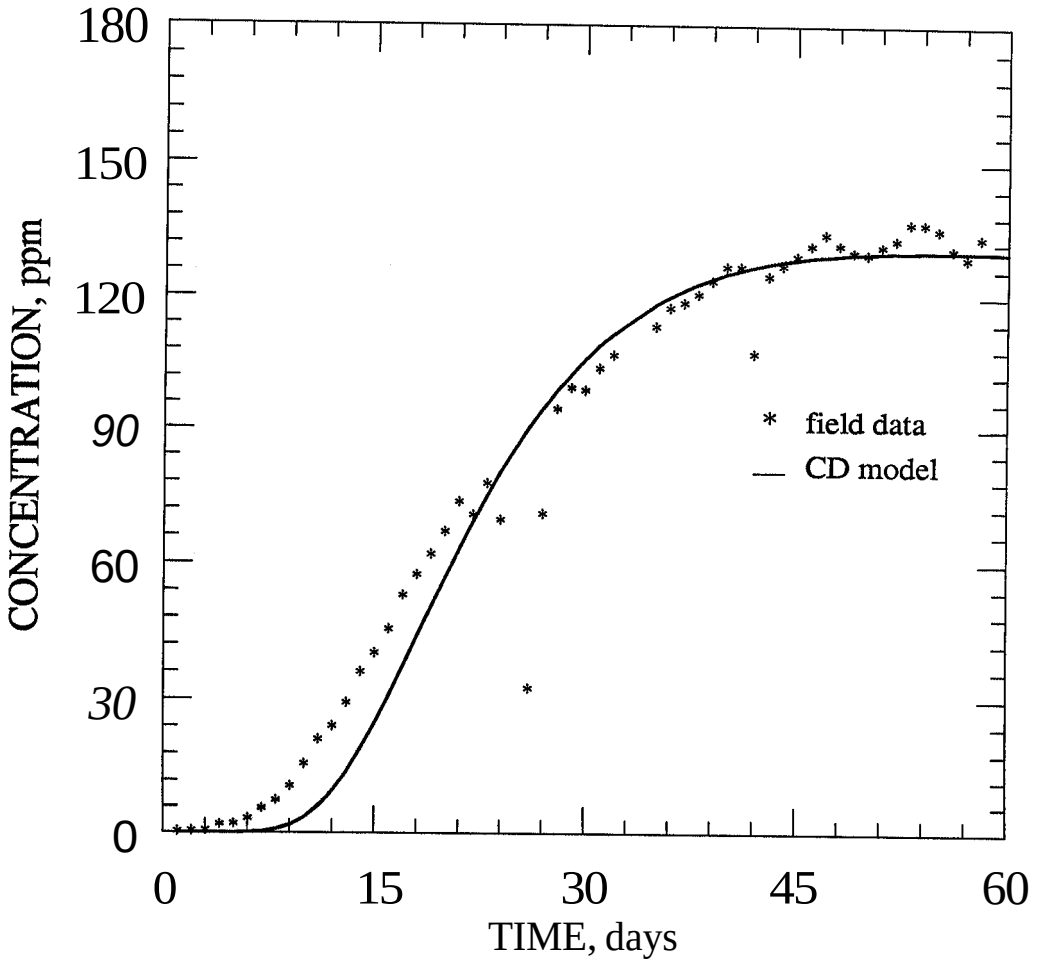

Figure **3.13:** Matching of Broadland Test Data by the CD Model

is to start from the simplest case and to add complications as the problem requires.

The fracture aperture estimated from the match values of the CD model did not satisfy **Eq. 3.3.** This was expected, since the shape of the profile was not well captured by the model. This example however is not a characteristic profile one would expect to obtain from a fast flow path. Therefore, it is more appropriate to test the model on other data, which have the desired characteristics, including strong recirculation effects.

Tracer tests with recirculation were also used by Ito *et.al.*[42] to estimate the volume of fluid recirculating trough the system at Onuma field, Japan. We tried to estimate transport parameters of the Onuma field by matching tracer return profiles with the solutions of models. Since we did not have the actual data sets we digitized the tracer return profiles published by Ito *et. al.* The tail part of digitized tracer return profile matched solutions of the CD and **AD** models poorly, therefore, parameter estimates were rejected. Data match with the MD model did not satisfy the error criteria.

3.3 INJECTION-BACKFLOW TRACER TESTS

In an injection-backflow tracer test, the traced fluid is injected into the system at a well for a period of time, after which the same well is produced until the tracer is recovered. The flow conditions are assumed to be steady state and the flow due to injection to be dominant compared to the natural formation flow. Tracer return profiles obtained during the backflow period may be analyzed to determine dispersive flow characteristics of the flow region near the test well. The main purpose of an injection-backflow tracer test in a geothermal field is to identify high conductivity fractures intersecting the injection well. Therefore, we need to study the characteristics of tracer return profiles of injection-backflow tests when flow takes place in a high conductivity single vertical fracture.

Usually, in tracer tests in geothermal reservoirs, the tracer is introduced into the flow stream of the injection fluid, and concentrations of tracer in samples taken from the backflow stream are used to obtain tracer return profiles. In this case, both

injection and detection methods correspond to the flux concentration mode. Even though both injection and detection in resident concentration modes are difficult to perform, analytical solutions for both injection and detection in resident fluid and injection in resident fluid, and detection in flux are easy to compute. Therefore, for the cases where dispersion is not high, these formulas may be used instead of the solution for both injection and detection in flux concentration mode.

3.3.1 Injection Period Solutions

Injection period solutions are the same as solutions derived for the analysis of interwell tracer tests without recirculation.

3.3.2 Backflow Period Solutions

Since the flow directions in injection and backflow periods are opposite, the sign of the convective transport term in the transport equation of the backflow period is of opposite sign from the convective transport term in the equation of the injection period. For the convection-dispersion model, Eq. 1.1 is the injection period transport equation, and the backflow period transport equation is:

$$\frac{\partial C}{\partial t} - u\frac{\partial C}{\partial x} - D\frac{\partial^2 C}{\partial x^2} = 0 \qquad \textbf{(3.16)}$$

The positive sign before the second term in Eq. 1.1 becomes negative in Eq. **3.16.** To obtain the solution for tracer return profiles during the backflow period, Eq. **3.16** must be solved subject to appropriate initial and boundary conditions. The tracer distribution at the end of the injection period is the initial tracer distribution for the backflow period. Therefore, the injection period solution provides the initial condition of the backflow period solution.

Convection-Dispersion Model

In this study, we consider four cases of injection-detection modes, namely both injection and detection in resident concentration mode, injection in resident

concentration mode and detection in flux concentration mode, injection in flux concentration mode and detection in resident concentration mode, and finally, both injection and detection in flux concentration mode. The solutions for the continuous injection of tracer fluid during the injection period will be considered.

To obtain both injection and detection in resident concentration solution, Eq. **3.16** will be solved with C_{CRR} solution for the injection period as the initial condition. Solution was obtained by Fourier transformation method. The solution to Eq. **3.16** is[37]:

$$C(x,t) = \int_{-\infty}^{\infty} f(x') \frac{1}{2\sqrt{\pi Dt}} \exp\left(-\frac{(x+ut-x')^2}{4Dt}\right) dx' \qquad (3.17)$$

where $f(x')$ is the initial condition. **Eq. 3.17** is the convolution of the initial condition with the influence function of Eq. 3.16. Therefore, the Fourier transform of Eq. **3.17** is the scalar product of the Fourier transforms of the functions $f(x')$ and the influence function. If the infinitely extended injection in resident fluid and detection in resident fluid concentration is the initial condition for the injection period, the Fourier transform of the solution C_{CRR} for the injection period is:

$$\overline{C}_{CRR} = B(\omega) \exp\left(-D_j t_j \omega^2\right) \exp(u_j t_j i\omega) \qquad (3.18)$$

where $B(\omega)$ is the Fourier transform of $[1 - H(x)]$ and $H(x)$ is the Heaviside step function. The Fourier transform of Eq.3.17 is:

$$\overline{C} = B(\omega) \exp\left(-(D_j t_j + Dt)\omega^2\right) \exp((u_j t_j - ut)i\omega) \qquad \mathbf{(3.19)}$$

Using the convolution theorem, Eq. 3.19 can be inverted:

$$C(x,t) = \frac{1}{2\pi} \int_{-\infty}^{0} \frac{\sqrt{\pi}}{\sqrt{D_j t_j + Dt}} \exp\left(-\frac{(x - ujtj + ut - x')^2}{4(D_j t_j + Dt)}\right) dx' \qquad (3.20)$$

and Eq.3.20 can be integrated to yield:

$$C(x,t) = \frac{1}{2} erfc\left(\frac{x - ujtj + ut}{2\sqrt{D_j t_j + Dt}}\right) \qquad (3.21)$$

To determine the tracer return profile, Eq. **3.21** is evaluated at $x = 0$. An advantage of this solution is that the injection and backflow rates do not have to be equal. Using this method, solutions for any number of sequences of constant rate periods may be found.

The solutions of injection in resident fluid and detection in flux concentration modes can be obtained by two methods. However, the easiest is application of the transformation T_1 to Eq. **3.21.** Because of the change in the sign of the convective flux, the transformation T_1 in Table **1.3** for the backflow period is:

$$C_F = C_R + \frac{D}{u}\frac{\partial C_R}{\partial x} \tag{3.22}$$

When backflow starts, the initial flux concentration solution can be found by substituting Eq. **3.21** into Eq. **3.22.** The flux concentration is chosen to be positive if the net tracer transport is in the flow direction. That means the values measured during the backflow will be taken as positive values.

To determine the solution for the case of both injection and detection in flux concentration mode, an important assumption is that the exit boundary does not influence the system. This is a challenging task, because it is necessary to avoid imposing a boundary condition at $x = 0$, which is the outlet of the system. Assuming an infinite domain for the backflow period permits the use of Eq. **3.17** in obtaining the solution. Eq. **3.17** requires an initial condition $f(x')$ from $-\infty$ to ∞. The solution for the injection period is the initial concentration distribution for $x \geq$, but the initial concentration distribution for $x \leq$ must be assumed. Care must be exercised so that initial condition does not cause material balance errors. To obtain the solution, either of the two methods can be used. First, express $f(x')$ in terms of the resident concentration distribution and apply the transformation T_1 to Eq. **3.17.** This method was used in Section **2.3.** Alternatively, express $f(x')$ in terms of the flux concentration by applying the transformation T_1 to the initial resident concentration function and substitute into Eq. **3.17.**

The injection period solution, C_{CFF} in Table **1.2,** gives the flux concentration distribution in a semi-infinite system during the injection period. Between the end of injection and the beginning of backflow there is a moment at which the flow

velocity becomes zero, and C_{CFF} becomes equal to C_{CFR}. The solution C_{CFR} in Table 1.2 gives the resident concentration distribution from 0 to ∞, and we must assume an initial resident concentration distribution from 0 to $-\infty$. Substituting a resident concentration distribution into Eq. 3.17 gives the resident concentration solution. Material balance can be ensured as follow: From C_{CFR}, there is a negative concentration gradient at $x = 0$. An initially symmetrical resident concentration profile with respect to the point $x = 0$ allows the system respond to the negative concentration gradient and prevents addition of material into the system. Further, during the backflow period, there will be no dispersive flux across the point of symmetry travelling with the mean speed of flow.

The initial flux concentration distribution is obtained by substituting initial resident concentration function into Eq. 3.22:

$$f(x') = \frac{1}{2} erfc\left(\frac{x' - ut_j}{2\sqrt{Dt_j}}\right) - \exp\left(\frac{ux'}{D}\right) erfc\left(\frac{x' + ut_j}{2\sqrt{Dt_j}}\right) \left[3 + \frac{u(x' + ut_j)}{D}\right] + \frac{2u\sqrt{t_j}}{\sqrt{\pi D}} \exp\left(\frac{(x' - ut)^2}{4Dt}\right) \quad x \geq 0 \qquad (3.23)$$

$$f(x') = \frac{1}{2}\left\{erfc\left(\frac{|x'| - ut_j}{2\sqrt{Dt_j}}\right) + \exp\left(\frac{u|x'|}{D}\right) erfc\left(\frac{|x'| + ut_j}{2\sqrt{Dt_j}}\right)\right\} \quad x \leq 0 \qquad (3.24)$$

Finally, substituting Eqs. 3.23 and 3.24 into Eq. 3.17 yields the flux concentration solution. The concentration values at the well can be found by numerical integration of Eq. 3.17 at $x = 0$. The solutions may be expressed in dimensionless variables which are defined in Section 2.3 as shown in Table 3.6.

Numerical differences between injection-backflow solutions are similar to numerical differences between the solutions for unidirectional flow. While for small t_D differences between profiles are small (see Fig. 3.14), for large values of t_D differences increases (see Fig. 3.15). In Fig. 3.14, the C_{CRR} solution yields the highest concentration values as opposed to C_{CFF} in the case of unidirectional flow. This is because, convective and dispersive fluxes are in opposite directions.

$$C_{CRR}(x_D, t_{Dp}) = \frac{1}{2} erfc\left(\frac{x_D - 1 + t_{Dp}}{2\sqrt{t_D(1+t_{Dp})}}\right)$$

$$C_{CRF}(x_D, t_{Dp}) = \frac{1}{2} erfc\left(\frac{x_D - 1 + t_{Dp}}{2\sqrt{t_D(1+t_{Dp})}}\right) - \frac{1}{2}\frac{\sqrt{t_D}}{\sqrt{\pi(1+t_{Dp})}} \exp\frac{-(x_D - 1 + t_{Dp})^2}{4t_D(1+t_{Dp})}$$

$$C_{CFR}(x_D, t_{Dp}) = \int_{-\infty}^{\infty} f(x'_D) \frac{1}{2\sqrt{\pi t_D t_{Dp}}} \exp\frac{-(x_D + t_{Dp} - x'_D)^2}{4t_D t_{Dp}} dx'_D$$

$$f(x'_D) = \frac{1}{2} erfc\left(\frac{|x'_D| - 1}{2\sqrt{t_D}}\right) - \frac{1}{2}\exp\frac{|x'_D|}{t_D} erfc\left(\frac{|x'_D| + 1}{2\sqrt{t_D}}\right)$$

$$\left[1 + \frac{(|x'_D| + 1)}{t_D}\right] + \frac{1}{\sqrt{\pi t_D}} \exp\frac{-(|x'_D| - 1)^2}{(4t_D)}$$

$$C_{CFF}(x_D, t_{Dp}) = \int_{-\infty}^{\infty} f(x'_D) \frac{1}{2\sqrt{\pi t_D t_{Dp}}} \exp\frac{-(x_D + t_{Dp} - x'_D)^2}{4t_D t_{Dp}} dx'_D$$

$$f(x'_D) = \frac{1}{2} erfc\left(\frac{x'_D - 1}{2\sqrt{t_D}}\right) - \frac{1}{2}\exp\frac{x'_D}{t_D} erfc\left(\frac{x'_D + 1}{2\sqrt{t_D}}\right)$$

$$\left[3 + \frac{2(x'_D + 1)}{t_D}\right] + \frac{2}{\sqrt{\pi t_D}} \exp\frac{-(x'_D - 1)^2}{(4t_D)} \qquad x \geq 0$$

$$f(x'_D) = \frac{1}{2} erfc\left(\frac{|x'_D| - 1}{2\sqrt{t_D}}\right) + \frac{1}{2}\exp\frac{|x'_D|}{t_D} erfc\left(\frac{|x'_D| + 1}{2\sqrt{t_D}}\right) \qquad x \leq 0$$

Table *3.6:* Dimensionless Backflow Period Solutions to the CD Model

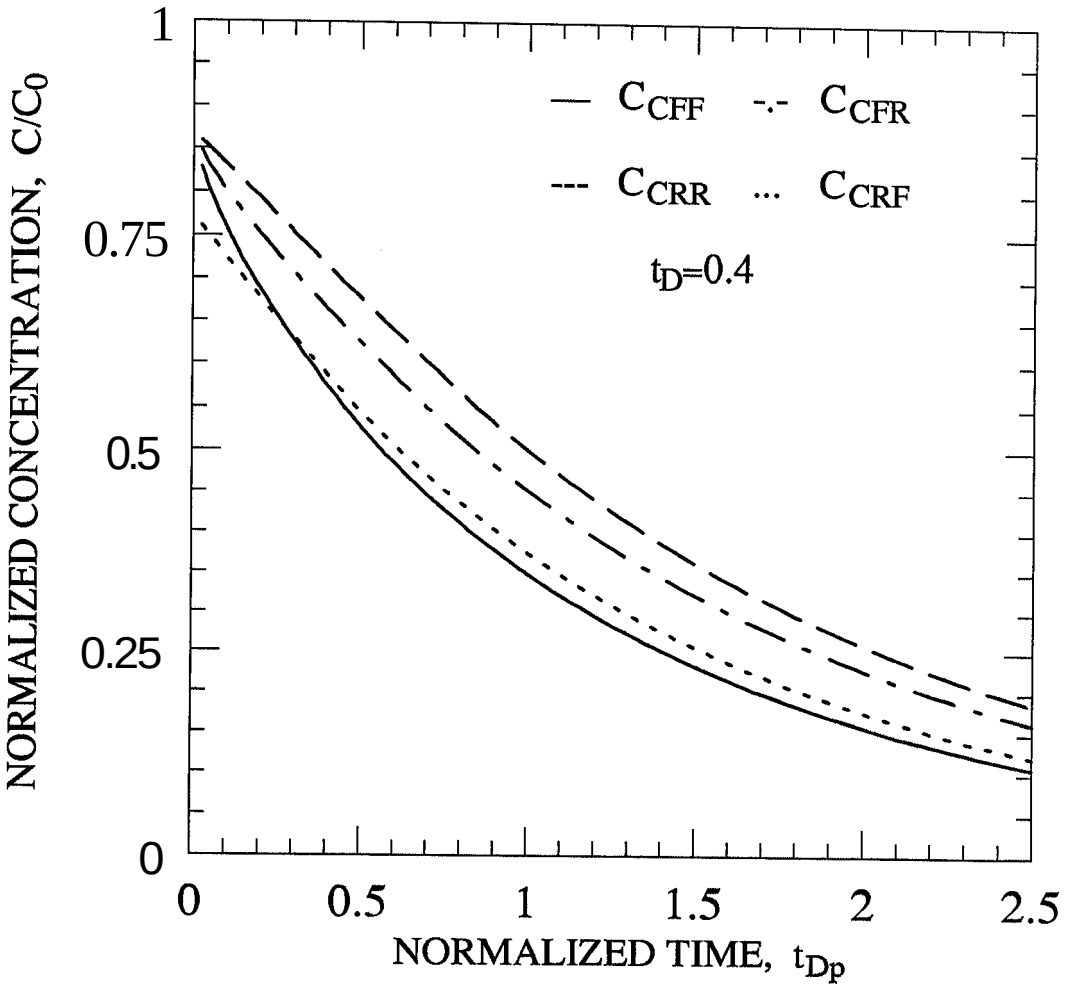

Figure 3.14: Solutions for Different Injection and Detection Modes-Medium t_D

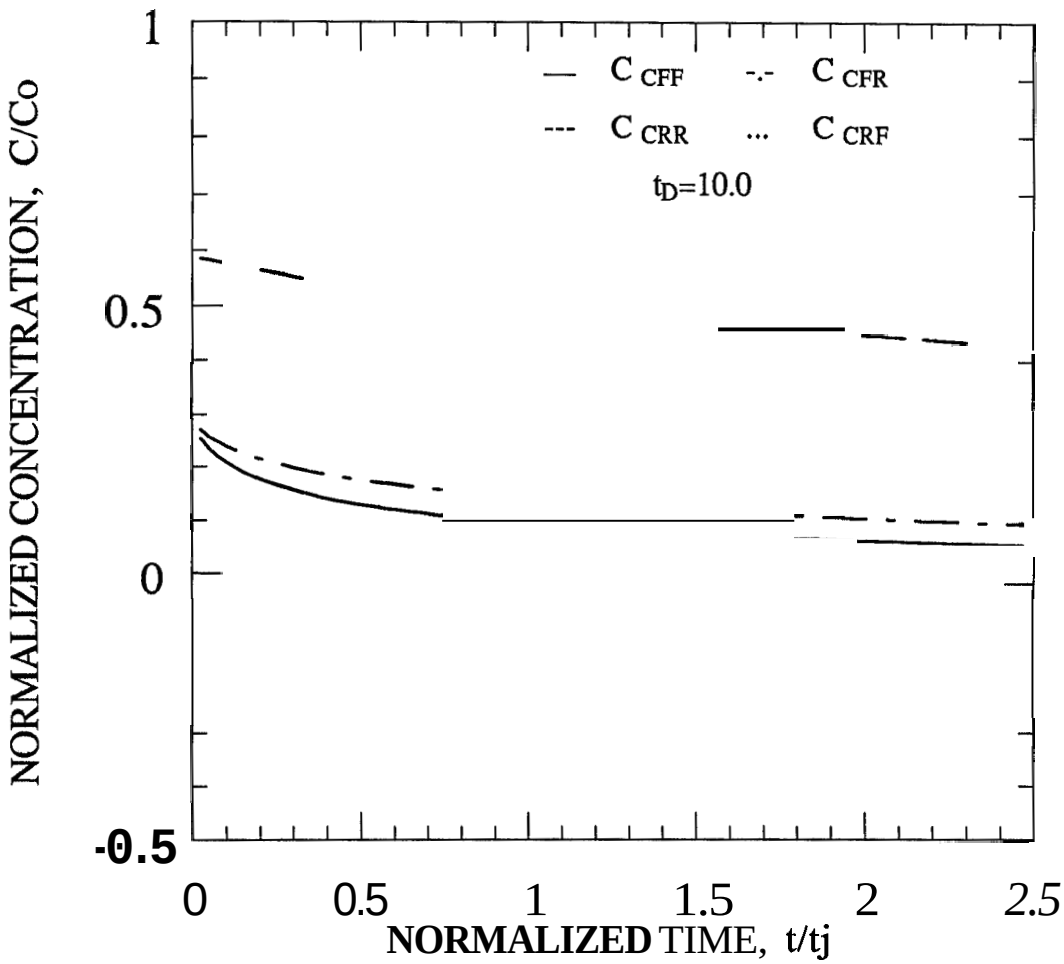

Figure 3.15: Solutions for Different Injection and Detection Modes-Large t_D

The C_{CRF} solution may yield negative concentrations which indicate that the net tracer transport is in opposite direction with flow. The initial condition which assumes an infinite amount of tracer is distributed along the negative axis of the domain can support a high concentration gradient so that dispersive flux becomes greater than convective flux. The basic assumption in using C_{CRR} and C_{CRF} is that the length of the transition region between tracer fluid and reservoir fluid is negligible compared to the distance traveled by convective front. Therefore, we should avoid using these solutions for short term injection-backflow tracer tests and for highly dispersive systems.

The difference between C_{CFR} and C_{CFF} solution profiles is smaller than the corresponding profiles for unidirectional flow. The source at the origin which gives rise to large concentration gradients ceases to be for the backflow period. As a result, dispersive flux decreases reducing the difference between C_{CFR} and C_{CFF} solutions.

Since the second group of terms in Eq. 3.23 is a product of a large number and a small number, we used an asymptotic expansion of the error function for large arguments, to evaluate the solution.

The instantaneous injection case solutions can also be found by the same method.

Matrix Diffusion Model

Solutions of transport equations for the backflow period were obtained by using a double Laplace transformation method. Transport equations were transformed first with respect to the injection period time variable t_j, and then with respect to the backflow period time variable, t. Using the Laplace transformation, the difficulties caused by the effect of the step function, which is in the solutions for the injection period, have been avoided.

The Laplace space solution for equal injection and backflow rates were presented in a previous work[45,46]:

$$\overline{\overline{C}} = \frac{1}{s+p+2\lambda(\sqrt{s}+\sqrt{p})}\left[\frac{1}{s}+\frac{2\lambda}{s\sqrt{p}}+\frac{2\lambda}{s-p}\left(\frac{1}{\sqrt{s}}-\frac{1}{\sqrt{p}}\right)\right] \qquad (3.25)$$

To obtain theoretical tracer return profiles, Eq. **3.25** was inverted by a double numerical inversion technique based on the Stehfest algorithm[82]. However, the effect of numerical dispersion on the Stehfest algorithm was not determined for the case of tracer return profiles with steep slopes, which are likely to be observed when the parameter, A, in Eq. 3.25 is small. To compute solutions for small A, either an accurate numerical inversion algorithm must be used or the real space solution must be found and evaluated.

Using the inversion method, *functions* **of** *functions,* discussed by Ditkin and Prudnikov[28], and the inversion formula given by Voelker and Doetsch[89], the real space function of **Eq.3.25** (see Appendix D), is obtained:

$$
\begin{aligned}
C_f = \int_0^{min(t_j,t)} \Bigg\{ & erfc\left(\frac{\lambda\theta}{\sqrt{t_j-\theta}}\right) \frac{\lambda\theta}{\sqrt{\pi(t_j-\theta)}} \exp\left(-\frac{\lambda^2\theta^2}{t_j-\theta}\right) + \\
& 2\lambda\, erfc\left(\frac{\lambda\theta}{\sqrt{t_j-\theta}}\right) + \sqrt{\pi(t_j-\theta)}\, \exp\left(-\frac{\lambda^2\theta^2}{t_j-\theta}\right) \Bigg\} d\theta \\
+ 2\lambda \int_0^{t_j} d\eta \int_0^{min(t_j-\eta,t+\eta)} & \left\{ \frac{1}{\sqrt{\pi(t_j-\eta-\theta)}} \exp\left(-\frac{\lambda^2\theta^2}{t_j-\eta-\theta}\right) \right. \\
& \left. \frac{\lambda\theta}{\sqrt{\pi(t+\eta-\theta)^3}} \exp\left(-\frac{\lambda^2\theta^2}{t+\eta-\theta}\right) \right\} d\theta \\
- 2\lambda \int_0^{t_j} d\eta \int_0^{min(t_j-\eta,t+\eta)} & \left\{ \frac{\lambda\theta}{\sqrt{\pi(t_j-\eta-\theta)^3}} \exp\left(-\frac{\lambda^2\theta^2}{t_j-\eta-\theta}\right) \right. \\
& \left. \frac{1}{\sqrt{\pi(t+\eta-\theta)}} \exp\left(-\frac{\lambda^2\theta^2}{t+\eta-\theta}\right) \right\} d\theta \qquad (3.26)
\end{aligned}
$$

Eq. **3.26** may be interpreted to show that there are two parameters, λ and t_j, affecting tracer return profiles. However, the influences of both parameters on the tracer return profiles are not independent. Both parameters can eliminate the concentration discontinuity at the convective front. For every λ, there is a corresponding t_j which can moderate the concentration discontinuity at the convective front. This can be verified as follows. Defining a new variable, λ_D:

$$\lambda_D = \lambda\sqrt{t_j} \tag{3.27}$$

and normalizing the time variables by t_j, Eq. 3.26 becomes:

$$\begin{aligned} C_f = \int_0^{min(1,t_{Dp})} & \left\{ erfc\left(\frac{\lambda_D\theta}{\sqrt{1-\theta}}\right) \frac{\lambda_D\theta}{\sqrt{\pi(1-\theta)^3}} \exp\left(-\frac{\lambda_D^2\theta^2}{t_{Dp}-\theta}\right) + \right. \\ & \left. 2\lambda_D\, erfc\left(\frac{\lambda_D\theta}{\sqrt{1-\theta}}\right) + \frac{1}{\sqrt{\pi(1-\theta)}} \exp\left(-\frac{\lambda_D^2\theta^2}{t_{Dp}-\theta}\right) \right\} d\theta \\ + 2\lambda_D \int_0^1 d\eta \int_0^{min(1-\eta,t_{Dp}+\eta)} & \left\{ \frac{1}{\sqrt{\pi(1-\eta-\theta)}} \exp\left(-\frac{\lambda_D^2\theta^2}{1-\eta-\theta}\right) \right. \\ & \left. \frac{\lambda_D\theta}{\sqrt{\pi(t_{Dp}+\eta-\theta)^3}} \exp\left(-\frac{\lambda_D^2\theta^2}{t_{Dp}+\eta-\theta}\right) \right\} d\theta \\ - 2\lambda_D \int_0^1 d\eta \int_0^{min(1-\eta,t_{Dp}+\eta)} & \left\{ \frac{\lambda_D\theta}{\sqrt{\pi(1-\eta-\theta)^3}} \exp\left(-\frac{\lambda_D^2\theta^2}{1-\eta-\theta}\right) \right. \\ & \left. \frac{1}{\sqrt{\pi(t_{Dp}+\eta-\theta)}} \exp\left(-\frac{\lambda_D^2\theta^2}{t_{Dp}+\eta-\theta}\right) \right\} d\theta \end{aligned} \tag{3.28}$$

To obtain Eq. 3.28, θ and η of Eq. 3.26 were also normalized by t_j, but since they are dummy variables we left them unchanged. The Laplace space solution can be expressed (see Appendix D) in terms of the new variable as:

$$\overline{\overline{C}} = \frac{1}{s+p+2\lambda_D(\sqrt{s}+\sqrt{p})}\left[\frac{1}{s} + \frac{2\lambda_D}{s\sqrt{p}} + \frac{2\lambda_D}{s-p}\left(\frac{1}{\sqrt{s}} - \frac{1}{\sqrt{p}}\right)\right] \tag{3.29}$$

Eq. 3.29 has the same form as Eq. 3.25, but the Laplace space variables s and p correspond to different real space variables. In Eq. 3.29, s corresponds to the variable $t_j/t_j = 1$, and p corresponds to the variable t_{Dp}.

From Eqs. 3.28 and 3.29, that the influences of λ and t_j are indistinguishable; and λ_D, a combination of λ and t_j, determines shapes of tracer return profiles.

Eq. 3.28 was evaluated numerically for several values of λ_D, and Eq. 3.29 was inverted numerically by using a double numerical inversion technique based on the Stehfest[82] algorithm.

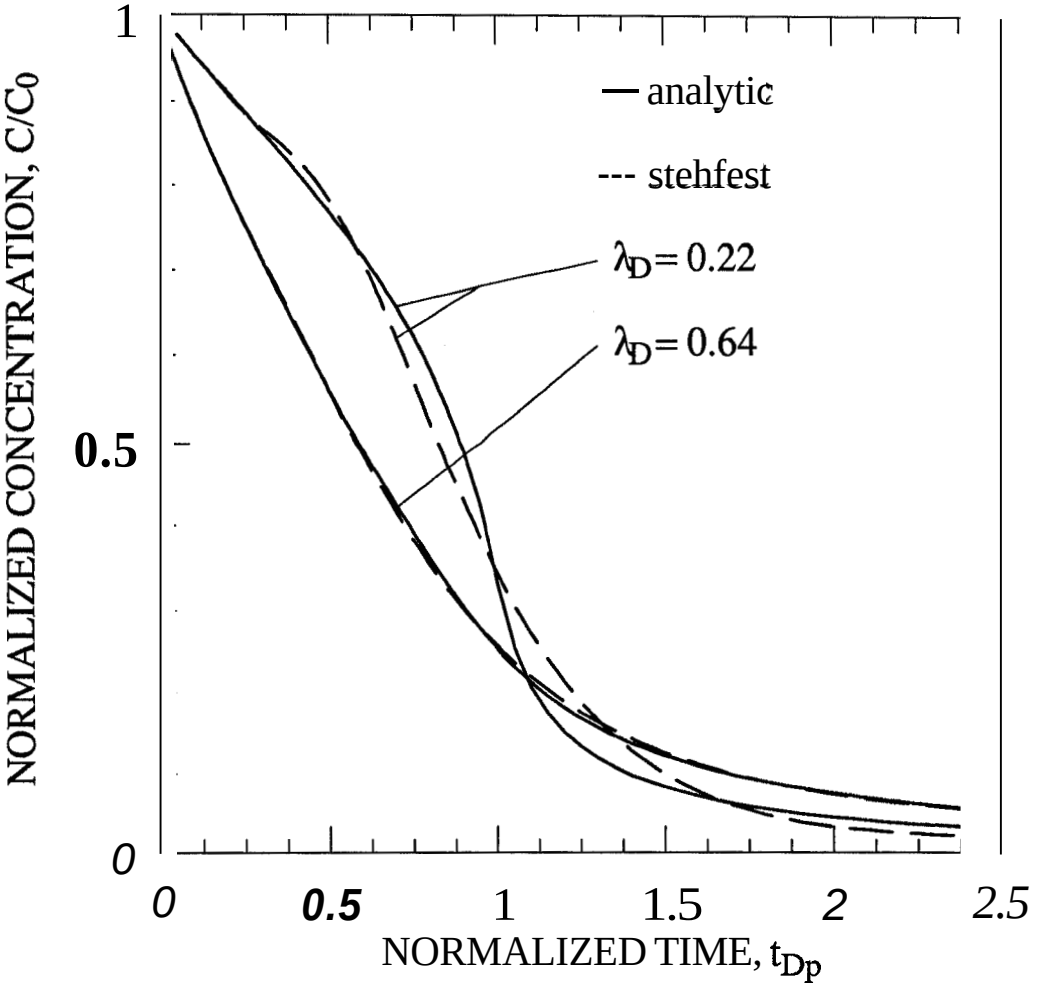

Figure 3.17: Solutions to MD Model for Medium λ_D

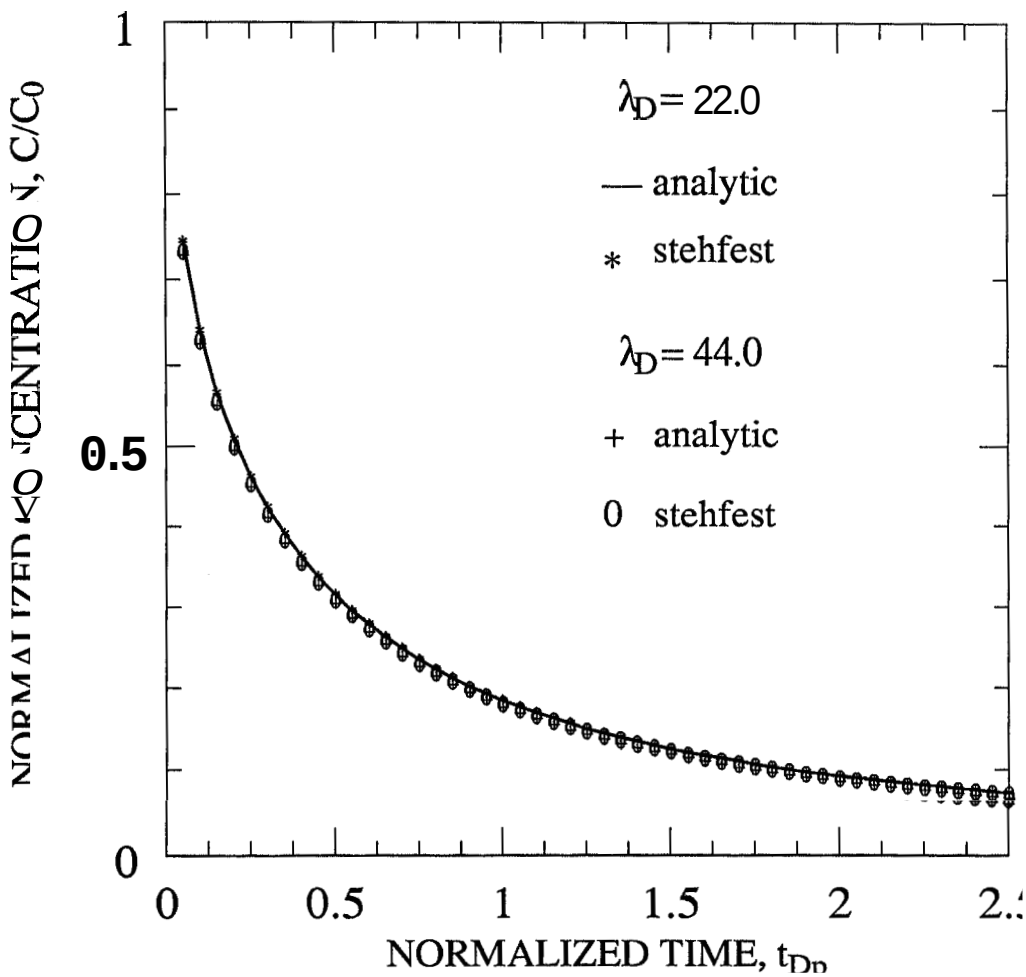

Figure 3.18: Solutions to MD Model for Large λ_D

Figs. 3.16 to 3.18 show the results of numerical integration of the solution as well as the numerically inverted Laplace space solution. From these figures, all of the profiles computed by either method preserve a material balance. The material balance can be checked by drawing a vertical line at $t_{Dp} = 1$, and determining whether the areas above the curve before the line and under the curve after the line are equal or not. All of the tracer return profiles have a common feature: Since the matrix provides a time-dependent storage, for all of the injected tracer to be recovered, an infinitely long backflow period is required. For small values of λ_D, the curves for the two methods differ considerably. For large values of λ_D, the profiles become smooth, and both methods produce the same result. Based on these new results, the tracer return profiles with steep fronts, which were interpreted in a previous work [45] by using the Stehfest[82] algorithm, should be reinterpreted.

Fig. **3.16** shows the tracer return profiles for small values of λ_D. **A** small λ_D may occur because of either λ or t_j being small. While a small λ means that the rate of diffusion into the matrix is small, a small value for t_j means that the time is not enough for diffusion into the matrix. In Fig. 3.16, since the total amount of diffusion is small, the concentration discontinuity at the convective front is reduced slightly. **As** a result, when $t_{Dp} = 1$ in each of those return profiles, a large sudden drop of concentration is observed.

In Fig. 3.17, values of λ are large and there is much diffusion, but the rate of transfer is not enough to smooth the concentration discontinuity at the convective front. In Fig. 3.18, λ_D values are high, which means either a high X or t_j value or both being moderate such that the product λ_D is high. If X is high, then the injected fluid loses most of the tracer content to the matrix before it travels far in the fracture. Thus, the concentration discontinuity is virtually eliminated. Tracer return profiles have high slopes at early times since the injected fluid has lost most of the tracer content to the matrix. For the tracer which has diffused into the matrix to be recovered, the gradient at the fracture-matrix interface must to be reversed, which occurs as the reservoir fluid follows the injected fluid during the backflow. As a result, most of the tracer is recovered slowly, because it is controlled by diffusive transfer between the fracture and the matrix. If t_j is high, the continuous sorption of

the tracer reduces the magnitude of the concentration discontinuity at the convective front, and during the backflow period the tracer is slowly recovered.

The porosities of most geothermal reservoirs are low, ranging from 0.01 to 0.1 fraction of bulk volume. Generally, fracture apertures range from 0.05 to 2 *mm*, and diffusion into the porous matrix is about ten times smaller than molecular diffusion in water. Therefore, assuming the following values for each of the parameters:

$$\phi = 0.05$$
$$b = 1\ mm$$
$$D_a = 1.10^{-6} cm^2/sec$$
$$(0.36\,10^{-6} m^2/hr)$$

A representative field parameter value of λ can be calculated as:

$$\lambda = \frac{\phi\sqrt{D_a}}{b} = 0.03\frac{1}{\sqrt{hr}} \qquad (3.30)$$

In short injection period field tests, 2 to 48 hrs, tracer return profiles should be similar to the ones in Figs. 3.16 and 3.17. Hence, using the Stehfest[82] algorithm to evaluate theoretical tracer return profiles should be avoided.

Evaluation of solutions by numerical integration requires long computation times making a regression analysis in a small computer infeasible. On the other hand, numerical Stehfest inversion of the solutions requires little computation time.

3.4 THERMAL INJECTION-BACKFLOW TESTS

In this section, the possibility of determining thermal characteristics of a system by thermal injection-backflow tests is explored. Tracer tests identify fast flow paths, but estimation of the thermal breakthrough based on tracer data has sometimes been considered ambiguous[66] because of the assumptions about the geometry of the flow path, and other properties of the system such as the porosities of the

flow path and the adjacent matrix. The fracture aperture is the most important parameter affecting the propagation of the thermal front. It can be estimated by Eq. **3.8.** However, Eq. **3.8** can be used only if the condition of Taylor Dispersion, Eq. **3.3,** is satisfied. Therefore, nonisothermal injection tests have been proposed to determine the thermal characteristics of a system[66].

Pruess *et. al.*[66] argued that while tracer breakthrough time is determined by the volume of the flow path, thermal breakthrough is determined by the available surface area for heat transfer from the matrix to the fracture. **As** a result, the speed of the thermal front is only partially determined by the speed of the tracer. They proposed thermal interference tests to make reliable estimates of the thermal characteristics of fast flow paths. They reported that these tests had been carried out in several small experimental hot dry rock reservoirs[33,86]. However, a thermal interference test on a large scale requires a test period of duration similar to the thermal breakthrough time. **A** small scale test is also unattractive, since it requires drilling a new observation well into the zone connecting the injector and the producer, which is a costly operation. It is also possible that the observation well would not intersect the fast flow path. Therefore, if no thermal drawdown data **are** available, which is the case for most fields, the thermal interference analysis must be based on nonthermal means.

3.4.1 The Analysis Technique

A thermal injection-backflow test may be the best way to estimate the thermal characteristics of a system to avoid high cost or extremely long test period of thermal interference tests. The heat and the tracer transport mechanisms in porous media are nearly identical in form. The transport of both heat and tracer may be modelled by the same differential equations. In fact, the MD and AD models were originally developed to study the temperature distribution in an oil layer during a hot fluid injection. The solution to the MD model, which was developed for the analysis of injection-backflow tracer tests is used to interpret temperature return profiles from thermal injection-backflow tests. In this case, the dependent variable of the system is temperature, and the parameter of the model, λ_D, for flow in a porous stream

tube, is:

$$\lambda_D = \frac{\sqrt{k_m \rho_m c_m}}{\phi_f b \rho_w c_w} \sqrt{t_j} \tag{3.31}$$

Whether the Taylor dispersion condition is satisfied or not, the fluid transit time, t_j, from the interwell tracer tests and **Eq. 3.31** can be used to estimate the thermal breakthrough time.

In heat transport problems, a dimensionless temperature variable is:

$$T_D = \frac{T - T_o}{T_{in} - T_o} \tag{3.32}$$

The thermal breakthrough time, if equal the breakthrough time of $T_D = 0.75$, is[66]:

$$t_t = \frac{\rho_1 c_1}{\rho_w c_w} \frac{t_w}{\phi_f} + \frac{\lambda_D^2}{tj} \frac{t_w^2}{0.81342} \tag{3.33}$$

The contribution of the first group of terms in **Eq.3.33** is small compared to the contribution of the second group of terms, because the lateral heat conduction is the main mechanism retarding propagation of the thermal front. In other words, it is the parameter λ which influences the thermal breakthrough time most. The parameter, t_w, must be determined by tracer tests.

3.4.2 Estimation of the Thermal Breakthrough

Determining the parameter λ_D from a thermal injection-backflow test and t_j from an interwell tracer test, the thermal breakthrough time can be estimated. The only assumption is that flow occurs in a single vertical fracture and lateral heat conduction is the main mechanism retarding the propagation of the thermal front. In fact, the assumption that the flow path is vertical can be removed since the solution (Eq. **3.29)** is valid for both linear and radial flow geometries, and for other general flow paths. The breakthrough time (Eq. 3.33), however, must be modified according to the assumed geometry. Eq. **3.33** can be used to estimate the breakthrough time for any flow path with a constant surface to volume ratio independent of the position. As for radial flow, a similar expression can be derived by using the solution for unidirectional flow.

ϕ	k_w $W/m°C$	PW kg/m^3	c_w $kJ/kg°C$	k_r $W/m°C$	ρ_r kg/m^3	c_r $kJ/kg°C$	t_j hrs	t_w hrs
0.05	0.677	890	4.371	2.855	2640	0.82	1	50

Table 3.7: Thermal Properties of the System

$\phi_f b\,(mm)$	0.5	1	2	5	10	50
$\lambda_D/\sqrt{t_j}$	76.6	38.3	19.2	7.6	3.8	0.76
$t_t\,(years)$	2531	633	159	25	6	0.25

Table 3.8: Estimated Thermal Breakthrough Times

Using the values given in Table 3.7 for the rock and fluid properties[38,71] and for $t_j = 1\,hr$ and $t_w = 50\ hrs$, corresponding thermal breakthrough times were calculated and are given in Table 3.8.

From Table 3.8 and Fig. 3.18, for $\phi_f b$ values less than $2\,mm$, temperature return profiles of the zones with $\phi_f b \leq 2\,mm$ cannot be differentiated from each other. However, premature breakthrough is not a concern for any of these paths. In cases of $\phi_f b \geq 5\,mm$, it is important to design short injection period tests since as t_j increases, the return profiles tend to converge to a single curve. Therefore, a carefully designed thermal injection-backflow test with a small t_j is essential for an estimation of the thermal breakthrough time.

While the effect of temperature on some of the rock and the fluid properties such as $\rho_w c_w$ and $\rho_r c_r$ are not important others such as k_w and k_r may be affected

by temperature. In Table 3.7 the properties of water were evaluated at $176°C$, and the reservoir rock was assumed to be granitic. It is reported[71] that k_r of granite may have values ranging from 1.73 to 3.98. If k_r is taken to be 1.73, then for $\phi_f b = 1mm$, the corresponding thermal breakthrough time in Table 3.8 would have decreased from 633 to 398 years. This demands an accurate determination of the thermal conductivity of the rock. An in-situ determination of thermal conductivity and other parameters as well may be achieved by using thermal injection-backflow tests.

Thus, the results of a well-planned thermal injection-backflow test and the results of an interwell tracer test can provide estimates of thermal breakthrough times during reinjection processes.

In summary, any method of estimating the thermal breakthrough time must be based on both tracer and thermal data. This section contains quantitative interpretation techniques of tracer tests and thermal injection-backflow tests, and development of a new method to estimate thermal breakthrough times.

Depending on the scale of heterogeneities relative to the scale of flow, one of the four approaches namely, the very near field, the near field, the far field and the very far field may be used to model tracer and heat transport through fractures. In geothermal reservoirs, extremely fast fluid movements and asymmetric tracer return profiles of interwell tracer tests indicate that the scale of fractures is in the order of the scale of flow. Therefore, tracer return profiles should be interpreted by using the very near field approach. Based on this approach, quantitative interpretation techniques of interwell tracer tests with and without recirculation, and injection-backflow tests are presented.

Tracer return profiles are matched with the solutions of three mathematical models(CD,MD and **AD)** developed to study tracer transport through a single vertical fracture. Matching tracer return profiles with solutions of mathematical models provides estimates of three parameters:

- t_w, a measure of flow speed,
- D, a measure of dispersive characteristics,

- λ, a measure of fracture-matrix interaction.

Estimating the thermal breakthrough time may be based solely on tracer data. The two parameters D, and λ can be used to estimate the fracture aperture b, the most important parameter controlling the propagation of thermal front. However, estimating b from D requires that $P_e \simeq 500 - 1000$. For most of the tracer return profiles $P_e \ll 500$. Estimating b from λ is also questionable, since D_a and ϕ are usually unknown.

Alternatively, estimation of the thermal breakthrough time may be based solely on thermal interference tests. Thermal interference tests are infeasible, because durations of these tests are similar to thermal breakthrough times. Small scale thermal interference tests are also unattractive mainly because of high cost.

Finally, a new method of forecasting the thermal breakthrough time is developed by using interwell tracer tests and thermal injection-backflow tests. If Lauwerier model[50], which is equivalent to the MD model for tracer transport, is used to represent heat transport in the system, the thermal breakthrough time is given by Eq.3.33. Eq.3.33 requires two important parameters namely, water transit time t_w and λ_D which is a measure of thermal interaction between fracture and matrix. The parameter t_w is estimated from interwell tracer tests and λ is estimated from thermal injection-backflow tests.

In conclusion, the new method requires the following steps to estimate the thermal breakthrough time during reinjection:

1. estimate the water transit time t, from interwell tracer tests,
2. estimate the parameter λ_D from thermal injection-backflow tests,
3. substitute values of t, and λ_D into Eq. **3.33** to evaluate the thermal breakthrough time.

This new technique does not have the disadvantages of previously suggested methods namely, ambiguity of estimates from non-thermal methods and high cost and long periods of thermal interference tests.

Chapter 4

CONCLUSIONS

Major contribution of this study is development of a new method to estimate the thermal breakthrough time during reinjection in geothermal reservoirs. Following is a summary of this study on different aspects of tracer and thermal transients during reinjection. Also, recommendations for future work are listed.

4.1 SUMMARY

We presented a study of tracer and thermal transients during reinjection processes in geothermal reservoirs. Three mathematical models were used, namely, the CD, MD and AD models, developed to study tracer and heat transport in a single vertical fracture. The CD and AD models account for dispersive effects in the system.

In tracer studies, use of two concentration variables, namely resident and flux concentrations, has been equally common. The two concentrations differ whenever a system is dispersive, and there is a concentration gradient. Many solutions have been developed for the CD and AD models in both variables. Even though these solutions give similar numerical results in most cases, they differ significantly when dispersive effects are dominant. Therefore whenever a system is highly dispersive it is necessary to use a solution which is consistent with the conditions of the experiment. A distinction between these two concentration variables is also necessary

in:

- multidimensional simulators of tracer transport,
- miscible displacement experiments,
- water flooding, if modelled as a convective-dispersive process[73], especially in plotting the saturation profiles and the fractional flow curves,
- thermal injection processes[75,80] when dispersive effects are included, and
- thermal energy storage operations[76].

There are two approaches in treatment of the outlet boundary of a system. A zero gradient condition and the assumption that the outlet boundary does not affect the velocity distribution inside the system giving rise to the infinite medium flux-flux solution C_{CFF}. Many researchers are of the opinion that the second approach represents real systems better than the first approach. Since there is no proof supporting either, an example from the injection-backflow tracer tests have been evaluated to compare the two approaches. Fortunately, both approaches gave identical numerical results for observed field parameters. The C_{CFF} solution was used for interpreting tracer return profiles, first because of some experimental data supporting[26,61] it, and second because of its simple form.

We interpreted the return profiles from interwell tracer tests without recirculation in Wairakei, New Zealand. For the dispersive models, we used the C_{IFF} solutions, which are consistent with the actual conditions of the tests. The parameters were estimated by using a nonlinear regression technique. For all the tests, the estimates did not satisfy the Taylor dispersion condition. The fracture apertures estimated by using **Eq.** 3.9 were also high compared with values reported in the literature. However, the estimated fracture apertures were consistent with the tracer return profiles, which showed unusually high flow speeds indicating fast flow paths between injectors and producers. The estimated fracture apertures, however, are uncertain, because it was necessary to assume the matrix porosity.

Interwell tracer tests with recirculation are useful for determining both the degree of connectivity between the injector and producers, and the recirculating fluid

volume between them. New solutions to the mathematical models were developed to interpret the tracer return profiles from these tests. The solutions appear to be superior to previous methods, since the solutions specifically include recirculation effects, and can account for any number of recirculations. A study of the theoretical tracer return profiles generated by using the new solutions were presented.

Injection-backflow tests are useful to study dispersive characteristics of a reservoir near the test well. Solutions to the CD and MD models to interpret the tracer return profiles from injection-backflow tracer tests were developed. The CD model solutions depend on a parameter t_D which is the ratio of the dispersivity, a characteristic length of the system, to the length travelled by convective front during the injection period. If the condition for Taylor dispersion is satisfied, then the parameter t_D allows estimation of the fracture aperture b. If conducting a series of tests is economically feasible, using the results of tests with different flow rates, it is possible to determine whether dispersivity is scale dependent or not. The MD model solutions are dependent on the parameter λ_D, which allows an estimation of the product of the fracture porosity and the fracture aperture, $\phi_f b$.

The uncertainities of the estimates of thermal characteristics from tracer tests led to the investigation of thermal interference tests. We proposed thermal injection-backflow tests, which do not have high cost and extremely long test period disadvantages of thermal interference tests. To interpret temperature return profiles, the solution developed for analyzing tracer return profiles can be used. Using the parameters λ_D obtained from thermal injection-backflow tests, and t, obtained from interwell tracer tests, the thermal breakthrough time can be estimated which will help in designing the best reinjection scheme.

To develop the solutions to the models, single and double Laplace transformation methods were used. When the Laplace solutions were too complicated to invert analytically, or resulted in complicated integrals in real space, single and double numerical inversion methods based on Dubner and Abate[29], and Stehfest[82] algorithms were used. Double Laplace transformation has frequently been used to solve differential equations for semi-infinite mediums. We have used it to solve the MD model for injection-backflow tests. This allowed avoiding difficulties caused by

discontinuities in the injection period solutions in real space. It is a useful tool whenever an injection-backflow process such as thermal recovery processes and single well tests to estimate the residual oil saturations are involved. Especially using Dean's[24] model, it is possible to derive analytical solutions of single-well tracer test problems. It is also useful in well testing problems where superposition does not work such as a flow period followed by a shut-in period with different wellbore storage.

4.2 RECOMMENDATIONS

One of the main problems of tracer tests in geothermal reservoirs is to account for tracer flow in the wellbore. Since most of the time the tracer is introduced at the wellhead, the effect of flow in the wellbore on the concentration of the fluid stream entering the reservoir should be quantified. Similarly in thermal injection-backflow tests the heat gained by the cold fluid in the wellbore should be considered so that the temperature of the fluid entering the formation can be specified accurately.

Another important issue is the effect of temperature on the thermal properties of the reservoir. It seems that the properties $\rho_w c_w$ and $\rho_r c_r$ are not strongly dependent on temperature, however, the effect of temperature on the thermal conductivities should be investigated. If thermal conductivity decreases with decreasing temperature, the thermal breakthrough time may decrease significantly since the thermal breakthrough time is directly proportional to the thermal conductivity of the adjacent matrix. In such a case, use of pseudo temperature functions similar to the pseudo pressures in gas flow, or a temperature-square model may allow a better estimation of the thermal breakthrough time.

Using the method of Grove and Beetem[36], and the new solutions derived for interwell tests with recirculation, tracer return profiles from homogeneous formations can be analyzed. The new solutions have two advantages over solutions used by previous researchers. First, they can consider any number of recirculations. Second, they are easier to evaluate than the finite-system solution. Furthermore, a regression technique can be used to estimate parameters, rather than using trial

and error. In particular, assuming a dispersion coefficient proportional to the velocity squared, the problem can be simplified to a regression analysis for a single parameter function.

Double Laplace transformation may be used for well testing problems when the superposition technique does not work, such as for a flow period followed by a shut-in period with a different wellbore storage. The double Laplace transformation method may also be used for single well tracer tests to estimate residual oil saturations. Since, in Dean's model, the mass transfer coefficient between the flowing and the stagnant phases can be related to physical parameters [68,70,88], the technique becomes very attractive.

Bibliography

[1] Avdonin, N. A.: "Some Formulas for Calculating the Temperature Field of a Stratum Subject to Thermal Injection," *Nefti Gaz,* (1964), *3,* 37-41.

[2] Bahralolom, I., Bretz, R. E. and Orr, F. M. Jr.: " Experimental Investigation of the Interaction of Phase behavior With Microscopic Heterogeneity in a CO_2 Flood," *SPE Reservior Engineering,* (May 1988), 662-672.

[3] Baker,L. E.: "Effects of Dispersion and Dead-End Pore Volume in Miscible Flooding," *Soc. Pet. Eng. J.,* (June 1977), 219-227.

[4] Barker, J. A. : "Laplace Transform Solutions for Solute Transport in Fissured Aquifers," *Adv. Water Resour.,* (1982), *6,* 98-104.

[5] Barker, J. A. : "Block Geometry Functions Characterizing Transport in Densely Fissured Media,'' **J.** *Hydrol.,* (1985), *7,* **263-279.**

[6] Barry, D. A. and Sposito, G.: " Application of the Convection-Dispersion Model to Solute Transport in Finite Soil Columns," *Soil Sci. Am. J.,* (1988), **52, 3-9.**

[7] Bear, J.: *Dynamics of Fluids in Porous Media,* Elsevier, New York, (1972), **579-582** and **629.**

[8] Bear, J. and Berkowitz, B: " Groundwater Flow and Pollution in Fractured Aquifers," *Developments in Hydraulic Engineering, Vol.4* , P. Novak (Editor), Elsevier, London, (1987), **175-235.**

[9] Brenner, H.: "The Diffusion Model of Longitudinal Mixing in Beds of Finite Length. Numerical Values," *Chem. Eng. Sci.,* (1962), *17,* 229-249.

[10] Bretz, R. E. and Orr, F. M. Jr.: " Comparison of Analytical and Explicit Finite Difference Solutions of the Convection-Dispersion Equation," PRRC report 85-6, (1985), New Mexico petroleum Recovery Research Center.

[11] Bretz, R. E., Specter, R. M. and Orr, F. M. Jr.: " Mixing During Single Phase Flow in Reservoir Rocks: Models, Effects of Pore Structure and Interpretaion of Experiments," *Reservoir Characterization,* Lake, L. W. and Carroll, H. B. Jr.(Editors) Academic Press Inc., Orlando, (1986), 584-641.

[12] Bretz, R. E. and Orr, F. M. Jr.: " Interpretation of Miscible Displacements in Laboratory Cores," *SPE Reservior Engineering,* (Nov. 1987) 492-500

[13] Bretz, R. E. and Orr, F. M. Jr.: " Eeffect of Pore Structure on Miscible Displacement in Laboratory Cores," *SPE reservior Engineering,* (Aug. 1988), 857-866.

[14] Bullivant, D. P.: "Tracer Testing of Geothermal Reservoirs," Ph.D. Thesis, Department of Theoretical and Applied Mechanics, School of Engineering, University of Auckland, Auckland, New Zealand, (1988).

[15] Brigham, W. E., Reed, P. W. and Dew, J. N.: "Experiments on Mixing During Miscible Displacement in Porous Media," *Soc. Pet. Eng. J., Trans. AIME, 222,* (March 1961), 1-8.

[16] Brigham, W. E.: "Mixing Equations in Short Laboratory Cores," *Soc. Pet. Eng.* J., (1974), *14,* 91-99.

[17] Budd C. F. Jr.: " Geothermal Energy for Electrical Generation," J. *Pet. Tech.,* (Feb. 1984), 189-195.

[18] Carslaw, H. S. and Jeager, J. C.: *Conduction of Heat in Solids,* Clarendon Press, Oxford, (1986), 75-77

[19] Clark, R. T.: "A Review of Some Mathematical Models Used in Hydrology with Observations on Their Calibration and Use," *J. Hydr.,* (1973), *19,* 1-20.

[20] Coats, K. H. and Smith, B. D. : "Dead-end Pore Volume and Dispersion in Porous Media,'' *Soc. Pet. Eng. J., Trans. AIME, 231,* (March 1964), 73-84.

[21] Correa, A. C., Pande, K. K., Ramey, H. J. Jr. and Brigham, W. E.: "Prediction and Interpretation of Miscible Displacement Using a Transverse matrix Dispersion Model," (Sep. 1987), *SPE Paper # 16704.*

[22] Danckwerts, P. V.: "Continuous Flow Systems," *Chem. Eng. Sci.,* (1953), *2,* 1-13.

[23] Davies, B. and Brian, M.: "Numerical Inversion of the Laplace Transform: a Survey and Comparison of Methods," *J. Comput. Phys.,* (1979), *33,* 1-32.

[24] Deans, H. A. : "A Mathematical Model for Dispersion in the Direction of Flow in Porous Media,'' *Soc. Pet. Eng. J., Trans. AIME, 228,* (March 1963), 49-52.

[25] De Marsily, G.: *Quantitative Hydrology: Groundwater Hydrologyfor Engineers,* Academic Press Inc. , Orlando, (1986), 242-243.

[26] De Smedt, F., Wierenga, P. J. and Van der Beken, A.: *Theoretical and Experimental Study of Solute Movement Through Porous Media with Mobile and Immobile Water,* Vrije Universtait Brussel, Brussel, (1981).

[27] De Vries, M.: "Applicability of Fluorescent Tracers," *Tracer Techniques in Sediment Transport,* Int. Atomic Energy Agency I.A.E.A., Vienna 1973, 105-123.

[28] Ditkin, V.A. and Prudnikov, A. P.: *Operational Calculus in Two variables,* Int. Ser. Pure Appl. Math., Pergamon Press, London, (1962), 46-47.

[29] Dubner, H. and Abate, J.: "Numerical Inversion of Laplace Transforms by Relating Them to the Finite Fourier Cosine Transform," *J. ACM.,* (Jan. 1968) 15, 1, 115-123.

[30] Fried, J. J. : *Groundwater Pollution* Elsevier, New York, (1971a), 6-8.

[31] Fossum, M. P.: "Tracer Analysis in a Fractured Geothermal Reservoir: Field Results From Wairakei, New Zealand," Stanford Geothermal Program, SGP-TR-56, Stanford, **CA,** (1982).

[32] Fried, J. J. and Combarnous, M. A. : "Dispersion in Porous Media," *Adv. Hydrosciences,* (1971b), *7,* 169-282.

[33] Gringarten, A. C., Witherspoon, P. **A.** and Ohnishi, Y.: "Theory of Heat Extraction From Fractured Hot Dry Rock," **J.** *Goephys. Res.,* (1975), 80, 8, 1120-1**124.**

[34] Grisak, G. E. and Pickens, J. F. : "Solute Transport Through Fractured Media, 1. The Effect of Matrix Diffusion," *Water Resour. Res.,* (1980a), *16,* 719-730.

[35] Grisak, G. E., Pickens, J. F. and Cherry, J. **A.** : "Solute Transport Through Fractured Media, 2. Column Study of Fractured Till ," *Water Resour. Res.,* (1980b), 16, 731-739.

[36] Grove, D. B. and Beetem, W. **A.:** "Porosity and Dispersion Constant Calculations for a Fractured Carbonate Aquifer Using the Two Well Tracer Method,'' *Water Resour. Res.* (1971), *7,* **128-134.**

[37] Haberman, **R.:** *Elementary Applied Partial Differential Equations,* Prentice-Hall, Englewood Cliffs, (1983), **360-361.**

[38] Holman, J. P.: *Heat Transfer,* 4th ed., Mc-Graw-Hill Kogakusha LTD., Tokyo, (1976), 499-507.

[39] Horne, R. N. and Rodriguez, J.: "Dispersion in Tracer Flow in Fractured Geothermal Systems," *Proceedings, 7th Annual Stanford University Geothermal Workshop,* (1981).

[40] Horne, R. N.: "Geothermal Reinjection Experience in Japan," **J.** *Pet. Tech.,* (March 1982a), 495-503.

[41] Horne, R. N.: "Effects of Water Injection into Fractured Geothermal Reservoirs : A Summary of Experience Worldwide," *Geothermal Resources Council*, Davis, CA (1982), Special Report 12, 47-63.

[42] Ito, J. Kubota, Y. and Kurosawa, M.: " Tracer Tests of the Geothermal Hot Water at the Onuma Geothermal Power Station," *Japan Geothermal Energy Association Journal,* Vol. **15,** no. 2, (series **57**), (June 1978), p.87 (in Japanese).

[43] Jensen, C. L. and Horne, R. N.: "Matrix Diffusion and Its Effect on the Modelling of Tracer Returns From the Fractured Geothermal Reservior at Wairakei, New Zealand," *Proceedings,* Ninth Workshop on Geothermal Engineering, Stanford U., Stanford, CA (Dec. 1983).

[44] Johns, R. A.: " Experimental Investigation of the Flow of Tracers in Fractured Cores," Stanford Geothermal Program, SGP-TR-113, Stanford, CA (June 1987).

[45] Kocabas, I. and Horne, R. N.: "Analysis of Injection-Backflow Tracer Tests in Fractured Geothermal Reservoirs," *Proceedings,* Thirteenth Workshop on Geothermal Engineering, Stanford U., Stanford, CA (Jan. 1987).

[46] Kocabas, I. : "Analysis of Injection-backflow Tracer Tests" Stanford Geothermal Program, SGP-TR-96, Stanford, CA, (1986).

[47] Kreft, **A.** and Zuber, A.: "On the Physical Meaning of the Dispersion Equation and its Solutions for Different Initial and Boundary Conditions," *Chem. Eng. Sci.* **33,** (1978), **88, 1471-1480.**

[48] Kreft, A. and Zuber, A.: "On the Use of the Dispersion Model of Fluid Flow," *Int. J. Appl. Rad. Isot.* (1979), *30,* 705-708.

[49] Kreft, A. and Zuber, A.: "Comments on Flux-Averaged and Volume Averaged Concentrations in Continuum Approaches to Solute Transport by J. C. Parker and M. Th. van Genuchten," *Water Resour. Res.,* (1986), *22,* **7, 1157-1158.**

[50] Lauwerier, H. **A.:** "The Transport of Heat in an Oil Layer Caused by the Injection of Hot Fluid," *Appl. Sci. Res.*, (1955), **5,** 2-3, 145-150.

[51] Levenspiel, **O.** and Turner, J. C. R.: "The Interpretation of Residence-Time Experiments," *Chem. Eng. Sci.,* (1970), **25,** 1605-1608.

[52] Malozewski, P. and Zuber, A. : "Interpretation of Artificial and Environmental Tracers in Fissured Rocks with **a** Porous Matrix," Isotope Hydrology, Int. Atomic Energy Agency (I.A.E.A), Vienna, (1983), 635-651.

[53] Malozewski, P. and Zuber, A. : "On the Theory of Tracer Experiments in Fissured Rocks with **A** Porous Matrix," *J. Hydr.,* (1985), 79, 333-358.

[54] McCabe, J. W., Manning, M. R. and Barry, B. J.: "Tracer Tests-Wairakei," *Institute* of *Nuclear Sciences Report* INS-R-275, Dept. of Scientific and Industrial research, Lower Hutt, New Zealand, (1980), Geothermal Circular WJMcC 2.

[55] Nauman, E. B.: "Residence Time Distributions in Systems Governed by Dispersion Equation," *Chem. Eng. Sci.,* (1981), *36,* 957-966.

[56] Nauman, E. B. and Buffham, B. **A.:** "Mixing in Continuous Flow Systems," John Wiley & Sons Inc., New York, (1983), 97-100.

[57] Neretnieks, I. : "Diffusion in the **Rock** Matrix. An Important Factor in Radionuclide Retardation?" J. *Geophys. Res.,* (1980), *85,* B8, 4379-4397.

[58] Neretnieks, I., Eriksen, T. and Tahtinen, P. : "Tracer Movement in a Single Fissure in Granitic Rock. Some Experimental Results and Their Interpretation," *Water Resour. Res.,* (1982), *18,* 849-858.

[59] Neretnieks, I. : **"A** Note on Fracture Flow Mechanisms in the Ground," *Water Resour. Res.,* (1983), *19,* 364-370.

[60] Parker, J. C. and van Genuchten M. Th.: "Flux-Averaged and Volume-Averaged Concentrations in Continuum Approaches to Solute Transport," *Water Resour. Res.* (1984a), *LO* 7, 866-872.

[61] Parker, J. C.: "Analysis of Solute Transport in Column Tracer Studies," *Soil. Sci. Soc. Am.*, (1984b), *48,* 719-724.

[62] Parlange, J. Y., Barry, D. A. and Starr, J. L.: "Comments on Boundary Conditions for Displacement Experiments Through Short Laboratory Soil Columns," *Soil Sci. Soc. Am. J.*, (1985), *49,* 1325-1326.

[63] Passioura, J. B.: "Hydrodynamic Dispersion in Aggregated Media: I. Theory," *Soil Sci.*, (1971a), 9, 6, 339-344.

[64] Passioura, J. B. and Rose, D. A.: "Hydrodynamic Dispersion in Aggregated ,Media: 2. Effects of Velocity and Aggregate Size," *Soil Sci.*, (1971b), *3,* 6, 345-351.

[65] Perkins, R. K. and Johnstone, O. C. : "A Review of Diffusion and Dispersion in Porous Meida," *Soc. Pet. Eng. J.*, (March 1963), 70-84.

[66] Pruess, K. and Bodvarsson, G. S.: "Thermal Effects of Reinjection in Geothermal Reservoirs With Major Vertical Fractures,'' J. *Pet. Tech.*, (September 1984), 1567-1578.

[67] Pickens, J. F. and Grisak, G. E.: "Scale-Dependent Dispersion in a Stratified Granular Aquifer," *Water Resour. Res.*, **(1981) 2 7 4,** 1191-1211.

[68] Rao, P. S. C., Jessup, R. E., Rolston, D. E., Davidson, J. M., and Kilcrease, D. P.: "Experimental and Mathematical Description of Nonadsorbed Solute Transfer by Diffusion in Spherical Aggregates," *Soil. Sci. Soc. Am. J.*, (1980a), *44,* 684-688.

[69] Rao, P. S. C., Jessup, R. E., Rolston, D. E., Davidson, J. M., and Kilcrease, D. P.: "Solute Transport in Aggregated Porous media: Theoretical and Experimental Evaluation," *Soil Sci. Soc. Am. J.*, (1980b), *44,* 1139-1146.

[70] Rao, P. S. C. and Jessup, R. E. and Addiscott, T. M.: "Experimental and Theoretical Aspects of Solute Diffusion in Spherical and Nonspherical Aggregates," *Soil Sci.*, (1982), *133,* 6, 342-349.

[71] Reynolds, W. C. and Perkins, H. C.: *Engineering Thermodynamics,* 2nd ed., McGraw-Hill, New York, (1977).

[72] Riley, M. F.: Personal Communication, (1989), Department of Petroleum Engineering, Stanford University, Stanford, CA.

[73] Rosales, C. P., Cardenas, F. C. P., and Hernandez, J. C.: "Waterflooding as a Convection-Dispersion Process," (Aug. 1988), *SPE Paper # 18732.*

[74] Satman, **A.:** " Reinjection, " *Reservoir Engineering Assessment of Geothermal Systems,* H. J. Ramey, Jr., (Editor), Department of Petroleum Engineering, Stanford University, (1981), 10.3-10.18.

[75] Satman, A., Zolotukhin, A. B. and Brigham, W. E.: "A New Approach for Predicting the Thermal Behavior in Porous Media During Fluid Injection," *Geoth. Resour. Council, Trans.,* (1979), 621-624.

[76] Sauty, J. P., Gringarten, A. C. and Landel, P. A.; "The Effect of Dispersion on Injection of Hot Water in Aquifers," *Proceedings* of *Second Invitational Well Testing Symposium,* Lawrence Berkeley Lab., Berkeley, Calif., (1979), 122-131.

[77] Sauty, J. P. : "An Analysis of Hydrodispersive Transfer in Aquifers," *Water Resour. Res.,* (1980), *16,* 1,69-103.

[78] Snyder, W. M. and Stall, J. B. : "Men, Models, Methods and Machines in Hydrologic Analysis,'' J. *Hydr. Div., ASCE,* (1965), *91,* 85-89.

[79] Spiegel, M. R.: *Mathematical Handbook: of Formulas and Tables, Schaum's Outline Series in Mathematics,* McGraw-Hill, New-York, (1968), 110-111.

[80] Spillette, A. G.: "Heat Transfer During Hot Fluid Injection into an Oil Reservoir," J. *Can. Pet. Tech.,* (1965), 213-217.

[81] Stakgold, I.: *Green's Functions and Boundary Value Problems,* John Wiley & Sons, New York, (1979), 45-46 and 77-80.

[82] Stehfest, H.: "Numerical Inversion of Laplace Transforms," *Communications, ACM 13,* (1970), 144-149.

[83] Tang, D. H., Frind, E. O. and Sudicky, E. A. : "Contaminant Transport in a Fractured Porous Media: Analytical Solution for a Single Fracture," *Water. Resour. Res.,* (1981), *18,* 1634-1642.

[84] Taylor, G.: "Dispersion of Soluble Matter in Solvent Flowing Slowly Through a Tube," *Proc. Roy. Soc. Ser. A 219,* (1953), 186-203.

[85] Taylor, G.: "Conditions Under Which Dispersion of a Solute in a Stream of Solvent can be Used to Measure Molecular Diffusion," *Proc. Roy. Soc. Ser. A 225,* (1954), 473-477.

[86] Tester, J. N., Bivins, R. L. and Potter, R. M.: " Interwell tracer Analysis of a Hydraulically Fractured Granitic Geothermal Reservoir," *SPEJ*, (Aug. 1982), 537-554.

[87] van Genuchten, M. Th. and Parker, J. C.: "Boundary Conditions for Displacement Experiments Through Short Laboratory Soil Columns," *Soil Sci. Soc. Am.,* (1984), *48,* 703-708.

[88] van Genuchten, M. Th.: "A General Approach to Modelling Solute Transport in Structured Soils," *International Association of Hydrogeologists Memoires, Hydrogeology of Rocks of Low Permeability, XVII, Part 2 Proceedings,* Tucson, Arizona, (1985), 513-524.

[89] Voelker, D. and Doetsch, G.: *Die Zwiedimensionale Laplace-Transformation* Birkhauser, Basel Switzerland, (1950), 186-187.

[90] Webster, D. S., Proctor, J. F. and Marine, I. W.: "Two-Well Tracer Test in Fractured Crystalline Rock," *U.S. Geol. Surv. Water Supply Pap.,* 1544-1, (1964), 215-230.

[91] Wehner, J. F. and Wilhelm, R. H.: "Boundary Conditions of Flow Reactor," *Chem. Eng. Sci.,* (1956), *6,* 89-93.

[92] White, C. D.: Personal Communication, (1986), Department of Petroleum Engineering, Stanford University, Stanford, CA.

[93] Zuber, **A.:** "Theoretical Possibilities of the Two-Well Pulse Method," *Isotope Techniques in Grounwater Hydrology, Int. Atomic Energy Agency (I.A.E.A),* Vienna, (1974), **I.,** 277-297.

[94] Zuber, **A.:** "Models for Tracer Flow," *Tracer Methods in Isotope Hydrology. Int. At. Energy Agency (I.A.E.A),* Report TECDOD-291 Vienna, (1983), 67-112.

[95] Zuber, **A.:** "Mathematical Models for the Interpretation of Environmental Radioisotopes in Groundwater Systems,'' *Handbook* **of** *Environmental Isotope Geochemistry, Vol. 2.*, P. Fritz and J. CH. Fontes (Editors), Elsevier, Amsterdam, (1985), 1-60.

Appendix A

Nomenclature

A = cross-sectional area of preferential flow path

b = fracture aperture

C = resident concentration variable of fracture transport equations

C_F = flux concentration variable (ratio of the tracer flux to volumetric flux)

C_m = concentration variable of matrix transport equations (related to the resident concentration of the fracture equations)

C_0 = concentration of the injected fluid

C_R = resident concentration variable (amount of tracer per unit volume of the system)

C_r = a reference concentration (concentration that would be obtained if all the injected tracer were to mix in the recirculating fluid volume)

C^* = a reference concentration (ratio of the total tracer generated per unit time by a source to the volumetric flow rate in the system)

C_1 = concentration of the first unit in a three-unit system to study specification of boundary conditions

C_2 = concentration of the last (third) unit in three unit system to study specification of boundary conditions

c_m = specific heat of the immobile(matrix) phase

c_r = specific heat of the reservoir rock

c_w = specific heat of water

c_1 = specific heat of the mobile(fracture) phase
D = longitudinal dispersion coefficient
D_a = apparent diffusion coefficient (diffusion coefficient in a porous matrix in this study)
D_j = longitudinal dispersion coefficient during injection period if injection and backflow rates are different
D_m = coefficient of molecular diffusion in water
D_1 = longitudinal dispersion coefficient in the first unit
D_2 = longitudinal dispersion coefficient in the third(last) unit
H = Heaviside step function
i = complex constant, $\sqrt{-1}$
J = total tracer flux
J_m = dependent variable of matrix transport equation when fracture transport equation has J as its dependent variable
k = constant in a linear reaction term
k_m = thermal conductivity of the immobile(matrix) phase
k_r = thermal conductivity of the reservoir rock
k_w = thermal conductivity of water
L = length of a finite system (distance between the injector and the producer in interwell tracer tests)
L_t = length over which the tracer has spread
m = amount of tracer injected into the system (or generated by a source in the system)
m' = amount of tracer generated per unit time by a source in the system
Δm = tracer in AV of fluid
$\Delta m'$ = tracer crossing A in At
P_e = Peclet number
p = Laplace space variable (corresponding to the backflow time variable)
Q = volumetric flow rate in the system
Q_r = volumetric injection rate
q = a source/sink in the system (amount of tracer generated/lost per

unit volume of the system per unit time)

s = Laplace space variable (corresponding to the injection period time variable)

T = temperature of the fracture

T_D = dimensionless fracture temperature

T_{Dm} = dimensionless matrix temperature

T_i = i^{th} transformation linking two solutions of dispersive models

T_{in} = temperature of the injected fluid

T_0 = initial temperature of the system

t = time variable of the transport equations

t_b = tracer breakthrough time

t_D = inverse Peclet number scaled to the distance travelled by the convective front during the injection period

t_{Di} = dimensionless injection time variable

t_{Dp} = dimensionless backflow time variable

t_j = injection period

t_p = peak arrival time of a tracer slug

t_t = thermal (temperature) breakthrough time

t_{tr} = tracer transit time in a constant volume system

t_w = water transit time (breakthrough time of the convective front)

t' = integration variable of time

Δt = a small time interval

u = flow velocity (volumetric flux)

u_j = flow velocity during injection period, if injection and backflow rates are unequal

u_1 = flow velocity in the first unit

u_2 = flow velocity in the third(last) unit

x = space variable along the flow direction

x_D = dimensionless space variable

x' = integration variable of space

x'_D = dimensionless integration variable

Δx = length of a small segment of the system
y = space variable perpendicular to the flow direction
V = total injected fluid volume in an injection-backflow test
V_r = recirculating fluid volume in an interwell tracer test
ΔV = a small volume of fluid in the system
$\Delta V'$ = a small volume of fluid crossing A in At
α_i = i^{th} nonlinear parameter of a regression function
β_i = i^{th} linear parameter of a regression function
$\delta(x)$ = Dirac delta function for space variable
$\delta(t)$ = Dirac delta function for time variable
η = integration variable of the solution of the MD model for injection-backflow tests
θ = integration variable of the solution to the MD model for injection-backflow tests
λ = parameter accounting for tracerwise or thermal interaction between fracture and matrix
λ_D = dimensionless parameter accounting for fracture matrix interaction
ρ_m = density of immobile(matrix) phase
ρ_r = reservoir rock density
ρ_w = water density
ρ_m = density of mobile(fracture) phase
ϕ = matrix porosity
ϕ_f = preferential flow path(fracture) porosity
ω = Fourier space variable (corresponding to the space variable x)
Ω = domain of a partial differential equation
$\partial\Omega$ = boundaries of the domain of a partial differential equation
$-$ = indicates single Laplace transformation
$=$ = indicates double Laplace transformation

Appendix B

Derivatives of Solutions-No Recirculation

The regression routine VARPRO uses the derivatives of the function with respect to nonlinear parameters (See Fossum[31] for details of using VARPRO). Hence, the derivatives of solutions to transport models are presented in the following:

B.1 Derivatives of the CD Model

The CD Model solution has two nonlinear parameters and its derivatives are:

$$C_{IFF} = \frac{\beta}{\sqrt{4\pi\alpha_1\alpha_2 t^3}} \exp\left(-(1-\alpha_2 t)^2/(4\alpha_1\alpha_2 t)\right) \tag{B.1}$$

$$\frac{\partial C_{IFF}}{\partial \alpha_1} = \left[\frac{(1-\alpha_2 t)^2}{4\alpha_1\alpha_2 t} - \frac{1}{2}\right] \frac{C_{IFF}}{\alpha_1} \tag{B.2}$$

$$\frac{\partial C_{IFF}}{\partial \alpha_2} = \left[\frac{2\alpha_2 t(1-\alpha_2 t) + (1-\alpha_2 t)^2}{4\alpha_1\alpha_2 t} - \frac{1}{2}\right] \frac{C_{IFF}}{\alpha_2} \tag{B.3}$$

B.2 Derivatives of the MD Model

The MD Model solution has two nonlinear parameters and its derivatives are:

$$C_I = \beta H(t-\alpha_2)\,\frac{\alpha_1\alpha_2}{\sqrt{\pi(t-\alpha_2)^3}}\,\exp\left(-\frac{(\alpha_1\alpha_2)^2}{(t-\alpha_2)}\right) \tag{B.4}$$

$$\frac{\partial C_I}{\partial \alpha_1} = \left[1 - \frac{2(\alpha_1\alpha_2)^2}{t-\alpha_2}\right]\,\frac{C_I}{\alpha_1} \tag{B.5}$$

$$\frac{\partial C_I}{\partial \alpha_2} = \left[1 + \frac{3\alpha_2}{2(t-\alpha_2)} - \frac{2(\alpha_1\alpha_2)^2}{t-\alpha_2} - \frac{\alpha_1^2\alpha_2^3}{(t-\alpha_2)^2}\right]\,\frac{C_I}{\alpha_2} \tag{B.6}$$

B.3 Derivatives of the AD Model

The **AD** Model solution has three nonlinear parameters and its derivatives are:

$$\overline{C}_{IFF} = \beta\,\exp^{(1/(2\alpha_1))}\,\exp\left(-\sqrt{1/(4\alpha_1^2) + (s+2\alpha_3\sqrt{s})/(\alpha_1\alpha_2)}\right) \tag{B.7}$$

$$\frac{\partial \overline{C}_{IFF}}{\partial \alpha_1} = \left[\frac{1/(2\alpha_1) + (s+2\alpha_3\sqrt{s})/\alpha_2}{\sqrt{1/(4\alpha_1^2) + (s+2\alpha_3\sqrt{s})/(\alpha_1\alpha_2)}} - 1\right]\,\frac{\overline{C}_{IFF}}{2\alpha_1^2} \tag{B.8}$$

$$\frac{\partial \overline{C}_{IFF}}{\partial \alpha_2} = \left[\frac{(s+2\alpha_3\sqrt{s})/(\alpha_1\alpha_2)}{\sqrt{1/(4\alpha_1^2) + (s+2\alpha_3\sqrt{s})/(\alpha_1\alpha_2)}}\right]\,\frac{\overline{C}_{IFF}}{2\alpha_2} \tag{B.9}$$

$$\frac{\partial \overline{C}_{IFF}}{\partial \alpha_3} = \left[\frac{-\sqrt{s}/(\alpha_1\alpha_2)}{\sqrt{1/(4\alpha_1^2) + (s+2\alpha_3\sqrt{s})/(\alpha_1\alpha_2)}}\right]\,\overline{C}_{IFF} \tag{B.10}$$

Appendix *C*

Derivation of Solutions-Recirculation

Solutions to transport models for recirculating flow are derived as follows:

C.1 The AD Model Solution

The **AD** model transport equation of flow in a fracture, in terms of the flux concentration variable, is:

$$\frac{\partial C}{\partial t} + u\frac{\partial C}{\partial x} - D\frac{\partial^2 C}{\partial x^2} + q = 0 \tag{C.1}$$

The equation of the transport in the matrix is:

$$D_a \frac{\partial^2 C_m}{\partial y^2} = \frac{\partial C_m}{\partial t} \tag{C.2}$$

The fluxes and the concentrations at the fracture matrix interface are equated by:

$$q = -\frac{2\phi D_a}{b} \left.\frac{\partial C_m}{\partial y}\right|_{y=0} \tag{C.3}$$

$$C(x,t) = C_m(x,0,t) \tag{C.4}$$

Initially, both the fracture and the matrix are assumed to be tracer free. Thus initial conditions are:

$$C(x,0) = C_m(x,y,0) = 0 \tag{C.5}$$

The matrix is assumed to be infinite, therefore, the outer boundary condition for the matrix equation is:

$$\lim_{y\to\infty} C_m(x,t) = 0 \tag{C.6}$$

Assuming that the outlet boundary does not influence the velocity distribution inside the system, we can follow a semi-infinite medium approach. Thus, the outer boundary condition becomes:

$$\lim_{x\to\infty} C(x,t) = 0 \tag{C.7}$$

The inner boundary condition is specified in terms of flux concentrations so that a flux concentration is obtained. Assume that the outflowing fluid at the production end is immediately reinjected into the system. Thus the lower boundary condition is:

$$C(0,t) = \frac{m}{Q}\delta(t) + C(L,t) \tag{C.8}$$

Taking the Laplace transformation of Eq. C.2 and imposing Eqs. C.4, C.5 and C.6 results:

$$\overline{C}_m = \overline{C}\exp\left(-(\sqrt{s}/\sqrt{D_a})y\right) \tag{C.9}$$

Substituting Eq. C.9 into the Laplace transform of Eq. **C.3** yields:

$$\overline{q} = -\lambda\sqrt{s}\,\overline{C} \tag{C.10}$$

The Laplace transform of Eq. C.1 is:

$$D\frac{\partial^2\overline{C}}{\partial x^2} - u\frac{\partial\overline{C}}{\partial x} - (s+\lambda\sqrt{s})\overline{C} = 0 \tag{C.11}$$

The source term, q, was transformed by using Eq. C.10. The solution of Eq. C.11 subject to the Laplace transforms of Eqs. C.5, C.7 and C.8, is:

$$\overline{C} = \frac{m}{Q}\frac{1}{(1-\exp(\kappa L))}\exp(\kappa x) \tag{C.12}$$

where:

$$\kappa = \frac{U}{2D} - \sqrt{u^2/(4D^2) + (4s/D) + (4/D)(2\lambda\sqrt{s})} \tag{C.13}$$

Solving Eq. C.12 at $x = L$ and rearranging, the Laplace space solution to the AD model in terms of the the variables β, α_1 and α_2 are:

$$\overline{C} = \beta\left(\exp^{-1/(2\alpha_1)}\exp\sqrt{1/(4\alpha_1^2)+(s+2\alpha_3\sqrt{s})/(\alpha_1\alpha_2)} - 1\right)^{-1} \tag{C.14}$$

C.2 The CD Model Solution

To obtain the CD model solution, it is not necessary to repeat the same procedure, since the solution can be derived from the **AD** model solution. When $\lambda = 0$, Eq. C.13 reduces to:

$$\kappa' = \frac{u}{2D} - \sqrt{u^2/(4D^2) + (4s/D)} \tag{C.15}$$

Replace x in Eq. C.12 by x' to obtain the Laplace space solution to the CD model:

$$\overline{C} = \frac{m}{Q}\frac{1}{(1-\exp(\kappa' L))}\exp(\kappa' x) \tag{C.16}$$

Using the binomial series expansion[79] given by:

$$\frac{1}{1-X} = \sum_{n=0}^{\infty} X^n = 1 + X + X^2 + \ldots \quad for \ |X| \leq 1 \tag{C.17}$$

Rewrite Eq. C.16 as:

$$\overline{C} = \frac{m}{Q}\exp(\kappa' x)\sum_{n=0}^{\infty}\exp(n\kappa' L) \tag{C.18}$$

Eq. C.18 may be inverted to obtain the real space solution to the CD model:

$$C = \frac{m}{Q}\sum_{n=0}^{\infty}\frac{nL+x}{2\sqrt{\pi D t^3}}\left(\frac{-(nL+x-ut)^2}{4Dt}\right) \tag{C.19}$$

Eq. C.19 can be solved at $x = L$ and rewritten in terms of parameters β, α_1 and α_2 as:

$$C = \frac{\beta}{2\sqrt{\pi\alpha_1\alpha_2 t^3}}\sum_{n=0}^{\infty}(n+1)\exp\left(-((n+1)-\alpha_2 t)^2/(4\alpha_1\alpha_2 t)\right) \tag{C.20}$$

C.3 The MD model Solution

The transport equation of the fracture is:

$$\frac{\partial C}{\partial t} + u\frac{\partial C}{\partial x} + q = 0 \tag{C.21}$$

Since Eq. C.21 is first order in the x variable, only one boundary condition must be specified along the flow direction. The matrix transport equation and the initial and boundary conditions are the same as those of the **AD** model.

The Laplace space solution of the matrix transport equation is given by Eq. C.9 and the source term is given by Eq. C.10. If we take the Laplace transform of Eq. C.21 and substitute Eq. C.10 in it we obtain

$$u\frac{\partial \overline{C}}{\partial x} - (s+\lambda\sqrt{s})\overline{C} = 0 \tag{C.22}$$

The solution of Eq. C.22 is:

$$\overline{C} = A\exp\left(-\frac{x}{U}s\right)\exp\left(-\frac{2x\alpha}{u}\sqrt{s}\right) \tag{C.23}$$

The constant **A** is determined by using the boundary condition given by Eq. C.8. The solution is:

$$\overline{C} = \frac{m}{Q}\frac{1}{(1-\exp(-\kappa_m L))}\exp(-\kappa_m x) \tag{C.24}$$

where κ_m is:

$$\kappa_m = \frac{s}{u} + \frac{2x}{u}\sqrt{s} \tag{C.25}$$

Using Eq. C.17, Eq. C.24 becomes:

$$\overline{C} = \frac{m}{Q}\exp(-\kappa_m x)\ \sum_{n=0}^{\infty}\exp(-n\kappa_m L) \tag{C.26}$$

Eq. C.26 may be inverted to obtain the real space solution to the MD model:

$$C = \frac{m}{Q}\sum_{n=0}^{\infty} H(t - \frac{nL + x}{u})\frac{2\lambda((nL + x)/u)}{2\sqrt{\pi(t - (nL + x)/u)^3}}\exp\left(-\frac{(2\lambda(nL + x)/u)^2}{4(t - (nL + x)/u)}\right) \tag{C.27}$$

Eq. C.27 may be solved for $x = L$, and the resultant equation expressed in terms of the parameters β, α_1 and α_2 of the MD model to obtain:

$$C = \beta\sum_{n=0}^{\infty} H(t - (n+1)\alpha_2)\frac{(n+1)\alpha_1\alpha_2}{\sqrt{\pi(t - (n+1)\alpha_2)^3}}\exp\left(-\frac{((n+1)\alpha_1\alpha_2)^2}{(t - (n+1)\alpha_2)}\right) \tag{C.28}$$

Appendix D

Derivatives of Solutions-Recirculation

Derivatives of solutions with respect to nonlinear parameters are presented in the following:

D.1 Derivatives of the CD Model

The CD model solution has two nonlinear parameters and its derivatives are:

$$C_{IFF} = \beta \frac{1}{\sqrt{4\pi\alpha_1\alpha_2 t^3}} \sum_{n=o}^{M} (n+1) \exp\left(-((n+1)-\alpha_2 t)^2/(4\alpha_1\alpha_2 t)\right) \tag{D.1}$$

$$\frac{\partial C_{IFF}}{\partial \alpha_1} = \left[\frac{((n+1)-\alpha_2 t)^2}{4\alpha_1\alpha_2 t} - \frac{1}{2}\right] \frac{C_{IFF}}{\alpha_1} \tag{D.2}$$

$$\frac{\partial C_{IFF}}{\partial \alpha_2} = \left[\frac{2\alpha_2 t((n+1)-\alpha_2 t) + ((n+1)-\alpha_2 t)^2}{4\alpha_1\alpha_2 t} - \frac{1}{2}\right] \frac{C_{IFF}}{\alpha_2} \tag{D.3}$$

D.2 Derivatives of the MD Model

The MD model solution has two nonlinear parameters and its derivatives are:

$$C_I = \beta \sum_{n=0}^{\infty} H(t-(n+1)\alpha_2) \frac{(n+1)\alpha_1\alpha_2}{\sqrt{\pi(t-(n+1)\alpha_2)^3}} \exp\left(-\frac{((n+1)\alpha_1\alpha_2)^2}{(t-(n+1)\alpha_2)}\right) \quad \text{(D.4)}$$

$$\frac{\partial C_I}{\partial \alpha_1} = \left[1 - \frac{2(n+1)(\alpha_1\alpha_2)^2}{t-(n+1)\alpha_2}\right] \frac{C_I}{\alpha_1} \quad \text{(D.5)}$$

$$\frac{\partial C_I}{\partial \alpha_2} = \left[1 + \frac{3(n+1)\alpha_2}{2(t-(n+1)\alpha_2)} - \frac{2((n+1)\alpha_1\alpha_2)^2}{t-(n+1)\alpha_2} - \frac{\alpha_1^2((n+1)\alpha)_2^3}{(t-(n+1)\alpha_2)^2}\right] \frac{C_I}{\alpha_2} \quad \text{(D.6)}$$

D.3 Derivatives of the AD Model

The AD model solution has three nonlinear parameters and its derivatives are:

$$\overline{C}_{IFF} = \beta\left(\exp(-(1/(2\alpha_1)))\exp(\sqrt{1/(4\alpha_1^2) + (s+2\alpha_3\sqrt{s})/(\alpha_1\alpha_2)}) - 1\right)^{-1} \quad \text{(D.7)}$$

$$\frac{\partial \overline{C}_{IFF}}{\partial \alpha_1} = \left[\frac{1 - 1/(2\alpha_1) - (s+2\alpha_3\sqrt{s})/\alpha_2}{\sqrt{1/(4\alpha_1^2) + (s+2\alpha_3\sqrt{s})/(\alpha_1\alpha_2)}}\right] \frac{\overline{C}_{IFF}^2}{2\alpha_1^2} \quad \text{(D.8)}$$

$$\frac{\partial \overline{C}_{IFF}}{\partial \alpha_2} = \left[\frac{-(s+2\alpha_3\sqrt{s})/(\alpha_1\alpha_2)}{\sqrt{1/(4\alpha_1^2) + (s+2\alpha_3\sqrt{s})/(\alpha_1\alpha_2)}}\right] \frac{\overline{C}_{IFF}^2}{2\alpha_2} \quad \text{(D.9)}$$

$$\overline{C}_{IFF} = \frac{\partial \overline{C}_{IFF}}{\partial \alpha_3} = \left[\frac{\sqrt{s}/(\alpha_1\alpha_2)}{\sqrt{1/(4\alpha_1^2) + (s+2\alpha_3\sqrt{s})/(\alpha_1\alpha_2)}}\right] \overline{C}_{IFF}^2 \quad \text{(D.10)}$$

Appendix E

MD Solution- Injection-Backflow

Derivation of solutions to the CD model for injection-backflow case has been explained in detail in section **3.3.** The solution to the MD model may be derived as follows:

E.1 The MD Model Solution

In a previous **work,** the Laplace space solution was presented without nondimensionalizing the variables. Here we will use dimensionless variables and a slightly different approach to reach the same solution and show how the real space solution is obtained.

Define the following dimensionless variables:

$$x_D = \frac{x}{ut_j} \tag{E.1}$$

$$t_{Di} = \frac{t}{t_j} \tag{E.2}$$

$$y_D = \frac{\mathrm{Y}}{b} \tag{E.3}$$

$$\lambda_D = \frac{\phi\sqrt{D_a}}{b}\sqrt{t_j} \tag{E.4}$$

The dimensionless injection period equations are:

$$\frac{\partial C}{\partial t_{Di}} + \frac{\partial C}{\partial x_D} + q_D = 0 \tag{E.5}$$

$$\left(\frac{1}{\phi\lambda_D}\right)^2 \frac{\partial^2 C_m}{\partial y_r^2} - \frac{\partial C_m}{at_{;}} \tag{E.6}$$

The fluxes at the fracture matrix interface are equated by:

$$q_D = -\frac{2\lambda_D^2}{\phi} \left.\frac{\partial C_m}{\partial y_D}\right|_{y_D=0} \tag{E.7}$$

The initial and boundary conditions are:

$$C(x_D, 0) = C_m(x_D, y_D, 0) = 0 \tag{E.8}$$

$$C(0, t_{Di}) = 1 \tag{E.9}$$

$$C(x_D, t_{Di}) = C_m(x_D, 0, t_{Di}) \tag{E.10}$$

$$\lim_{y_D \to \infty} C_m(x_D, t_{Di}) = 0 \tag{E.11}$$

The Laplace space solution of the fracture transport equation subject to these conditions is:

$$\overline{C_m} = \frac{1}{s} exp(-(x_D s)) \ \exp(-(2\lambda_D x_D \sqrt{s})) \tag{E.12}$$

and the Laplace space solution of the matrix transport equation is:

$$\overline{C} = \frac{1}{s} exp(-(x_D s)) \ \exp(-(2\lambda_D x_D)\sqrt{s}) \ \exp\left(-\frac{\phi\sqrt{s}}{\lambda_D} y_D\right) \tag{E.13}$$

The fracture transport equation of the backflow period is different from the injection period equation in the sign of the convective term, because of the change in the direction of the flow velocity (or convective flux):

$$\frac{\partial C}{\partial t_{Dp}} - \frac{\partial C}{\partial x_D} + q_D = 0 \tag{E.14}$$

In Eq. E.14, the time variable is defined as:

$$t_{Dp} = \frac{t}{t_j} \tag{E.15}$$

In Eq. E.15, the time variable t is understood to be the backflow time. Since Eq. C.l is first order in the x_D variable, only one boundary condition must be specified along the flow direction:

$$C = 0 \quad at \quad x_D = \frac{L}{ut_j} = 1 \tag{E.16}$$

The matrix transport equation and other boundary conditions remain the same as in the injection period. Only the time variable, t_{Di}, in Eq. E.6 should be changed to the backflow time variable t_{Dp}. The injection period solutions, Eqs. E.12 and E.13, become the initial conditions in the backflow period. In these equations, the Laplace transformation variables correspond to $t_{Di} = 1$, since at the end of the injection period, the time variable t becomes t_j. The double Laplace transformation of Eq. E.6 with respect to the injection and backflow time variables is:

$$\left(\frac{1}{\phi\lambda_D}\right)^2 \frac{\overline{\overline{C}}_m}{\partial y_D^2} - p\overline{\overline{C}}_m = \overline{C}_m \tag{E.17}$$

where $\overline{C}_m$ is the initial condition given by Eq. E.13. Eq. E.6 is an inhomogeneous ordinary differential equation, and a solution may be obtained by the method of undetermined coefficients:

$$\overline{\overline{C}}_m = A\exp\left(-\frac{\phi\sqrt{s}}{\lambda_D}y_D\right) + B\exp\left(-\frac{\phi\sqrt{p}}{\lambda_D}y_D\right) + \frac{\overline{C}}{(p-s)}\exp\left(-\frac{\phi\sqrt{s}}{\lambda_D}y_D\right) \tag{E.18}$$

Applying the boundary conditions yields:

$$\overline{\overline{C}}_m = \overline{\overline{C}}exp\left(-\frac{\phi\sqrt{p}}{\lambda_D}y_D\right) + \frac{\overline{C}}{(p-s)}\left[exp\left(\frac{\phi\sqrt{s}}{\lambda_D}y_D\right) - exp\left(-\frac{\phi\sqrt{p}}{\lambda_D}y_D\right)\right] \tag{E.19}$$

Substituting Eq. E.19 into Eq. E.7 yields:

$$\left.\frac{\partial \overline{\overline{C}}_m}{\partial y_D}\right|_{y_D=0} = \frac{\phi\sqrt{p}}{\lambda_D}\overline{\overline{C}} + \frac{\phi \overline{C}}{\lambda_D(\sqrt{p}+\sqrt{s})} \tag{E.20}$$

The double Laplace transformation of the fracture equation is:

$$\frac{\partial \overline{\overline{C}}}{\partial x_D} - (p + 2\lambda_D\sqrt{p})\,\overline{\overline{C}} = -\overline{C}\left[1 + \frac{2\lambda_D}{\sqrt{p}+\sqrt{s}}\right] \tag{E.21}$$

The solution to Eq. E.21 is:

$$\overline{\overline{C}} = \frac{1}{s}\left[1 + \frac{2\lambda_D}{\sqrt{p}+\sqrt{s}}\right]\frac{}{(s)+(p)+(2\lambda_D)(\sqrt{s}+\sqrt{p})}\exp(-(x_D s)) \exp -((2\lambda_D x_D\sqrt{s})) + A\exp(-(x_D p))\exp(-(2\lambda_D x_D\sqrt{p})) \tag{E.22}$$

Applying the boundary condition specified at $x_D = 1$ by Eq. E.16, and solving the resultant equation at $x_D = 0$:

$$\overline{\overline{C}} = \frac{1}{s + p + 2\lambda_D(\sqrt{s}+\sqrt{p})}\left[\frac{1}{s} + \frac{2\lambda_D}{s(\sqrt{s}+\sqrt{p})}\right] \tag{E.23}$$

To obtain the inverse transform, rewrite Eq. E.23 as:

$$\overline{\overline{C}} = \frac{1}{s + p + 2\lambda_D(\sqrt{s}+\sqrt{p})}\left[\frac{1}{s} + \frac{2\lambda_D}{s\sqrt{p}} + \frac{2\lambda_D}{s-p}\left(\frac{1}{\sqrt{s}} - \frac{1}{\sqrt{p}}\right)\right] \tag{E.24}$$

Use the method of *functions offunctions* described by Ditkin and Prudnikov[28]. Supposing:

$$F(s) = \int_0^\infty \exp(-s\theta) f(\theta)\, d\theta \tag{E.25}$$

and the validity of following operational relations:

$$\mathcal{L}_{t_{Di}}\{A(t_{Di},\theta)\} = \alpha(s)\exp(-\theta\rho(s)) \tag{E.26}$$

$$\mathcal{L}_{t_{Dp}}\{B(t_{Dp},\theta)\} = \beta(p)\exp(-\theta\sigma(p)) \tag{E.27}$$

Writing $[\rho(s) + \sigma(p)]$ for s in Eq. E.25, and multiplying both sides by $\alpha(s)\beta(p)$, we obtain:

$$\alpha(s)\beta(p)F(\rho(s)+\sigma(p)) = \alpha(s)\beta(p)\int_0^\infty \exp\left(-(\rho(s)+\sigma(p))\theta\right)f(\theta)d\theta \qquad \text{(E.28)}$$

From relations Eq. E.26 and Eq. E.27, Eq. E.28 can be written as:

$$\alpha(s)\beta(p)F(\rho(s)+\sigma(p)) = \mathcal{L}_{t_{Di}}\mathcal{L}_{t_{Dp}}\int_0^\infty A(t_{Di},u)B(t_{Dp},\theta)f(\theta)d\theta \qquad \text{(E.29)}$$

Using Eq. E.29, Eq. E.24 can be inverted term by term as follows. Let:

$$\alpha(s) = \frac{1}{s} \quad \rho(s) = s + 2\lambda_D\sqrt{s} \qquad \text{(E.30)}$$

$$\beta(p) = 1 \quad \sigma(p) = p + 2\lambda_D\sqrt{p} \qquad \textbf{(E.31)}$$

Using Eqs. E.26 and E.30:

$$A(t_{Di},\theta) = H(t_{Di}-\theta)erfc\left(\frac{\lambda\theta}{\sqrt{t_{Di}-\theta}}\right) \qquad \text{(E.32)}$$

Using Eqs. E.27 and E.31:

$$B(t_{Dp},\theta) = H(t_{Dp}-\theta)\frac{\lambda_D\theta}{\sqrt{\pi(t_{Dp}-\theta)^3}}\exp\left(-\frac{(\lambda_D\theta)^2}{t_{Dp}-\theta}\right) \qquad \text{(E.33)}$$

To invert the second term, we assume:

$$\alpha(s) = \frac{1}{s}, \quad \rho(s) = s + 2\lambda_D\sqrt{s} \qquad \text{(E.34)}$$

$$\beta(p) = \frac{1}{\sqrt{p}}, \quad \sigma(p) = p + 2\lambda_D\sqrt{p} \qquad \text{(E.35)}$$

To invert the third term, we assume:

$$\alpha(s) = \frac{1}{\sqrt{s}}, \quad \rho(s) = s + 2\lambda_D\sqrt{s} \tag{E.36}$$

$$\beta(p) = 1, \quad \sigma(p) = p + 2\lambda_D\sqrt{p} \tag{E.37}$$

and use the transformation given by Voelker and Deutch [89], the $43rd$ transformation:

$$\frac{1}{s-p} f(s,p) = \int_0^{t_{Di}} F(t_{Di} - \eta, t_{Dp} + \eta) d\eta \tag{E.38}$$

Finally, to invert the fourth term, we assume:

$$\alpha(s) = 1, \quad \rho(s) = s + 2\lambda_D\sqrt{s} \tag{E.39}$$

$$\beta(p) = \frac{1}{\sqrt{p}}, \qquad \sigma(p) = p + 2\lambda_D\sqrt{p} \tag{E.40}$$

and use Eq. E.38.

As a result, the real space solution is:

$$\begin{aligned} C_f = \int_0^{min(1,t_{Dp})} \Bigg\{ & erfc\left(\frac{\lambda_D\theta}{\sqrt{1-\theta}}\right) \frac{\lambda_D\theta}{\sqrt{\pi(1-\theta)^3}} \exp\left(-\frac{\lambda_D^2\theta^2}{t_{Dp}-\theta}\right) + \\ & 2\lambda_D\, erfc\left(\frac{\lambda_D\theta}{\sqrt{1-\theta}}\right) + \frac{1}{\sqrt{\pi(1-\theta)}} \exp\left(-\frac{\lambda_D^2\theta^2}{t_{Dp}-\theta}\right) \Bigg\} d\theta \\ + \ 2\lambda_D \int_0^1 d\eta \int_0^{min(1-\eta, t_{Dp}+\eta)} & \Bigg\{ \frac{1}{\sqrt{\pi(1-\eta-\theta)}} \exp\left(-\frac{\lambda_D^2\theta^2}{1-\eta-\theta}\right) \\ & \frac{\lambda_D\theta}{\sqrt{\pi(t_{Dp}+\eta-\theta)^3}} \exp\left(-\frac{\lambda_D^2\theta^2}{t_{Dp}+\eta-\theta}\right) \Bigg\} d\theta \end{aligned}$$

$$- 2\lambda_D \int_0^1 d\eta \int_0^{min(1-\eta, t_{Dp}+\eta)} \left\{ \frac{\lambda_D \theta}{\sqrt{\pi(1-\eta-\theta)^3}} \exp\left(-\frac{\lambda_D^2 \theta^2}{1-\eta-\theta}\right) \right.$$
$$\left. \frac{1}{\sqrt{\pi(t_{Dp}+\eta-\theta)}} \exp\left(-\frac{\lambda_D^2 \theta^2}{t_{Dp}+\eta-\theta}\right) \right\} d\theta \quad \text{(E.41)}$$

In Eq. E.41 the term t_{Di} has been replaced by unity because its value is constant and equal to unity during the entire backflow period.